IMPROVED FAULT RIDE THROUGH CAPABILITY OF DFIG -WIND TURBINES USING CUSTOMIZED DEVICE

MASTER OF SCIENCE IN POWER SYSTEM AND ENERGY ENGINEERING

BY

BELAYNEH KAWATO HENTO

HAWASSA UNIVERSITY, HAWASSA, ETHIOPIA

March, 2021

IMPROVED FAULT RIDE THROUGH CAPABILITY OF DFIG -WIND TURBINES USING CUSTOMIZED DEVICE

BY

BELAYNEH KAWATO HENTO

A THESIS SUBMITTED TO DEPARTEMENT OF ELECTRICAL AND COMPUTER ENGINEERING, HAWASSA INSTITUTE OF TECHNOLOGY, SCHOOL OF GRADUATE STUDIES.

HAWASSA UNIVERSITY

HAWASSA, ETHIOPIA

IN PARTIAL FULFILLMENT OF THE REQUIREMENTS FOR THE DEGREE OF MASTER OF SCIENCE IN POWER SYSTEM AND ENERGY ENGINEERING

March, 2021

HAWASSA UNIVERSITY

INSTITUTE OF TECHNOLOGY

DEPARTMENT OF ELECTRICAL AND COMPUTER ENGINEERING

SCHOOL OF GRADUATE STUDIES

ADVISOR'S APPROVAL SHEET

This is to certify that the thesis entitled **"Improved Fault Ride Through Capability of DFIG -Wind Turbines Using Customized Device"** submitted in partial fulfillment of the requirements for the degree of Masters with specialization in Power System and Energy Engineering, The Graduate Program of the Department of Electrical and Computer Engineering, and has been carried out by **Belayneh Kawato Hento** ID No- PGPSER/003/10, under my supervision. Therefore, I recommend that the student has fulfilled the requirements and hence hereby can submit the thesis to the department.

Dr.Teshome.G	.....	.....
Advisor	Signature	Date
Mr.Mesfin.J (MSc)	.....	.....
Co-advisor	Signature	Date

SCHOOL OF GRADUATE STUDIES

HAWASSA UNIVERSITY

EXAMINER'S APPROVAL SHEET

We the under signed Board of examiners of the final open defense by **Belayneh Kawato** have read and evaluated his thesis entitled **"(Improved Fault Ride through Capability of DFIG -Wind Turbines Using Customized Device: Case Study on Ashegoda Wind Farm)"** and examined the candidate. This is therefore, to certify that the thesis has been accepted in partial fulfilment of the requirements for the degree.

Name	Signature	Date
_____ Chair Person	_____	_____
Dr.Teshome.G Advisor	_____	_____
Mr.Mesfin.J Co- advisor	_____	_____
_____ External Eximiner	_____	_____
_____ Internal Examiner I	_____	_____
_____ Internal Examiner II	_____	_____
_____ SGS	_____	_____

Final approval and acceptance of the thesis is contingent upon the submission of the final copy of the thesis to the school of graduate studies (SGS) through the department Graduate Committee (DGC) of Electrical and Computer Engineering.

Declaration

I declare that this thesis work entitled **"Improved Fault Ride through Capability of DFIG -Wind Turbines Using Customized Device"** is the result of my own work; it contains no materials previously published or written by another person except where due reference is made. This research has not been previously submitted for any degree to other higher academic or other institutions.

Belayneh Kawato ————————————- ————————————

HAWASSA UNIVERSITY, HAWASSA, ETHIOPIA

March, 2021

Acknowledgment

First and foremost, glory and thanks to the almighty God for the completion of this master's thesis. Next, I would like to take this opportunity to express my deep and sincere gratitude to my advisor, Dr. Teshome Gaa, for his guidance, support and encouragement throughout the thesis work. Without his unending help this thesis would not have been possible.

I am also very much grateful to all engineers who have given me unreserved assistance in obtaining the information and data needed for this work. My special thanks go to the professionals and Ashegoda wind farm for their willingness to provide me with all the necessary data and valuable information. In addition I gratefully acknowledge Hawassa University institution of Technology and Bona Zuria Woreda for sponsoring the whole Master's program including the research expense.

Finally, I want to thank you to my beloved family who has given their support and encouragement for me to complete my study. Lastly but not least, I want to thank all of my beloved friends who show their support and helping hands in order for me to complete my research study.

Contents

List of Tables

List of Figures

List of Abberivations

AWF	Ashegoda Wind Farm
BESS	Battery Energy Storage Systems
CRF	Capital Recovery Factor
D-FACTS	Distribution flexible alternative current transmission system
D-STATCOM	Distribution Static synchronous Compensators
DFIG	Doubly Fed Induction Generators
DSC	Distribution Series Capacitors
DVR	Dynamic Voltage Restorer
EACC	Equivalent Annual Capital Cost
FACTS	Flexible AC Transmission System
FRT	Fault Ride Through
GA	Genetic Algorithm
GSC	Grid Side Converter
LVRT	Low Voltage Ride-Through
MPPT	Maximum Power Point Tracking
PCC	Point of Common Coupling
PI	Proportional–Integral

PSO	Particle Swarm Optimization
PWM	Pulse Width Modulation
RER	Renewable Energy Resources
RSC	Rotor Side Convertor
SVC	Static VAR Compensator
TSO	Transmission System Operator
WEG	Wind Electric Generators
WPGS	Wind Power Generation System

List of Symbols

$(\alpha,\ \beta)$	Axes corresponding to the stator
$(d,\ q)$	Axes corresponding to the rotating field
$V_{sa},\ V_{sb},\ V_{sc}$	Three phase stator Voltages
$V_{ra},\ V_{rb},\ V_{rc}$	Three phase rotor Voltages
$V_{sd},\ V_{sq}$	Stator voltages in the frame $d-q$
$V_{s\alpha},\ V_{s\beta}$	Stator voltages in the frame $\alpha-\beta$
$i_{sa},\ i_{sb},\ i_{sc}$	Three phase stator currents
$i_{ra},\ i_{rb},\ i_{rc}$	Three phase rotor Currents
$i_{sd},\ i_{sq}$	Stator Currents in the frame $d-q$
$i_{s\alpha},\ i_{s\beta}$	Stator currents in the frame $\alpha-\beta$
$\lambda_{sa},\ \lambda_{sb},\ \lambda_{sc}$	Three phase stator fluxes
$\lambda_{ra},\ \lambda_{rb},\ \lambda_{rc}$	Three phase rotor fluxes
$\lambda_{sd},\ \lambda_{sq}$	Stator flux in $(d,\ q)$ coordinate system
$\lambda_{s\alpha},\ \lambda_{s\beta}$	Stator flux in $(\alpha,\ \beta)$ coordinate system
$R_s,\ R_r$	Stator and rotor resistances

L_s, L_r	Stator and rotor resistances
L_m	Mutual inductance between stator and rotor
f_r	Coefficient of friction
P_{mech}	Mechanical power
ω_m	Electrical angular speed
ρ	Air density
C_p	Power coefficient
T_{em}	Electromagnetic Torque
T_l	Load Torque
p	Number of pole pairs

Abstract

Expanding measure of wind turbines is associated with electrical power systems because of the ecological concern and mission of vitality security. One of the main concerns connected to the high level penetration of the wind turbine integrated grid is power system stability problem. Consequently, the stable operation of wind power generation systems is very important for power system stability.To evaluate the dynamic performance of the power system with and without the dynamic voltage support from Dynamic Voltage Restorer (DVR) for a three phase short circuit fault at point of common coupling. The main goal of this proposition is to create models of DVR, and Crowbar security at Point of Common Coupling (PCC) to help Doubly Fed Induction Generator (DFIG) based wind farm during disturbances. The main concern is the Fault Ride Through (FRT) capacity of the system when the generator voltage drops to exceedingly low values because of short out fault and furthermore unexpected burden changes. Integrating FACTS keep the grid connected DFIG-based wind farm from going disconnected during and after the disturbance. DFIG is usually used to satisfy standard grid requirements such as stability of the grid, grid synchronization, power quality improvement, power control and fault ride through in grid tied wind energy system. The proposed system DVR and Crowbar protection rides through the fault by improving voltage guideline and prevents wind turbine termination during grid faults. The proposed system is applied on Ashegoda wind farm in Ethiopia as a case study and a test modeling and simulation have been acted in Mat Lab/Simulink programming version 9.4.

Key words: *Doubly fed induction generation (DFIG), Dynamic voltage restorer (DVR), Fault ride through capabilities, Particle swarm optimization and Proportional integral controller*

Chapter 1

Introduction

In current years, wind power generation is in fast development and its contribution to the power sector has been increasing day by day. This situation has forced the necessity for evaluation of their impact on power system dynamics. During short circuit fault or severe load difference, voltage sags are detected in the network.

The increased energy demand and depletion of fossil fuels forced energy sectors to generate energy requirement through Renewable Energy Resources (RER). Among numerous RER, the Wind Power Generation System (WPGS) plays a vital role for its higher technology and low maintenance requirement in [1]. Among various WPGS, the flexible speed operated Doubly Fed Induction Generator (DFIG) based WPGS is preferred to large scale grid integration for their variable speed operation and reduced flicker effect in [2].

Just; many researchers have concentrated on different techniques to overcome the Low Voltage Ride Through (LVRT) issue. There are numerous different methods to mitigate voltage sags and swells, but the use of a custom power device is considered to be the most efficient method. Switching off a large inductive load or energizing a large capacitor bank is a typical system event that causes swells in [3].

Advanced control strategy for the DFIG converter has been proposed of doubly fed induction generator wind turbines for power system fault ride through. With the advanced control strategy, the Roter Side Controller (RSC) converts the imbalanced power into a kinetic energy of WT by increasing its rotor speed and enhances the LVRT capability according to the grid requirement in [4].

This method results in impact of wind turbine mechanical parts and might damage both the DFIG-WT as well as supporting towers. Consequently, this method is not flexible for effecient FRT. Machine magnetizing current control based FRT for DFIG WPGS has been proposed to improve the system reaction during balanced dips. The method uses an additional high rotor voltage for performing Low Voltage Ride-Through (LVRT) in [5].

However, using a high rotor voltage is not viable for the converter and further; the control strategy is preferred only for balanced conditions. Additionally, the behavior of control strategies for unbalanced conditions cannot be predicted. In order to overcome these issues, hardware modification based crowbar control strategy has been proposed to perform FRT in DFIG wind turbines in [6].

1.1 Statement of Problem

In order to fulfill the power demand needed by consumers, countries are applying various types of renewable energy sources in addition to the conventional sources. The main renewable energy resources that have been improving fault ride through capabilities exist in both the generator side and the grid side in the system. Due to the nature and increasing penetration level of wind power generation it is important to consider the interaction between the wind power generation systems and the grid, as large wind grid to use device starts to influence the overall system behavior and pose power system stability and control issues.

Earlier, disconnection of wind turbine was not of the important consideration whenever there was a problem of supplying voltage. Today this concept has changed because loss of such a considerable part of the power production due to network disturbances can't be accepted any more as it results in instability of the power grid. Voltage stability and an efficient a DVR device is the basic requirements for higher penetration. Under this condition, wind turbines have to be able to continue uninterrupted operation under transient voltage conditions to be in accordance with the grid codes and to support in grid voltage and frequency regulation.

Different methods to improve the dynamic performance of wind farms during system disturbances and hence maintain system stability have been proposed in different studies.

In order to maintain proper voltage level at the PCC and promote the improve fault through the wind farms into the electrical network. This thesis work proposed to use a DVR device at PCC to enhance system stability and to increase the LVRT capability of the wind turbine generators. The main motivation for choosing a DVR device in wind farm is its ability to provide fast and dynamic voltage support at PCC either by supporting or absorbing reactive power in to the system. The proposed system in to the system in applied on Ashegoda wind farm in Ethiopia as a case study.

1.2 Objectives of the study

1.2.1 General Objective

The general objective of this thesis is to improve fault ride through capability of Doubly Fed Induction Generators (DFIG) - wind turbines using customized dynamic voltage restorer device.

1.2.2 Specific Objectives

- To model doubly fed induction generator wind power systems.
- To improve the fault ride through capability using optimal placed of DVR device.
- To evaluate the behavior of wind turbine with and without dynamic voltage restorer device using Mat Lab/Simulink software.
- To obtain appropriate and economical solution.

1.3 Significance of the study

This work provides important insight into potential improvements to the studied wind farm and can be used as an input for other existing wind farms and for those which are under construction. It also helps to:

- Understand the operational challenges on a power system containing large wind farm.

- Evaluate the possible solutions for improved performance of grid connected wind farms, and hence comply with grid connection requirements (grid codes).
- Investigate the applicability of FACTS devices in improving dynamic performance of wind farms.

In addition, this thesis can be used as input for further research work.

1.4 Scope of the study

The scope of this study is to investigate the causes of faults in Ashegoda wind farm and identify the linkage of these causes to specific system weaknesses. With these system weaknesses computer simulations (by using Mat Lab software) for some selected faults are performed to corroborate whether the suggested causes could possibly have caused the previous system collapses. This in turn helps us to identify the system vulnerabilities and propose solutions to minimize the occurrence of faults and the optimal placement of the DVR device be analyzed using Particle Swarm Optimization (PSO) method. Due to the random nature, fault imposed on the grid can occur anywhere within the connected system. Moreover, advanced control strategies have been proposed and developed for an efficient and reliable operation during normal condition. The faults occurred in 2017 G.C in the Ashegoda wind farm.

Chapter 2

Literature Review

2.1 Overview of Doubly Fed Induction Generations.

The electrical power supplied to the end consumer should be of high quality. Power Quality concerns about the utility ability to deliver uninterrupted power source. The Doubly Fed Induction Generator (DFIG) can supply power at constant voltage and constant frequency while the rotor speed varies. This makes it suitable for variable speed wind energy applications.

The stator of Doubly Fed Induction Generators (DFIG) is directly connected to the grid while the rotor is connected to the utility grid by means of a partially rated variable frequency ac/dc/ac converter, which just needs to deal with a fraction (25%-30%) of the total DFIG power to acquire full control of the generator. By the help of these converters the magnitude and phase of the rotor voltage can be controlled, so as to make active and reactive power control possible. The Fault Ride -Through (FRT) capability of DFIG WPGS can be achieved either by hardware adaptation or modifying the control strategy of a Doubly Fed Induction Generator (DFIG) converter controller.

The term custom power means the utilization of power electronic controllers for distribution systems. The custom power devices will increases the quality and reliability of the power that is delivered to the customers. Customers are increasingly demanding more exigent quality in the power supplied by the electrical company. Generally during grid faults, as stator of DFIG based WPGS is directly coupled to the grid, the stator terminal voltage falls and stator current increases enormously in [7, 8].

2.1.1 Back-to-Back Converter

A back-to-back converter is connected between the rotor and stator of the DFIG. The back-to-back converter is used in the rotor circuit, the speed range can be extended above synchronous speed and power can be generated both from the stator and the rotor. An advantage of this type of Doubly Fed Induction Generator (DFIG) drive is that the rotor converter can only be rated for a fraction of the total output power, the fraction depends on the acceptable sub- and super-synchronous speed range.

2.1.2 Rotor Side Converter (RSC) Controller

The aim of the rotor side converter is to control independently the active and reactive power. The active and reactive powers are not controlled directly, but by controlling the impressed rotor current. The rotor side converter operates in a stator flux d-q reference frame, where the rotor current is split into a parallel and orthogonal component to the stator flux, respectively. A very fast inner control loop regulates the active and the reactive component of the rotor current.

According to [9] a feed-forward transient current control method for Rotor Side Converter (RSC) of the DFIG has been proposed. This method enhances the Doubly Fed Induction Generators (DFIG) Low Voltage Ride-Through (LVRT) capability by controlling the RSC. The current set points are defined by the slower outer control loop regulating the active and reactive power. The controller provides set point values of the quadrature and direct axis component of the rotor current (iqr and idr). In normal operation the goal of the rotor side converter controller is to control active and reactive power independently.

Further, as stator and rotor are magnetically coupled, rise in stator current results in an increase of rotor current, raising the DC – link voltage, electromagnetic torque and damages the rotor circuit. The reference active power is provided by a maximum power tracking depending on the actual generator speed, which assures operation with maximum aerodynamic efficiency. During normal operation the mention reactive power is usually set to zero. For high wind speeds the speed of the turbine is limited to its rated speed, which implies indirectly that the power is limited to its rated value, too in [10, 11].

According to [12] magnetizing current control based Fault Ride -Through (FRT) for

DFIG WPGS has been proposed to enhance the system response during balanced dips. The method uses an additional high rotor voltage for performing Low Voltage Ride-Through (LVRT). However, using a high rotor voltage is not viable for the converter and further; the control strategy is preferred only for balanced conditions. Additionally, the behavior of control strategies for unbalanced conditions cannot be predicted.

According to [13] in order to overcome these issues, hardware modification based crowbar control strategy has been proposed to perform Fault Ride-Through (FRT) in Doubly Fed Induction Generators (DFIG) wind turbines. The crowbar control scheme uses crowbar circuit which is additionally added up with the RSC for FRT. Using crowbar strategy during fault isolates the Rotor Side Convertor (RSC) and makes DFIG behave like a squirrel-cage induction generator, which could lead to absorb plenty of reactive power from the grid network and causes stability issues in the grid.

2.1.3 Grid Side Converter (GSC)Controller

The main idea of this scheme is to modify the active power outer control loop of the GSC. The generated active power value of the DFIG is regulated to be constant and equal to the reference power (average power). This reference active power value is compared with the instantaneous output active power and the error is fed to a Proportional–Integral (PI) controller to generate the q-axis current reference component that will be compared with the q-axis actual value component of the generator current. This means that the grid side converter exchanges with the grid only active power, and therefore the transmission of reactive power from DFIG to the grid is done only through the stator. The dc-voltage and the reactive power are controlled indirectly by controlling the grid side converter current in [14].

The aim of the grid side converter controller for normal operation is to maintain the DC-link capacitor voltage and to guarantee a converter operation with unity power factor. Detailed explanations about the control concept of the DFIG wind turbine concept for normal operation conditions can be found in [15].

As for reactive power control loop of the GSC, the idea is to regulate or control the stator reactive power. This control loop allows us to control the reactive power sharing between the Grid Side Converter (GSC) and the DFIG and then provide the total reactive

power that matches the requirement of the grid (Grid = Stator +QGSC). The resulted d-q reference currents that produced from comparing the reference d-q current components with actual d-q current components of the DFIG will be fed to the PWM controller of the GSC to control both active and reactive power.

2.2 FACTS Devices

Flexible AC Transmission System (FACTS) technology is the ultimate tool for getting the most out of existing equipment via faster control action and new capabilities. The greatest outstanding feature is the ability to directly control transmission line flows by operationally changing parameter of the grid and to implement high gain type controller based on fast switching.

The application of FACTS devices to power system safety has been a good-looking ongoing area of research. In most of the reported studies attention has been focused on the ability of these devices to improve the power system security by damping system oscillation and minimal attempts have been made to investigate the effect of these devices on power system reality.

According to [16] described the power electronic devices and technical review in various power engineering levels. In addition, the power electronics-based equipment, which are called power conditioners are used to solve power quality problems. Power conditioners are also called Distribution FACTS (D-FACTS)devices.

There are many types of Custom Power devices. About of these devices include Active Power Filters (APF), Surge Arresters (SA). Battery Energy Storage Systems (BESS), Super conducting Magnetic Energy Systems (SMES), Static Electronic Tap Changers (SETC), Solid State Fault Current Limiter (SSFCL), Solid-State Transfer Switches (SSTS), Static VAR Compensator (SVC), Distribution Series Capacitors (DSC), Dynamic Voltage Restorer (DVR), Distribution Static synchronous Compensators (D-STATCOM) , Uninterruptible Power Supplies (UPS) , Unified power flow controller (UPFC),Unified power quality conditioner (UPQC) and Crowbar protection. But in this work, the main focus is kept only on a dynamic voltage restorer device and Crowbar protection device.

2.2.1 Dynamic Voltage Restorer (DVR) Device

Dynamic Voltage Restorer device is a series connected solid state device which injects voltage in to the system and regulate the load-side voltage. It is normally installed in between the supply and the feeder in a distribution system. In the event of a disturbance it boosts up the load-side voltage and avoids any power disruption to that load. There are various control schemes and circuit topologies that can be used to implement a DVR.

To demonstrate that power quality measures can be applied both at the user end and also at the utility level. The work identifies some important measures that can be applied at the utility level without much system upset. The models of custom power equipment, namely DVR and D-STATCOM are existing and practical to mitigate voltage dip which is very prominent as per utilities are disturbed using a new Pulse Width Modulation (PWM)-based control system. A dynamic voltage restorer system based on downstream fault limiting function and a flux charge model feedback controller can be found in [17, 18].

It would act as a large virtual inductance in series with the distribution feeder in fault condition. It can protect from sudden sags and swells and it minimizes the stress on the DC Link. For the compensation of power quality problems with voltage sags, voltage harmonics and voltage imbalances a two level DVR with repetitive controller can be found in [19].

They oberved that repetitive controller specialty is fast transient response and it ensures for any sinusoidal input and any sinusoidal disturbance to zero error in steady state condition. For the implementation of controller, they used either stationery reference frame or rotating reference frame. To overcome these issues, traditional Dynamic Voltage Regulator (DVR) based compensating devices. A DVR is an efficient voltage compensation device and well known for its fast response time as well as the better effect of restraining flicker. A DVR is energized using DC- capacitor or batteries, which are linked to the grid, though a Voltage Source Converter (VSC) and boost transformer. In traditional DVR, the energy storage gets charged during normal operation and discharges during compensation requirement can be found in[20].

The major drawback of the traditional DVR is lack of adequate control strategy and energy storage devices. Particularly, the traditional DVR based on batteries is by parasitic losses when it draws power while the system is in operation. Dynamic voltage restorer

is used to compensate voltage sags and swells, as well as it can compensate line voltage harmonics, reduce transients in voltage and fault current limitations. Dynamic voltage restorer consists of an injection / booster transformer, a harmonic filter, a Voltage Source Converter (VSC), DC charging circuit and a control and protection system as shown in Figure 2.1. The DVR injects active power into the distribution line in sag correction techniques during the compensation period. Hence, for long duration sags the capacity of the DC-link or energy storage unit becomes a limiting factor in the disturbance compensation process in [21].

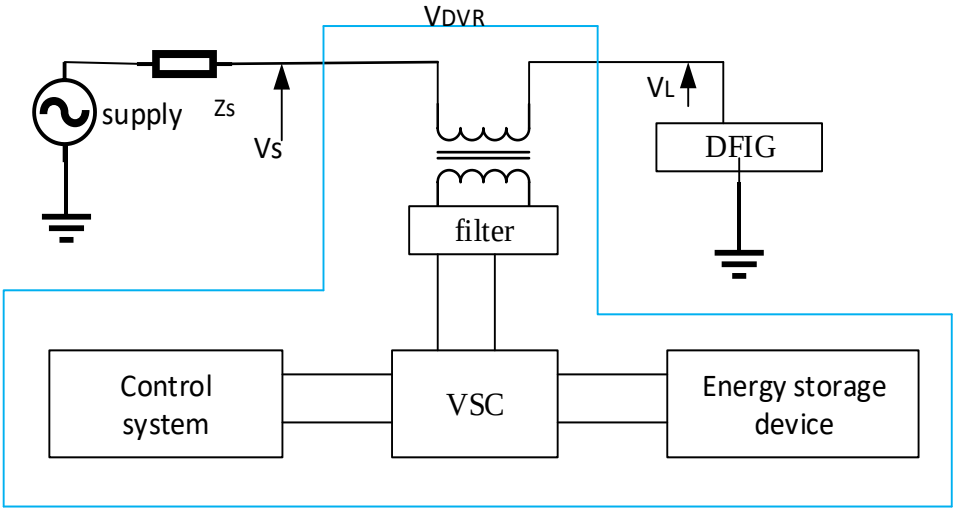

Figure 2.1: Block diagram of basic structure of dynamic voltage restorer

2.2.2 Selection of Dynamic Voltage Restorer Components

The basic structure of dynamic voltage restorer divided in depending up on figure 2.1. It is divided in to five categories selection of DVR components.

2.2.2.1 Voltage injection transformer

The high voltage side of the injection transformer is connected in series to the distribution line, while the low voltage side is connected to the DVR power circuit. Three single-phase or three-phase voltage injection transformers can be connected to the distribution line for a three-phase DVR and for single phase DVR one single-phase transformer is connected. For the three-phase DVR the three single - phase transformers can be connected either

in delta/open or star/open configuration.

2.2.2.2 Passive filter

Filters are used to convert the inverted PWM waveform into a sinusoidal waveform. This is achieved by eliminating the unwanted harmonic components generated by VSI action.

2.2.2.3 Inverter

An Inverter system is used to convert dc storage into ac form. These inverters have low voltage ratings and high current ratings as step up transformers are used to boost up the injected voltage.

2.2.2.4 Energy storage unit

It is responsible for energy storage in DC form. Flywheels, batteries, Superconducting Magnetic Energy Storage (SMES) and super capacitors can be used as energy storage devices. It is supplies the real power requirements of the system when DVR is used for compensation.

2.2.2.5 Capacitor

DVR has a large DC capacitor to ensure a proper DC voltage input to Inverter. Capacitor terminal voltage reduces when energy is drawn from energy storage capacitors. Therefore, there is a minimum voltage required below which the inverter of the Dynamic Voltage Restorer (DVR) cannot generate the require voltage thus, size and rating of capacitor is very important for DVR power circuit. The most important advantage of these capacitors is the capability to supply high current pulses repeatedly for hundreds of thousands of cycles.

2.2.3 Dynamic Voltage Restorer Operating Modes

1. **During a voltage sag/swell on the line:** The DVR injects the difference between the pre-sag and the sag voltage, by supplying the real power requirement from the energy storage device together with the reactive power. The maximum injection capability of the Dynamic Voltage Restorer (DVR) is limited by the ratings of

the DC energy storage and the voltage injection transformer ratio. In the case of three single-phase DVRs the magnitude of the injected voltage can be controlled individually. The injected voltages are made synchronized (i.e. same frequency and the phase angle) with the network voltages can be found in [22].

2. **During the normal operation:** As the network is working under normal condition the DVR is not injecting any voltages to the system. In that case, if the energy storage device is fully charged then the DVR operates in the standby mode or otherwise it operates in the self-charging mode. The energy storage device can be charged either from the power supply itself or from a different source.

3. **During a short circuit or fault in the downstream of the distribution line:** In this particular case the by-pass switch is activated to provide an alternate path for the fault currents. Hence the inverter is protected from the flow of high fault current through it, which can damage the sensitive power electronic components.

2.2.4 Control Strategy of Customized Dynamic Voltage Restorer (DVR) Device

The purpose of a dynamic voltage restorer is to inject voltage in to a grid network in order to minimize voltage disturbances in the grid and load voltage during grid faults. There are several techniques to implement and control methods of the dynamic voltage restorer for power quality enhancements. The control of dynamic voltage restorer is very important factor. The control strategy of the system plays a major role by controlling the dynamic voltage restorer device to operate according to the requirement such as:-

- Voltage control.
- Power control.
- Rated torque control can be found in [23]. Hence, the proposed processes proportional-integral controller to minimize the error and the regulate load voltage in to the system model mat lab/Simulink software.

2.2.5 Criteria of Dynamic Voltage Restorer Placement on Transmission Line

The functions of the dynamic voltage restorer placement on transmission line are

1. Protect load voltage from any short duration voltage disturbances.
2. Reduces the losses and improve power quality at the load bus.
3. The protection of sensitive loads from voltage sags/swells coming from the network.

2.2.6 Crowbar Protection device

When a voltage dip occurs in the network, current transients in the stator windings (due to the stator's direct connection to the grid) and grid side converter are produced. A crowbar is a device widely used to protect electronic circuits against an overvoltage condition in their power supply. It operates by putting a short- circuit or low resistance path between the terminals.

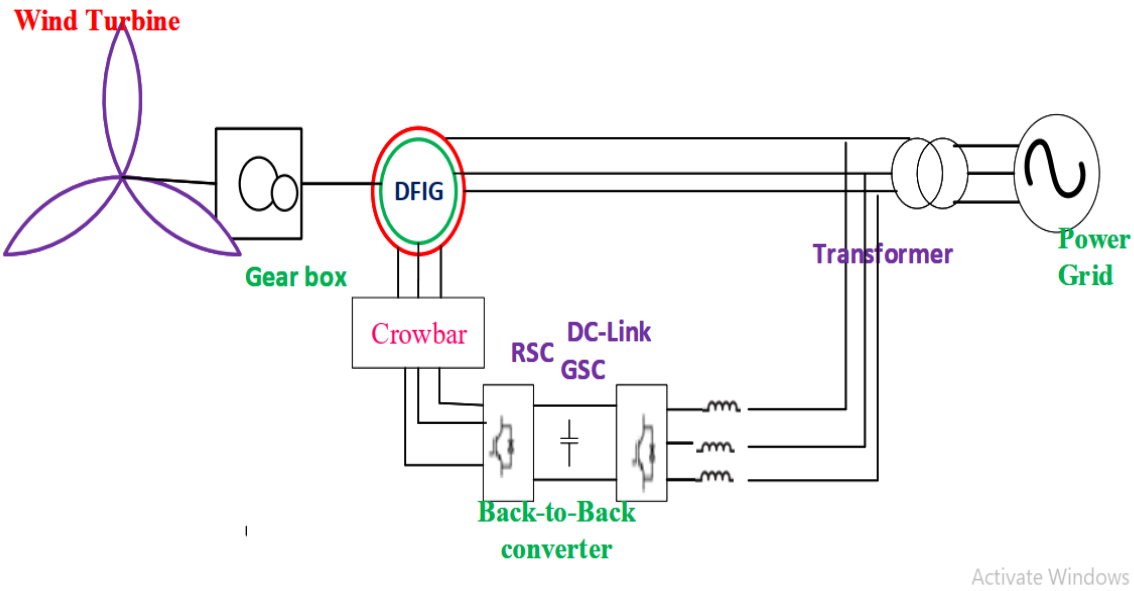

Figure 2.2: Crowbar protections with DFIG schemes block diagram

Hence, these two behaviors are completely different:

- The grid side converter doesn't lose current control in most cases.

- Stator disturbance is transmitted to the rotor, causing uncontrollable currents that can produce damage to the rotor converter due to the over currents and the over-voltage of the DC-link. Frequently, there is a high transformation ratio between the stator and rotor windings; thus, the rotor converter has restricted control over the generator.

A circuit called crowbar is connected to the rotor to protect the rotor side convertor. The crowbar avoids voltage bus exceed his maximum value once the rotor side convertor loses current control providing a path for the rotor currents.

The crowbar power converter may be affected with several power arrangements. In this section we will analyze two configurations that allow a passive and an active crowbar. Both diagrams rectify the rotor current and short-circuit the rotor by means of a resistance. The passive crowbar is constructed with a thyristor and allows closing the circuit but does not allow it to open until the crowbar current is extinguished. The active crowbar is built with an IGBT and allows opening the circuit in forced commutation.

In order to overcome these issues, hardware modification based crowbar control strategy has been proposed to perform fault ride through in doubly fed induction generator wind turbines. The crowbar control scheme uses crowbar circuit which is additionally added up with the rotor side convertor for fault ride through capability. Using crowbar strategy during fault isolates the rotor side convertor and makes doubly fed induction generator behave like a squirrel-cage induction generator, which could lead to absorb plenty of reactive power from the grid network and causes stability issues in the grid as in [24].

The control system of the crowbar may be materialized in many ways depending on the power converter structure and the desired performances. After a voltage dip, the rotor current regulators lose control and an energy flow from the stator to the rotor charges the bus capacitor. To avoid the bus voltage from reaching the converter limits, it is necessary to break this energy flow, and the simplest method is to short-circuit the rotor when the bus voltage reaches a limiting value.

With a passive control, the crowbar act as a defense system; the time essential to open the stator breaker is approximately 100 milliseconds, causing at the end the disconnection of the wind turbine. When the control objective is to keep the wind turbine connected to the grid during fault, it is necessary to control the bus voltage can be found in[25].

The simplest technique consists of comparing the bus voltage with its maximum and normal operation reference values and, depending on that comparison, keeping the crowbar circuit open or closed. This technique is called active crowbar control. The bus capacitor load dynamics is determined by the rotor–bus energy flow, and the discharge is determined by the capacity of the grid side inverter (bus to grid energy flow).

2.2.7 Reasons for choosing DVR and Crowbar Protection devices

The output of the wind power plants and the total load vary always in the day. Reactive power compensation is mandatory to continue normal voltage levels in the power system. Reactive power imbalances, which can seriously affect the power system, can be minimized by reactive power compensation by using devices such as dynamic voltage restorer and Crowbar protection.

Dynamic voltage restorer is used to compensate voltage sags and swells, as well as it can compensate line voltage harmonics reduce transients in voltage and fault current limitations. Crowbar technique is a useful way to solve fault ride through capability of Wind Electric Generators (WEG). The crowbar provides a safe route for the high transient rotor current by short circuiting the generator rotor windings, switching the crowbar to protect the Rotor Side Converter (RSC) during faults.

2.3 Fault ride-through Capability

One of the important requirements for wind power plant is provide fault ride-through capabilities. This means the wind power plant must withstand voltage dips to certain percentage of the nominal voltage and for a specific duration. The wind turbines will nowadays be likely to remain connected to the grid both during and after a fault. Upon voltage recovery, the wind turbines are not expected to consume excessive reactive power when re-exciting the generator, as this may result in a further voltage dip in [26].

During the occurrence of voltage sag, the turbines are required to remain connected for a specific amount of time before being allowed to disconnect. This condition is to confirm that there is no loss of generation for normally cleared faults. Disconnecting a

wind grid particularly dealing with large wind farms. In addition, some utilities require that the wind turbines help support the grid during faults. The cumulative and growth of wind power has set some new problems to power system. The power system with large scale wind power will include problems not only in steady state process but also in contingency condition. Fault Ride -Through (FRT) requires keep the Wind Turbines (WTs) on the grid during faults so that they can contribute to the stability to the power transmission system. In other word wind farm necessity not be separated from the grid during a fault or short circuit. Under grid faults, the Wind Turbines System (WTS) should remain connected to the grid and provide reactive power to support the grid, and the active power generation should be restored in a required time which is also referred to as fault ride through requirements. This fault ride-through can be described in figure 2.3 in[26].

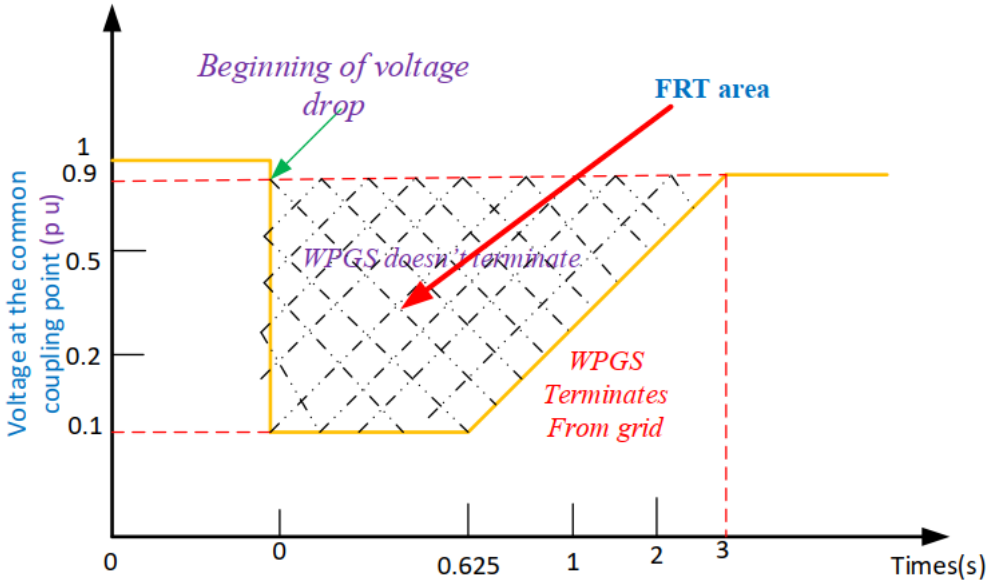

Figure 2.3: Voltage fault ride through requirement

The graph is described by the voltage (in p.u) versus time characteristic and minimum requirement of the wind farm. Under the fault conditions, there are two major problems for existing doubly fed induction generator based wind energy system.

1. Over voltage for rotor side converter and over voltage on dc-link.

2. Reconnection to recovered grid may cause stability issue.

Without proper control scheme, a dynamic voltage restorer Doubly Fed Induction Generator (DFIG) induces large currents on the rotor side as the excitation current is low during faults. The generator flux is not maintained when the stator voltage drops or negative rotating flux may appear if the system is severely unbalanced. At the voltage dip wind farm and the grid must remain connected until it is restored to prefault values.

In the transition of the voltage dip to prefault values, the wind farm and the grid has a accidental that it may be cut off. Wind power plant must provide fast transition time to bring the voltage to prefault value. One of Doubly Fed Induction Generators (DFIG) capability during a fault ride-through situation is to control the generator output active power and reactive power. In a fault ride-through situation, there is a risk in the RSC because it can only handle certain amount of current flow through the converter. In additional, there is also a risk of over voltage on the DC-link capacitor during this situation.

When the RSC current or DC-link voltage hit their limits, the over current or over voltage protection is activated, respectively. This protection is controlled by the DFIG crowbar. The crowbar deactivates the RSC, and this leads to the DFIG rotor to be disconnected from the network. When the fault is cleared crowbar will reconnect the RSC, and the DFIG rotor will be rejoined to the network. It has the ability to repair the situation to the prefault state.

2.4 Low Voltage Ride-Through (LVRT)

In the event of voltage sag, the wind turbines are necessary to remain connected for a specific amount of time before being allowable to separate. In addition, some utilities need that the wind turbines help maintenance grid voltage during faults. Period of fault or low voltage ride through be contingent on the magnitude of voltage drop at the Point of Common Coupling (PCC) during the fault and time taken by the grid system to improve to the normal state. Table 2.1 the fault clearing times for different nominal system voltages. The typical duration for fault clearing is 0.15s in [27].

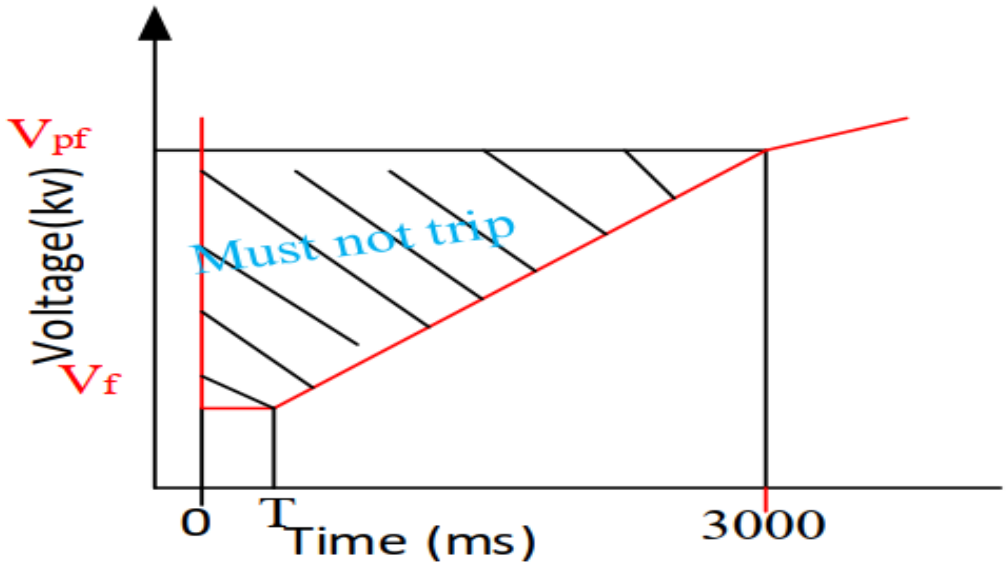

Figure 2.4: low Voltage fault ride through requirement

Where:-

Vf: 15% of nominal system voltage.

Vpf: Minimum voltage for normal operation of the wind turbine.

The typical duration is 0.15s.

Table 2.1: Fault clearing time and voltage limits

Nominal system voltage (kv)	Fault clearing time,T (ms)	Vpf(kv)	Vf(kv)
400	100	360	60
220	160	200	33
132	160	120	20
110	160	96	17
60	300	60	10

The LVRT fulfillment for wind turbines has become a main condition from the TSD-DSOs all around the world. The first wind turbines estabilished on squirrel cage asynchronous generators were very complex to grid outages. The securities were tuned in such a way that the wind turbine separeted with even minor disturbances. This caused two major problems for the TSO-DSO:

1. The protections were powerless to sense faults in lines close wind farms, due to loss of short-circuit current from the wind farms.

2. The loss of wind power generation (reconnection of a fixed speed wind farm takes several minutes) demands fast reaction generation plants (such as hydro) or an increase in the fast standby power.

So, as mentioned earlier, the first requirement of the Transmission System Operator (TSO) is to "keep connected." But wind turbine behavior during a grid fault is very different depending on the technology (fixed speed or variable speed, and full converter technologies or doubly fed induction generator) and also different from conventional power plants based on synchronous generators. Thus, the TSOs decided to standardize the pattern of current versus voltage during faults, that is, the current that the generator consumes during the fault. The control strategy of LVRT must allow the wind turbine:

- To continue linked to the power system and not consume active power during the fault.
- To be providing with reactive power during the fault to support voltage recovery.
- To return to normal operation situations next the fault

Voltage recovery is a balancing condition; wind generators try to minimize the influence of wind parks in the power system during a short circuit and fault clearing. Voltage recovery is achieved by reactive current injection of the wind generator.

2.5 The Problems of Ashegoda Wind Farm

The economic and social effects of loss of electric service in Ashegoda wind farm have problems in both the utility supplying electric energy and the customer of electric service. If a major power outage affects multiple distribution systems of customer services, then the expected interruption. Ashegoda wind farm power system is vulnerable to system abnormalities such as control failures, protection or communication system failures, transmission line failures, poor maintenances and disturbances, such as lightning, grounding, system overload and human operational errors. Therefore, maintaining a reliable power supply to the customer service is a very important issue for power systems design and operation of EEP and EEU.

In case study the system is subjected to symmetrical fault analysis is carried out to prove the effective power quality mitigation using the customized dynamic voltage restorer. The symmetrical fault rarely occurs in practice as majority of the faults are of unsymmetrical nature. However, symmetrical fault are enable the reader to understand the problems that short circuit conditions present to the power system.

Dynamic voltage restorer used for utility

- Increase the stability and reliability of in the system.
- To compensate voltage sags and swells, as well as it can compensate line voltage harmonics reduce transients in voltage and fault current limitations.
- The maximum inject voltage in to a grid network in order to mitigate voltage disturbances in the grid and load voltage during grid faults.
- Improving the utilization efficiency and decreasing the investment cost of wind turbine generation.

Short outcome for utility

- Decrease the efficiency of wind energy extraction.
- Electronic equipment is highly sensitive to power outages and deviations in voltage and frequency.
- Decrease the stability and reliability of the system.
- If cluster outages are eliminated from outage statistics, reliability at the transmission level.

Chapter 3

Mathematical Modeling and Block Diagram

3.1 Model and Operating Principle of Double Fed Induction Generator.

The schematic of the study system is shown in figure 3.1. The study system consists of a DFIG-WPGS generating power of 120 MW integrated in to a grid network at the Point of Common Coupling (PCC). The DFIG-WPGS stator is directly connected to the grid, whereas the rotor is connected to the grid through DC-link back to back convertor. The back to back convertor controls the speed and frequency of doubly fed induction generator. The generated power of WPGS is fed to the utility grid through a 230/33kV transformer. Here, the DFIG is considered as the main source of energy supplier. The absence of doubly fed induction generator could lead to grid instability.

Furthermore, the voltage 33kV is step-upped and fed in to the utility grid network. The utility grid considered in this study is characterized as 33kV bus system and 50Hz frequency. A proposed control strategy based customized DVR is connected between the PCC and DFIG. The customized DVR is doesn't operate during normal operation, but it feeds energy only when there is voltage drop in the grid network. Hence, to analyze te behavior of DFIG and customized DVR, a 3-phase fault is intruded between PCC and DFIG-WPGS. The parameters of study system are listed in the appendix A.1.

The modeling of Dynamic Voltage Restorer (DVR) device is carried out component

wise and their performances are analyzed using Mat Lab /Simulink software. Fig 3.1 show the general block diagram of the proposed doubly fed induction generator model.

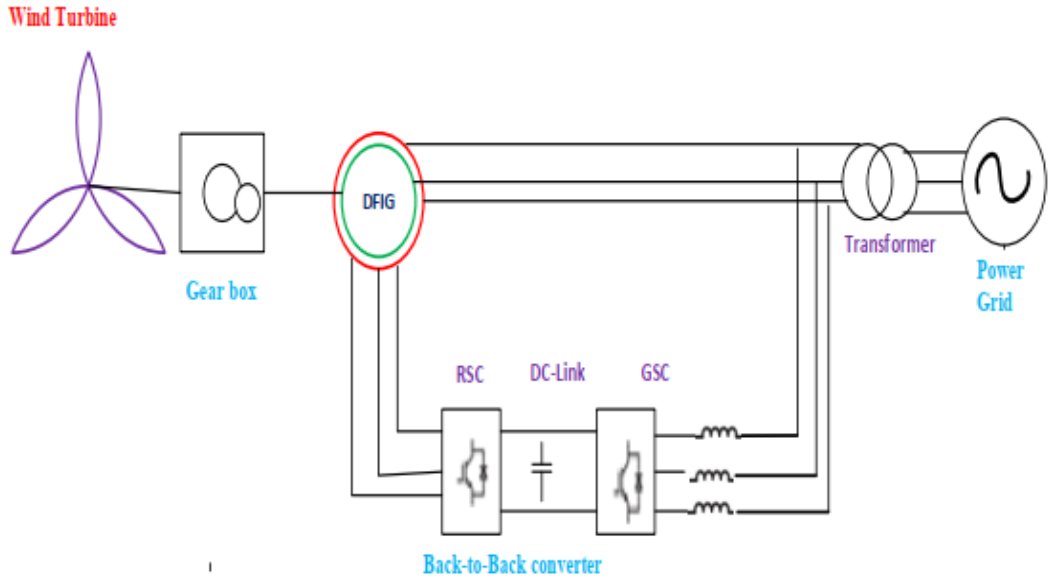

Figure 3.1: Grid connected double fed induction generation based wind power system

3.2 Doubly Fed Induction Generator Based Wind Power Generation System Configuration

The WPGS consists of an aerodynamic turbine connected to the Doubly Fed Induction Generator (DFIG) through a gear shaft system. The stator terminal of a DFIG is directly coupled to the grid, whereas the rotor terminal connects to the grid through a power electronic back to back VSC. The VSC is classified as Grid Side Converter (GSC) and Rotor Side Converter (RSC).

Where the function of the GSC is to regulate the DC-link capacitor voltage between the two converters and to inject independent reactive power into the grid according to grid requirement. Meanwhile, the RSC regulates the speed and torque to achieve optimal power output. The DFIG-WPGS converts the wind power (Pw) into mechanical power (Pm) and subsequently generates electrical power (Pe) which has been directly fed to the grid system.

3.3 Mathematical Modeling of Wind Turbines

Power developing by the wind machine is generally affected by wind speed, area swept by the rotor, density of air, rotational speed of the machine, radius of the rotor, number of blades, and total blade area. It is also affected by lift and drag appearances of the blade outline.

Some of the existing power in the wind is changed by the rotor blades to mechanical power acting on the rotor shaft of the wind turbine. For steady-state designs of the mechanical power from a wind turbine, the so called Cp (λ,β)-curve can be used. The mechanical power Pmech can be determined as follows:

$$P_{mech} = \frac{1}{2}\rho ArCp(\lambda,\ \beta)\,\omega^3 \tag{3.1}$$

Where Cp is the power coeffient, β is the pitch angle, λ is the tip speed ratio, ω is the wind speed, r is the rotor plane radius, ρ is the air density, and Ar is the area swept by the ratio.

Tip Speed Ratio

The power coefficient is at its maximum at a certain velocity of the wind turbines blade tip relative the velocity of the immidiate wind. The tip speed ratio, λ defines the ratio between the parameters.

$$\lambda = \frac{\omega R}{V} \tag{3.2}$$

Where ω is defined as the rotational speed of the rotor, R is the radius of the rotor and v is the speed of unobstructed wind flow.

The fundamentals of using a Doubly-Fed Induction Generator (DFIG) to convert the mechanical energy of the wind into valuable electrical power that can be used to supply electricity to any grid are presented. The effectiveness of the customized Dynamic Voltage Restorer (DVR) device and proposed strategy is analyzed for Doubly Fed Induction Generation (DFIG) based Wind Power Generation System (WPGS) under the symmetrical fault conditions.

3.4 Dynamic Model of Wind Turbines Based on the Doubly Fed Induction Generator

The steady-state equivalent circuit of a Doubly Fed Induction Generators (DFIG) is derived with the assumption that the DFIG works at steady state under the ideal grid condition. It is simplified as a one-phase system. It only describes the steady-state performance of the DFIG.

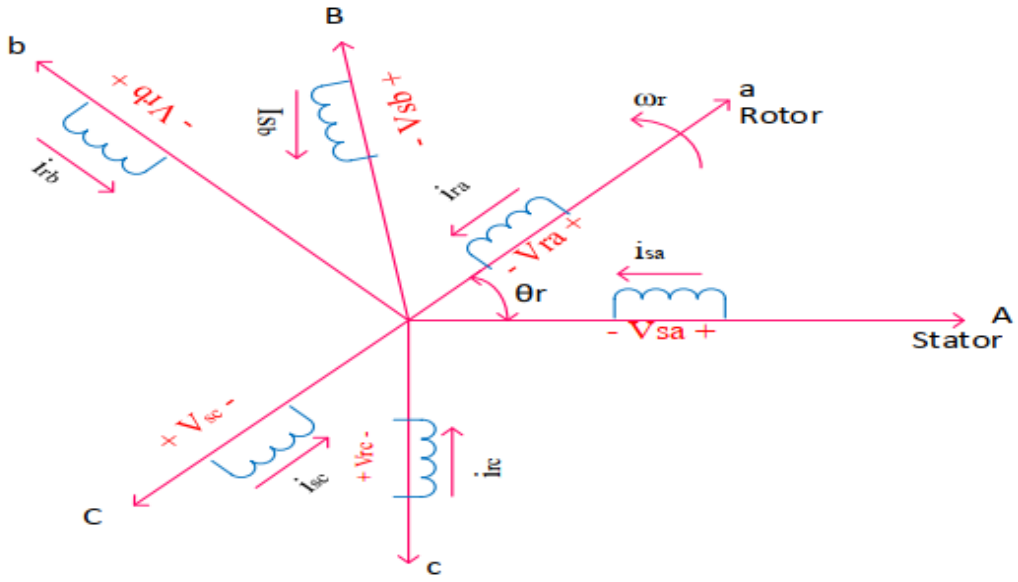

Figure 3.2: Stator and rotor windings of a double fed induction generation

For dynamic analysis and control system modeling dynamic voltage restorer device and crowbar protection device in Mat Lab/Simulink software, the dynamic model of the DFIG is needed. DFIG is a great order, nonlinear, and time-varying system. To simplify the dynamic analysis, the following assumption is introduced in [28]:

- Three-phase windings of the generator are balanced with Y connection, with 120◦ phase shift between each other in space. The induced magneto-motive force is distributed in a sinusoidal form along the air gap.
- The magnetic saturation of the stator and the rotor core is neglected.
- The iron loss of both the stator and the rotor core is neglected.
- The stator or rotor winding parasitic resistances do not change with the temperature and the frequency.

To simplify the study, all electrical variables on the rotor side are converted to the stator side. Positive reference direction for both the power and the current are selected to be the direction in which the power or the current flows into the stator or the rotor of the Doubly Fed Induction Generator (DFIG) in model of both dynamic voltage restorer and crowbar protection devices in Mat Lab/Simulink software depends in appendix's A.5 models .

3.4.1 ABC (abc) MODEL

With the conventions cited above, the DFIG is modeled as three static windings sitting on the stator (ABC), and three windings sitting on the rotor (abc) rotating with angular frequency ωr, as shown in Figure 3.2. If the initial angle between phase-a rotor winding and phase-A stator winding are zero, the angle θr between phase-a rotor winding and phase-A stator winding is described in [29]

$$\theta_r = \varpi_{rt} \tag{3.3}$$

In Figure above 3.2, vsa, vsb, vsc and vra, vsb, vsc are three-phase stator voltages and three-phase rotor voltages, respectively. isa, isb, isc and ira, irb, irc are three-phase stator currents and three-phase rotor currents, respectively. Stator equations are formulated as follows:

$$\begin{cases} V_{sa} = R_s I_{sa} + \frac{d}{dt}\psi_{sa} \\ V_{sb} = R_s I_{sb} + \frac{d}{dt}\psi_{sb} \\ V_{sc} = R_s I_{sc} + \frac{d}{dt}\psi_{sc} \end{cases} \tag{3.4}$$

Where R_s is the resistance of each winding, and ψ_{sa}, ψ_{sb}, ψ_{sc} are three-phase stator winding fluxes. Three equations in above can be expressed with matrix form:

$$V_s = R_s I_s + P\psi_s \tag{3.5}$$

Where stator voltage vector $V_s = [V_{sa}\ V_{sb}\ V_{sc}]^T$, stator current vector $i_s = [i_{sa}\ i_{sb}\ i_{sc}]^T$, stator flux vector $\psi_s = [\psi_{sa}\ \psi_{sb}\ \psi_{sc}]^T$, and

$$P = \frac{d}{dt} \tag{3.6}$$

Where stator winding mutual inductance matrix is expressed by.

$$L_{ss} = \begin{bmatrix} L_{ms} + L_{ls} & -\frac{1}{2}L_{ms} & -\frac{1}{2}L_{ms} \\ -\frac{1}{2}L_{ms} & L_{ms} + L_{ls} & -\frac{1}{2}L_{ms} \\ -\frac{1}{2}L_{ms} & -\frac{1}{2}L_{ms} & L_{ms} + L_{ls} \end{bmatrix} \tag{3.7}$$

Rotor winding mutual inductance matrix is expressed by

$$L_{rr} = \begin{bmatrix} L_{mr} + L_{lr} & -\frac{1}{2}L_{mr} & -\frac{1}{2}L_{mr} \\ -\frac{1}{2}L_{mr} & L_{mr} + L_{lr} & -\frac{1}{2}L_{mr} \\ -\frac{1}{2}L_{mr} & -\frac{1}{2}L_{mr} & L_{mr} + L_{lr} \end{bmatrix} \tag{3.8}$$

Stator and rotor winding mutual inductance matrix is described by

$$L_{ss} = L_{rr}^{T} = L_{ms} \begin{bmatrix} \cos\theta_r & \cos(\theta_r + 120^0) & \cos(\theta_r - 120^0) \\ \cos(\theta_r - 120^0) & \cos\theta_r & \cos(\theta_r + 120^0) \\ \cos(\theta_r + 120^0) & \cos(\theta_r - 120^0) & \cos\theta_r \end{bmatrix} \tag{3.9}$$

3.4.2 $\alpha\beta$ MODEL

For a three-phase power system, usually the three-phase variables xa, xb, and xc satisfy the relationship xa +xb +xc = 0. In this case, all the three-dimensional space vectors satisfying this condition are located on the subset in the three-dimensional space, which is actually a plane. Therefore,three-phas variables can be simply expressed as a complex vector X in the complex plane, which is called $\alpha\beta$ plane, with the following transformation as in [29]

$$\vec{X} = \frac{2}{3}\left(x_a + \alpha x_b + \alpha^2 x_c\right) = \frac{2}{3}\left[1\, \alpha\, \alpha^2\right] . \begin{bmatrix} x_a \\ x_b \\ x_c \end{bmatrix} \tag{3.10}$$

Where $\alpha = e^{j\frac{2\pi}{3}}$, and $\alpha^2 = e^{j\frac{4\pi}{3}}$. The complex plane is shown in Figure 3.3. Constant 2/3 of expression (3-10) is chosen to scale the complex vector to have the same amplitude as that of the three-phase variables.

Complex vector X is composed of the real part xα and the imaginary part xβ:

$$X^{\rightarrow} = X\alpha + jX\beta \tag{3.11}$$

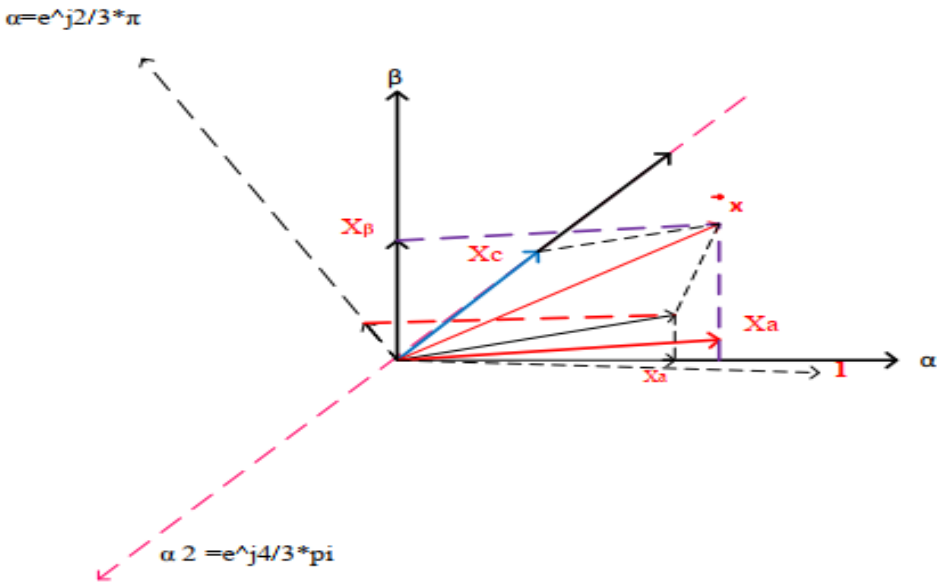

Figure 3.3: Vector representations in complex plane $\alpha\beta$

According to equations (3-12) and (3-13), the relationship between xa, xb, xc and xα, xβ are derived as in [29]:

$$\begin{cases} X_\alpha = \frac{2}{3}\left(X_a + X_b\cos\frac{2\pi}{3} + X_c\cos\frac{4\pi}{3}\right) \\ X_\beta = \frac{2}{3}\left(X_b\sin\frac{2\pi}{3} + X_c\sin\frac{4\pi}{3}\right) \end{cases} \tag{3.12}$$

Equation (3-14) can be written in the matrix form:

$$\begin{bmatrix} X_\alpha \\ X_\beta \end{bmatrix} = \frac{2}{3}\begin{bmatrix} 1 & \frac{-1}{2} & \frac{-1}{3} \\ 0 & \frac{\sqrt{3}}{2} & -\frac{\sqrt{3}}{2} \end{bmatrix} \cdot \begin{bmatrix} X_a \\ X_b \\ X_c \end{bmatrix} \tag{3.13}$$

The above transformation is called the Clarke transformation. The following matrix is called the Clarke transformation matrix:

$$T_C = \frac{2}{3}\begin{bmatrix} 1 & \frac{-1}{2} & \frac{-1}{3} \\ 0 & \frac{\sqrt{3}}{2} & -\frac{\sqrt{3}}{2} \end{bmatrix} \tag{3.14}$$

The inverse Clarke transformation can be derived as follows:

$$\begin{bmatrix} X_a \\ X_b \\ X_c \end{bmatrix} = \frac{2}{3}\begin{bmatrix} 1 & \frac{-1}{2} & \frac{-1}{3} \\ 0 & \frac{\sqrt{3}}{2} & -\frac{\sqrt{3}}{2} \end{bmatrix} . \begin{bmatrix} X_\alpha \\ X_\beta \end{bmatrix} \tag{3.15}$$

With regard to the DFIG, the stator voltage equations (3-3) can be changed into the complex vector equation form by using transform (3-12).

3.4.3 dq MODEL

If it is assumed that ωr is constant, these equations are linear. However, electrical variables of Doubly Fed Induction Generators (DFIG) such as the voltage, current, flux in $\alpha\beta$ reference frame are still AC components even at steady state modeling of system in Mat Lab/Simulink software. For the balanced three-phase system, if we observe its complex vectors in a certain rotating reference frame, it is possible to further simplify them as constant vectors with their axis components having DC values.

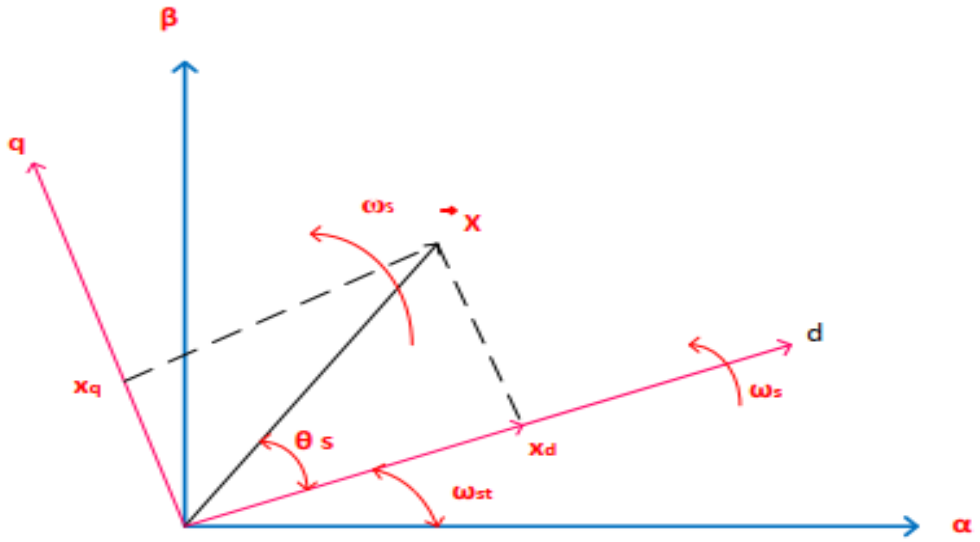

Figure 3.4: Relationship between the $\alpha\beta$ reference frame and the dq reference frame

As the analysis or control model for the DC system is much simpler than that of an AC system, it is natural to transform the three-phase system into the rotating reference frame, which is known as dq rotating reference frame.

As shown in Figure 3.4, the complex vector $\vec{X}$ of the three-phase system is usually rotating in $\alpha\beta$ reference frame. Now we introduce another reference frame: dq reference frame, which is rotating with angular frequency ωs. If the angular frequency is the same as the complex vector $\vec{X}$ rotating angular frequency, then the complex vector $\vec{X}$ becomes constant vector under the new dq reference frame. The relationship between $\alpha\beta$ reference frame and dq reference frame can be expressed as follows as in[29]:

$$\overrightarrow{X}_{dq} = e^{-j\omega st}\overrightarrow{X} \tag{3.16}$$

Where $\vec{X}$dq is the complex vector in the rotating dq reference frame, and $\vec{X}$dq = xd +jxq where xd is the d-axis component and xq is the q-axis component. Inverse transformation from dq reference frame to $\alpha\beta$ reference frame is

$$\overrightarrow{X} = e^{-j\omega st}\overrightarrow{X_{dq}} \tag{3.17}$$

Equation (3-18) can be written as

$$X_d + jX_q = (\cos \omega st - j \sin \omega st) \,.\, (X_\alpha + X_b) \tag{3.18}$$

The real and virtual components of $\vec{X}$dq in the dq reference frame can be expressed as

$$X_\alpha = X_\alpha \cos \omega s^t + X_\beta \sin \omega s^t \tag{3.19}$$

$$X_q = X_\beta \cos \omega s^t - X_\alpha \sin \omega s^t \tag{3.20}$$

The above two equations are often expressed in following matrix form which is known as rotating transformation from $\alpha\beta$ reference frame to rotating dq reference frame.

$$\begin{bmatrix} X_d \\ X_q \end{bmatrix} = \begin{bmatrix} \cos \omega_{st} & \sin \omega_{st} \\ -\sin \omega_{st} & \cos \omega_{st} \end{bmatrix} . \begin{bmatrix} X_\alpha \\ X_\beta \end{bmatrix} \tag{3.21}$$

3.5 Wind Farm Modeling

A very large wind power plant may contain hundreds of megawatt-size wind turbines. These turbines are interconnected by an intricate collector system. While the impact of individual turbines on the larger power system network is minimal, collectively, wind turbines can have a significant impact on the power systems during a severe disturbance such as a nearby fault. Since it is not practical to represent all individual wind turbines to conduct simulations, a simplified equivalent representation is required. Although it is very important to understand the dynamics of individual turbines, the collective behavior of the wind farm and the accuracy in modeling the collector systems are also very critical in assessing the wind farm characteristics.

As far as transient voltage stability study of a power system is concerned, it is usual practice to use reduced models of large wind farms that are implemented in detailed models of large power systems. In this case, the focus is on the collective impact of a large

wind farm on a large power system. This implies that a wind farm can be represented, for analysis, by a single machine equivalent of the wind turbines that constitute the farm with rescaled power capacity, power supply and reactive power exchanged between the wind farm and the entire transmission network at the connection point in [30].

This approach does not take into account the individual responses of many wind turbines and their possible mutual interaction. Among other aspects, the model of collector systems for wind power plants seeks to minimize losses and voltage drops within allowable constraints. This philosophy is generally applied regardless of the size of the wind farm, the types of the turbines, and reactive power compensation. Some wind farms are built with different types of wind turbines for different reasons. For example, recent unavailability of new turbines because wind turbine supply lags behind demand for wind turbines, the economic benefit of mixing wind turbine types within the same wind farm and repowering old windfarms with newer and bigger turbines.

In such cases analysis of wind farms must take into account the fact that each type of wind turbines in the wind farm should be represented by their respective single machine equivalents. An analytical approach can be used to derive the equivalent representation of a wind farm collector system. The methods used to develop an equivalence of a collector system in a large wind power plant are described in [31, 32].

3.5.1 General Assumptions

A modern utility-size wind turbine generates electrical power at a low voltage level (typically 690 V). Current utility-scale wind turbine ratings range from 1 MW to 5 MW per turbine. Each wind turbine is electrically attached to a pad- mounted transformer that steps up the voltage to a medium voltage level, typically 33 kV. The collector system is connected at the 33 kV levels, where the wind turbines are connected to each other in a string or "daisy chain" configuration as shown in Figure 3.5. Underground cables are most commonly used in the collector system. In the following derivation, the equivalent circuit is based on apparent power losses (i.e., real and reactive power losses). In the following two assumptions are made to derive the general equation for a circuit within a wind farm in [33].

1. The current injections from all the wind turbines have the same magnitude and angle and,

2. The reactive power generated by the line capacitive shunts is based on the assumption that the voltage is 1 p.u.

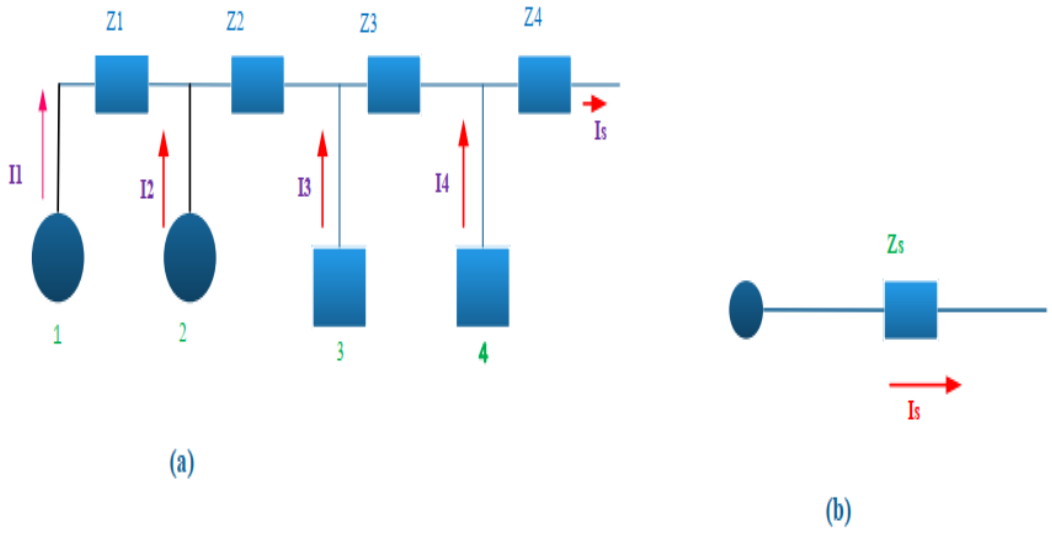

Figure 3.5: (a) Daisy-chain representation. (b) Equivalent circuit representation.

Let's first consider the voltage drops across the line impedances. Across Z1, the voltage drop can be written as:

$$\Delta V Z_1 = I_1 Z_1 = \left(\frac{S_1}{V}\right) Z_1 = \left(\frac{P_1}{V}\right) Z_1 \tag{3.22}$$

Note that I1 is substituted with S1/V where S1 is the rated apparent power of wind turbine 1. Based on the assumption that most wind turbines are compensated to have a very close to unity power factor, the apparent power S1 can be substituted by the rated power of wind turbine 1, P1. The rest of the equations, that can be used to describe the voltage drop across Z1 through Z4, can be written as:

$$\Delta V Z_2 = (I_1 + I_2) Z_2 = \left(\frac{P_1}{V} + \frac{P_2}{V}\right) Z_2 = (P_1 + P_2) \frac{Z_2}{V} \tag{3.23}$$

$$\Delta V Z_3 = (I_1 + I_2 + I_3) Z_3 = \left(\frac{P_1}{V} + \frac{P_2}{V} + \frac{P_3}{V}\right) Z_3 = (P_1 + P_2 + P_3) \frac{Z_3}{V} \tag{3.24}$$

$$\Delta V Z_4 = (I_1 + I_2 + I_3 + I_4)\, Z_4 = \left(\frac{P_1}{V} + \frac{P_2}{V} + \frac{P_3}{V} + \frac{P_4}{V}\right) Z_4 = (P_1 + P_2 + P_3 + P_4)\, \frac{Z_4}{V} \tag{3.25}$$

Next, let's define a new variable, PZi, as the total power flow in the line segment represented by Zi. The power loss in each line segment can be written as:

$$S_{loss} - Z_1 = \Delta V Z_1 I_1^* = \left(\frac{P_1}{V}\right)\left(\frac{P_1}{V}\right)^* Z_1 = P_1^2 \frac{Z_1}{V^2} = P Z_1^2 \frac{Z_1}{V^2} \tag{3.26}$$

$$S_{loss} - Z_2 = \Delta V Z_2 (I_1 + I_2)^* = (P_1 + P_2)^2 \frac{Z_2}{V^2} = P Z_2^2 \frac{Z_2}{V^2} \tag{3.27}$$

$$S_{loss} - Z_3 = \Delta V Z_3 (I_1 + I_2 + I_3)^* = (P_1 + P_2 + P_3)^2 \frac{Z_3}{V^2} = P Z_3^2 \frac{Z_3}{V^2} \tag{3.28}$$

$$S_{loss} - Z_4 = \Delta V Z_4 (I_1 + I_2 + I_3 + I_4)^* = (P_1 + P_2 + P_3 + P_4)^2 \frac{Z_4}{V^2} = P Z_4^2 \frac{Z_4}{V^2} \tag{3.29}$$

The total loss can be computed as:

$$S_{loss} = \frac{(P Z_1^2 Z_1 + P Z_2^2 Z_2 + P Z_3^2 Z_3 + P Z_4^2 Z_4)}{V^2} \tag{3.30}$$

From Figure 3.5 (b), the voltage drop across the equivalent impedance can computed as:

$$\begin{aligned} &\Delta V Z_s = I_s Z_s \\ &where\, I_s = \tfrac{P_1 + P_2 + P_3 + P_4}{V} \end{aligned} \tag{3.31}$$

The total loss in the equivalent impedance can be computed as:

$$S_{loss} - Z_s = \Delta V Z_s I_s^* = I_s I_s^* Z_s = \left(\frac{(P_1 + P_2 + P_3 + P_4)}{V^2}\right)\left(\frac{(P_1 + P_2 + P_3 + P_4)}{V^2}\right)^* Z_s = \frac{(P_1 + P_2 + P_3 +}{V^2} \tag{3.32}$$

By equating equation (3-32) and (3-33) the equivalent collector circuit impedance (ZS) can be calculated as:

$$\begin{aligned} S_{Loss} - Z_s &= S_{Loss} \\ PZ_4^2 Z_s &= \frac{PZ_1^2 Z_1 + PZ_2^2 Z_2 + PZ_3^2 Z_3 + PZ_4^2 Z_4}{V^2} \\ Z_s &= \frac{PZ_1^2 Z_1 + PZ_2^2 Z_2 + PZ_3^2 Z_3 + PZ_4^2 Z_4}{PZ_4^2} \end{aligned} \tag{3.33}$$

From equation (3-33) the general expression to calculate the equivalent collector circuit impedance for any number of turbines can be written as:

$$Z_s = \frac{\sum_{m=1}^{n} PZ_m^2 Z_m}{PZ_m^2} \tag{3.34}$$

For identical wind turbines of the same rated power (P) the above general expressions to calculate the equivalent collector circuit impedance reduce to:

For Connection at group level:

$$Z_s = \frac{\sum_{m=1}^{n} m^2 Z_m}{n^2} \tag{3.35}$$

Where: Zm = represents the individual series impedances

m = index

n = number of turbines in the group

For Connection at cluster level:

$$Z_s = \frac{\sum_{m=1}^{n} PZ_m^2 Z_m}{\left[\sum_{m=1}^{n} n_m\right]^2} \tag{3.36}$$

Where:

Zm = represents the equivalent impedance of the individual parallel groups.

nm = the number of turbine in each group.

3.5.2 Equivalence of Shunt Admittance

Consider an equivalent circuit for the transmission line shown in Figure 3.6. In a transmissions line, the line inductive reactance consumes the reactive power and the line capacitive reactance generates reactive power. The generated reactive power by the line capacitance is proportional to the square of the voltage across them.

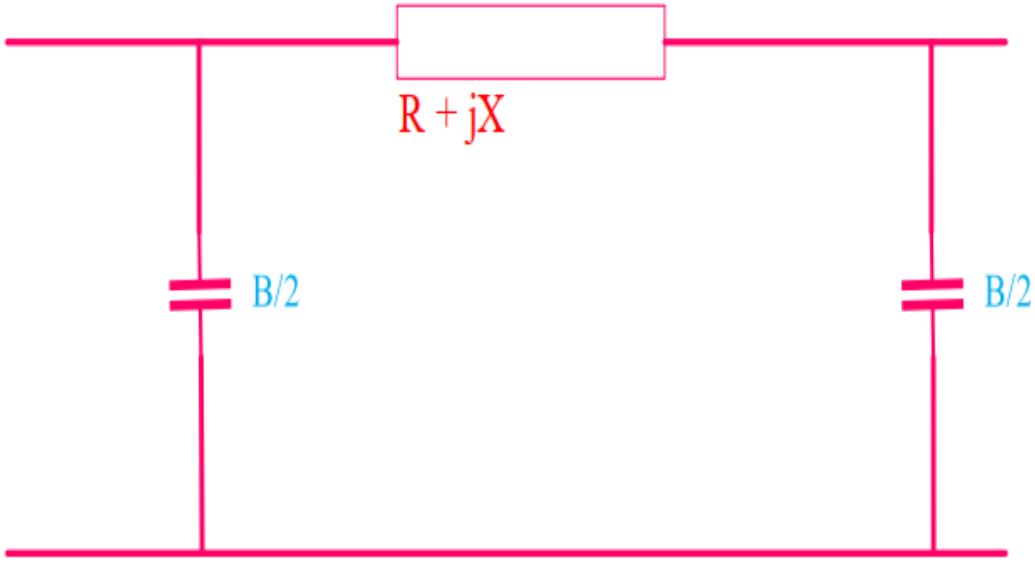

Figure 3.6: Representation of the line capacitance with in a wind power plant

Considering that the bus voltage is close to unity under normal conditions, the representation of the shunt can be considered as the sum of all the shunts in the wind farm networks. With this assumption is close to reality under normal conditions, the total shunt susceptance (B) within the wind farm can computed using equation (3-36).

$$B_{tot} = \sum_{m=1}^{n} B \tag{3.37}$$

3.5.3 Equivalence of Pad-Mounted Transformer (PMT)

The equivalence of the pad-mounted transformer at the turbine can be derived by using the illustration shown in Figure 3.7. In Figure 3.7 (a), the three-phase step up transformer connected to the wind turbines is shown. Figure 3.7 (b) shows the equivalent impedance to represent the entire group of the transformers (in this case, we have 4 turbines).

Let's consider a simple daisy chain of four turbines of different sizes connected to the same node. Originally, each turbine has its own transformer with different ratings and all turbines are producing at rated output. The transformer impedances for each turbine are ZT1, ZT2, ZT3, ZT4, respectively.

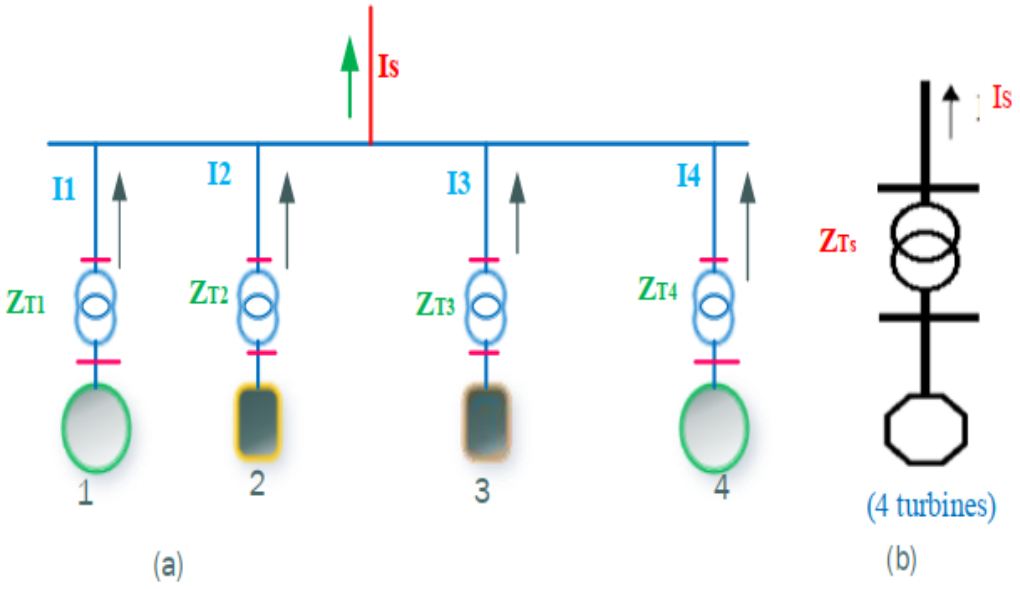

Figure 3.7: Parallel connections of four turbines of different sizes to find the equivalence of the pad-mounted transformers

Across ZT1, ZT2, ZT3, ZT4, the voltage drops can be written as:

$$\Delta V Z_{T1} = I_1 Z_{T1} = \frac{S_1}{V} Z_{T1} = \frac{P_1 Z_{TS}}{V} \tag{3.38}$$

$$\Delta V Z_{T2} = \frac{P_2 Z_{TS}}{V} \tag{3.39}$$

$$\Delta V Z_{T3} = \frac{P_3 Z_{TS}}{V} \tag{3.40}$$

$$\Delta V Z_{T4} = \frac{P_4 Z_{TS}}{V} \tag{3.41}$$

Losses in individual transformer would be:

$$S_{Loss} - Z_{T1} = \Delta Z_{T1} I^* = \frac{P_1 Z_{T1}}{V} * \left(\frac{P_1}{V}\right)^* = \left(\frac{P_1}{V}\right)\left(\frac{P_1}{V}\right)^* Z_{T1} = \frac{P_1^2 Z_{T1}}{V^2} \tag{3.42}$$

$$S_{Loss} - Z_{T2} = \frac{P_2^2 Z_{T2}}{V^2} \tag{3.43}$$

$$S_{Loss} - Z_{T3} = \frac{P_3^2 Z_{T3}}{V^2} \tag{3.44}$$

$$S_{Loss} - Z_{T4} = \frac{P_4^2 Z_{T4}}{V^2} \tag{3.45}$$

The total loss can be computed as:

$$S_{Loss} = \frac{P_1^2 Z_{T1}}{V^2} + \frac{P_2^2 Z_{T2}}{V^2} + \frac{P_3^2 Z_{T3}}{V^2} + \frac{P_4^2 Z_{T4}}{V^2} \tag{3.46}$$

From Figure 3.7 (b), the voltage drop across the equivalent transformer impedance can computed as:

$$\begin{aligned} &\Delta V Z_{Ts} = I_S Z_{TS} \\ &where \\ &I_S = \tfrac{P_1+P_2+P_3+P_4}{V} \\ &\Delta V Z_{Ts} = \left(\tfrac{P_1+P_2+P_3+P_4}{V}\right) Z_{TS} = \tfrac{P_{tot} Z_{Ts}}{V} \end{aligned} \tag{3.47}$$

The total loss in the equivalent transformer impedance can be computed as:

$$S_{Loss} - Z_{Ts} = \Delta V Z_{TS} I_S^* = \frac{P_{tot}^2 Z_{TS}}{V^2} \tag{3.48}$$

By equating equation (3-47) and (3-45) the equivalent transformer impedance (ZTS) can be calculated as:

$$\begin{aligned} &S_{Loss} - Z_{TS} = S_{Loss} \\ &\tfrac{P_{tot}^2 Z_{TS}}{V^2} = \tfrac{P_1^2 Z_{TS}}{V^2} + \tfrac{P_2^2 Z_{TS}}{V^2} + \tfrac{P_3^2 Z_{TS}}{V^2} + \tfrac{P_4^2 Z_{TS}}{V^2} \\ &Z_{TS} = \tfrac{P_1^2 Z_{T1} + P_2^2 Z_{T2} + P_3^2 Z_{T3} + P_4^2 Z_{T4}}{P_{tot}^2} \end{aligned} \tag{3.49}$$

From equation (3-48) the general expression to calculate the equivalent transformer impedance for any number of turbines can be written as:

$$Z_{TS} = \frac{\sum_{m=1}^{n} P_m^2 Z_{Tm}}{\left(\sum_{m}^{n} P_m\right)^2} \tag{3.50}$$

For identical wind turbines of the same rated power (P) and with identical pad-mounted transformers the above general expressions to calculate the equivalent transformer impedance would be reduced to:

$$Z_{TS} = \frac{Z_{Tm}}{n} \tag{3.51}$$

Where: n is the number of wind turbines aggregated in the group.

3.6 Modeling Equations of Dynamic Voltage Restorer Device

The system impedance ZTh - depends the fault level of the load bus. When the system voltage (VTh) the drops, the DVR injects a series voltage VDVR through the injection transformer so that the desired load voltage magnitude VL can be maintained in [34].

The series injected voltage of the DVR can be written as

$$V_{DVR} = V_L + Z_{TH} * I_L - V_{TH} \tag{3.52}$$

Where,

VDVR: The desired load voltage magnitude

ZTH: The load impedance.

IL: The load current

VTH : The system voltage during fault condition

The load current IL is given by,

$$I_L = \frac{P_{_L} + jQ_L}{V} \tag{3.53}$$

When VL is considered as a reference equation can be rewritten as,

$$V_{DVR<\alpha} = V_L < 0 + Z_{TH} < (\beta - \theta) - V_{TH} < \delta \tag{3.54}$$

α, β, δ are angles of VDVR, ZTH, and VTH respectively and θ is load power angles

$$\theta = \tan^{-1}\frac{Q_L}{P_L} \tag{3.55}$$

The complex power injection of the DVR can be written as,

$$S_{DVR} = V_{DVR} * I_L \tag{3.56}$$

It requires the injection of only reactive power and the DVR itself is capable of generating the reactive power.

3.7 Wind Farm Net Benefit Dynamic Voltage Restorer Device

The wind farm Dynamic Voltage Restorer (DVR) device is proposed to maximize the net economic benefits of wind farms and ensure that the power system is under an economical operating state based on the premise of ensuring the security and stability of the power system by combining the existing control measures and Dynamic voltage restorer device control strategies (e.g., minimize grid power loss). This thesis presents a Dynamic Voltage Restorer (DVR) device using the wind farm generation net benefit as the objective function, the installation number of WTGs and output power of the dispatched conventional generator units as the decision variables, and the system security operation requirements as model constraints to obtain the solution for dynamic voltage restorer device.

3.7.1 Wind power annual sale benefit

The renewable energy law in [35] prioritizes wind power sales and offers a favorable wind power electricity price to encourage renewable development. According to the policy, the total annual electricity sale benefit of wind energy generation is given by

$$B_{SB} = W_{price} * E_{year} \tag{3.57}$$

$$E_{year} = \sum_{k=1}^{K} (P(k)) * \sum_{t=1}^{T} (H_t * P_t) \tag{3.58}$$

$$P_t = \sum_{f=1}^{F} \sum_{g=1}^{WGT} N_{fg} * P_{fg}(\theta_{kt}(j)) \tag{3.59}$$

$$P_{fg} = \arg\max \{P_{fg}(h), h \in \Phi_{dis}\} \tag{3.60}$$

where B_{SB} is the annual electricity sale benefit; W_{price} is the electricity price for wind power sale; E_{year} is the annual wind energy generation amount; p(k) is the probability of the k^{th} scenario tree; Ht is the available generation time of the k^{th} time interval; N_{gf} is the installation number of the g^{th} WTG type in the f^{th} wind farm; g_{gf} is the optimal output of the g^{th} WTG type in the fth wind farm after processing the system optimization dispatch when the wind speed is set to θ_{kt}(j); θ_{kt}(j) is the corresponding wind speed scenario of the k^{th} scenario tree at the tth time interval; Φ_{dis} is the dispatch solution set corresponding to the θ_{kt}(j) scenario; and K, T, F and WGT represent the number of scenario tree branches, time intervals, wind farms, and WTG types, respectively.

3.7.2 Wind Farm Construction Capital Cost

WFCCC is the basic investment cost during the wind farm construction period. The loan mode is usually adopted as the mode of raising money because of the large amount of initial construction cost. To estimate the annual economic benefit of wind farms, WFCCC must be shared to the whole a proposed period equally so that an equivalent construction capital cost can be considered properly in the benefit calculation. This thesis utilizes the Capital Recovery Factor (CRF) in [36] to convert WFCCC to the Equivalent Annual Capital Cost (EACC). WFCCC using CRF, i.e., EACC, is calculated as follows:

$$C_{EA} = \sum_{f=1}^{F} \sum_{g=1}^{WGT} \frac{i(1+i)^n}{i(1+i)^n - 1} * C_{cg} * N_{fg} \tag{3.61}$$

Where C_{EA} is the C_{EA}, C_{cg} is the WFCCC of the g^{th} WTG type, i is the loan rate, and n is the loan term.

3.7.3 Maintenance and Operation Cost (M and O)

M and O is the cost spent for the promising routine operation of wind farms. It is composed of the equipment repair and maintenance expenses, insurance fees, labor fees, and necessary expenses. M and O is an important part of the wind farm economic benefit calculation considered during an annual time interval. The M and O of wind farms is given by

$$C_{MOA} = \sum_{f=1}^{F} \sum_{g=1}^{WGT} C_{MOg} * N_{fg} \tag{3.62}$$

Where C_{MOA} is the annual M and O of wind farms and C_{MOg} is the annual M and O of the g^{th} WTG type.

3.7.4 Wind Farm Net Generation Benefit

The wind farm net generation benefit consists of the wind power annual sale benefit, equivalent annual capital cost, and annual maintenance and operation cost. The goal of choosing the wind farm generation benefit as the objective function of the model in this thesis is to maximize the economic benefit brought by the wind energy generation. The objective function formula is expressed as follows:

$$Max(B_{PB}) = max(B_{SB} - C_{EA} - C_{MOA}) \tag{3.63}$$

3.7.5 Optimization Model Constraints

The constraints of the wind farm net benefit model are categorized into equation constraints and inequation constraints. The equation constraints are composed of the active power balance conditions and the reactive power balance conditions, which are expressed as follows:

$$\begin{cases} P_{Gi} + P_{Wi} - P_{Li} - U_i \sum\limits_{j \varepsilon i} U_i \left(G_{ij} \cos\theta_{ij} + B_{ij} \sin\theta_{ij}\right) = 0 \\ Q_{Gi} + Q_{Wi} - Q_{Li} - U_i \sum\limits_{j \varepsilon i} U_i \left(G_{ij} \sin\theta_{ij} - B_{ij} \cos\theta_{ij}\right) = 0 \end{cases} \tag{3.64}$$

where P_{Gi} ,Q_{Gi} represent the active output and the reactive output of the conventional generators at bus i, respectively; P_{Wi} , Q_{Wi} represent the active output and the reactive output of the wind turbine generators at bus i, respectively; P_{Li} , Q_{Li} represent the active load and the reactive load at bus i, respectively; U_i ,U_j represent the voltage amplitudes at bus i and bus j, respectively; θ_{ij} represents the difference in phase angles at bus i and bus j; and G_{ij} , B_{ij} represent conductance and susceptance located in row i and column j of system admittance matrix, respectively. The formula formats are assumed above to unify the description of each bus, and they do not indicate that conventional generators, wind turbine generators, and load are connected on each bus simultaneously. The formula format can be changed according to the actual situation. The inequation constraints are composed of the superior and inferior limit constraints of the decision variables and state variables. The active and reactive power output limits of conventional generators, active power output limits of wind turbine generators, branch power limits, bus voltage limits, and system spinning reserve constraints are considered the variable constraints in this thesis, and they are expressed as follows:

$$\begin{cases} P_{Gi}^{\min} \le P_{Gi} \le P_{Gi}^{\max} \\ Q_{Gi}^{\min} \le Q_{Gi} \le Q_{Gi}^{\max} \\ 0 \le P_{Wi} \le Q_{Gi}^{\max} \\ 0 \le S_L \le S_L^{\max} \\ U_i^{\min} \le U_i \le U_i^{\max} \\ \sum\limits_{i\varepsilon scg} (P_{Gi}^{\max} - P_{Gi}) > P_{res}^{up} \\ \sum\limits_{i\varepsilon scg} \left(P_{Gi} - P_{Gi}^{\min}\right) > P_{res}^{down} \end{cases} \tag{3.65}$$

Where S_L is the branch transmission power; P_{CG} is the conventional generators set; P_{res}^{up} and P_{res}^{down} are the system superior spinning reserve and the system inferior spinning reserve, respectively, which are usually considered as 5 % of the total system load. Superscript maximum and minimum represent the superior limits and inferior limits of the corresponding variables, respectively.

3.8 Proposed Method

In this thesis, the numbers of wind turbine is obtained and optimized for supplying the load. Find the best match distribution of data (PDF) in five clusters of Ashegoda wind farms. In equation (3.63) to maximization of the net economic benefit brought by wind energy generations is considered as objective function and the equations constraints are composed of the active power balance conditions and reactive power balance conditions. Uncertainty in power output of wind turbine is also considered.

Chapter 4

Methodology

The work of different authors haven been reviewed under the topic called literature review and it has been considered one of the methodology used to do this thesis. To achieve this work the methods have been used: namely data collection and case studies have been conducted. The data collected is available in Ashegoda wind farm include:-

1. Manufacturers data
2. From recorded data and equipment specifications and
3. By interviewing people working in Ashegoda wind farm

4.1 Description of the Study Area

The Ashegoda wind farm site is located in Tigray Regional State, approximately at 20 Km's south west of Mekele Town, 763 Km North from Addis Ababa capital city of Ethiopia. The wind farm has been finalized in 2013G.C in two phases. First phase consists of 30 GEV HP 1 MW WTG with squirrel cage induction generator connected to the grid through Full Scale Convertor Generator (FSCG). Second phase consists of 54 ALSTOM ECO 74 1.67 MW with Doubly Fed Induction Generator (DFIG). The total installed capacity of the wind farm is 120 MW.

The turbines are pitch- controlled, variable speed, two-blade (FCG) and three-blade (DFIG), upwind turbines. The generator terminal voltage is 690 V, and each wind turbine is attached to a pad-mounted transformer that steps up the generator terminal voltage (690 V) to a medium voltage level of 33 kV.

The Ashegoda wind farm is connected to Mekele and Alamata substations at the northern region of the national grid through 230kV/130MVA high voltage substation. The total 84 turbines are grouped into five clusters, with each cluster containing two or more groups of turbines ranging from 2 to 13 turbines in each group. Two outgoing 230kV overload lines link the WF to the grid at two locations, one at Mekele substation at a distance of 20km and another at Alamata substation, which is 120km away from the WF. The system includes 206 buses, 143 transmission lines, 109 transformers, 23 hydropower generating units and 10 groups of wind turbines, for which an aggregated model was used. The turbines within a group are connected to one another through underground cables, and 33 kV overhead lines connect each cluster to the central substation.

4.2 Data Analysis

The configuration and figurative summary of the topology of the Ashegoda wind farm is shown in Figure 4.1. 84 turbines are grouped into 5 clusters (CL_1 to CL_5), with each cluster containing turbines ranging from 2 to 13. The turbines within a cluster are connected through underground cables and 33 kV overhead lines connect each cluster to the central substation. The central substation itself has two 63 MVA (33/230 kV) transformers. Two outgoing 230 kV overhead lines link the wind farm to the grid at the Mekele substation. The collected data will help in calculating the improved fault ride through capability of doubly fed induction generator wind turbines by using a customized device. Finally, a conclusion and recommendation would be given based on the analysis result.

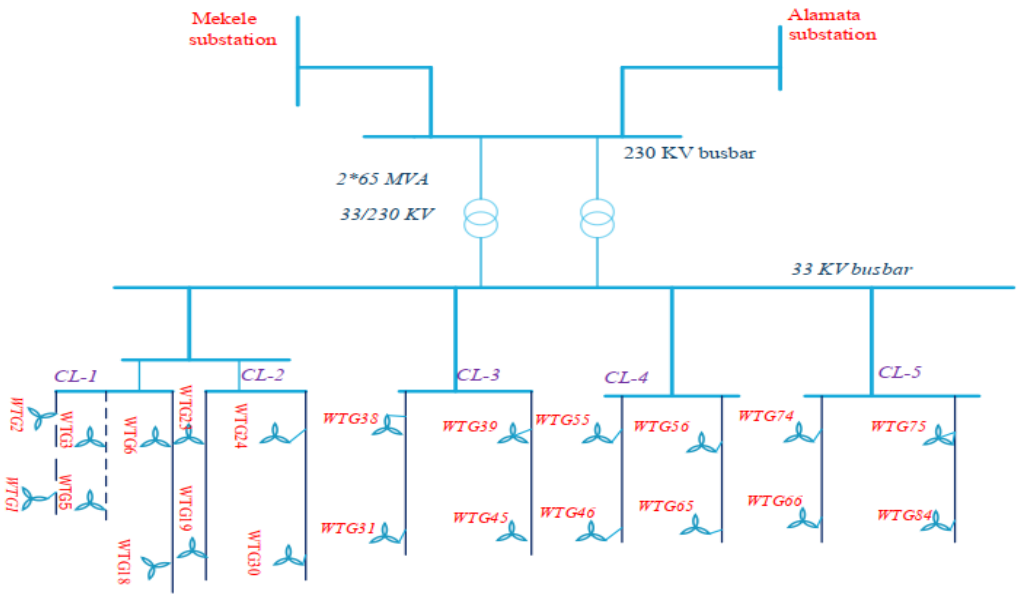

Figure 4.1: Configuration of Ashegoda wind farm

In this thesis work actual data collected from EEP are used to model the wind farm. The procedure followed to model the whole wind farm is demonstrated using cluster two and the final values for the rest of clusters have been summarized in tabular form in the appendixes A.2 and A.3.

Cable modeling

Underground cables are used to take power from each wind turbine. The maximum number of wind turbine connected in the group is not more than fourteen. The cable which carries power from each cluster to the central substation is between 21 MW and 30 MW. The required cable size and rating is determined based on a rating value of 15 MW and 30 MW using;

$$I = \frac{S}{\sqrt{3V_{LL}}} \tag{4.1}$$

Where the S is the apparent power and VLL is the line voltage of the cable (33 kV). The cable must be able to handle the maximum active and reactive power that can be generated in the wind farm. The maximum amount of active power generated by cluster wind turbines is 12 MW and the maximum reactive power for rated operation is 2.86 MVAR. For underground cable the current rating is calculated as;

$I_{underground-cable} = \frac{15}{\sqrt{3}*33} * 10^3 = 262.42A$

And for overhead

$I_{overhead-cable} = \frac{30}{\sqrt{3}*33} * 10^3 = 524.84A$

Appropriate cable size and cable parameter for the above current loading is taken from ABB in [37]. Underground cables with a conducting area of 50 mm^2, 95 mm^2, 150 mm^2, 240 mm^2 and overhead cable with a conducting are of 280 mm^2 is chosen. Underground cables are used to take power from each wind turbine and overhead lines are used to carry power from each cluster to the central high voltage substation. The resistance, capacitance and inductance of the cables and overhead lines used in this wind farm are shown in Table 4.1.

Table 4.1: Cables and overhead lines parameters

Installation Method	Cable type and rating	Capacitance (muF/ kM)	Inductance (mH/ kM)	Resistance ($omega$/kM)
Underground	1x50mm2Alu 18/30 kV	0.14	0.47	0.82195
	1x95mm2Alu 18/30 kV	0.17	0.42	0.41056
	1x150mm2Alu18/30kV	0.21	0.38	0.26462
	1x240mm2Alu18/30kV	0.27	0.35	0.16122
	1x240mm2Cu18/30 kV	0.23	0.37	0.09760
Overhead	ACSR 280mm2	0.001487	0.75	0.17267

From the parameters of the cables the collector system can be modeled as a π equivalent circuit in order to represent the collector in its impedances and admittances. The parameters are expressed in real unit to use it directly in Mat Lab/Simulink software for simulation analysis. The π equivalent values of the cables are summarized in Table 4.2.

Table 4.2: Summary of cables and overhead lines parameters

Installation Method	Cable type and rating	Xc(muF/kM)	Xl(mH/kM)	R(ω/kM)
Underground	1x50mm2Alu18/30kV	22747.95	0.1476	0.82195
	1x95mm2Alu18/30kV	18733.61	0.1319	0.41056
	1x150mm2Alu18/30kV	15165.3	0.1193	0.26462
	1x240mm2Alu18/30kV	11795.23	0.1099	0.16122
	1x240mm2Cu18/30 kV	13846.58	0.1162	0.09760
Overhead	ACSR 280mm2	2141704	0.2355	0.17267

4.3 Modeling of Cluster Two of Ashegoda Wind Farm

Cluster two has two groups each with five and seven wind turbines connected in parallel, see Figure 4.1. The distance between each wind turbine within the group and the cables used is given in appendix A.2 in table A.2. The modeling procedure is based on the

approach used in [38] and it is done in three steps to use model of dynamic voltage restorer device and crowbar protection device.

1. Equivalency of pad mounted transformers.
2. Equivalency of shunt admittances.
3. Equivalency of collector circuit impedance.

All steps are discussed in the following section step by step and results for other clusters summarized in appendix A.3.

4.3.1 Equivalency of Pad-Mounted Transformers [PMT]

The general expression to calculate the equivalent transformer impedance for any number of turbines in a group is given in equation (3.50). Since wind turbines have identical pad-mounted transformers, to determine their equivalent impedance first the impedance of a single pad- mounted transformer has to be determined based on the manufacturer data. The resistive and the reactive component of the pad mounted transformer impedance can be determined using equation (4.2) and (4.3) respectively.

$$R_{TS} = \frac{U_{Rr*}U_{rT}^2}{100 * S_{rT}}\Omega \tag{4.2}$$

$$X_{TS} = \frac{U_{Rr*}U_{rT}^2}{100 * S_{rT}}\Omega \tag{4.3}$$

Where: URr is rated resistive voltage drop (%)
UXr is rated reactive voltage drop (%)
UrT is transformer primary voltage (0.69 kV)
SrT is transformer apparent power (1.25 MVA)

The value of rated resistive voltage drop (URr = 1.25 %) is taken from the manufacturer data. Then, the value of reactive voltage drop (UXr) is calculated as follows.

$$U_{Xr} = \sqrt{U_{Kr}^2 - U_{Rr}^2} \tag{4.4}$$

Where UKr is the short circuit voltage of pad mounted transformer. The value of UKr is taken from the manufacturer data (equal to 6%), Substituting the values in equation(4.3).

$U_{Xr} = \sqrt{6^2 - 1.25^2} = 5.87\%$

Hence, the resistance component of pad mounted transformer impedance would be. $R_{Ts} = \frac{1.25*0.69^2}{100*1.25} = \frac{0.595125}{125} = 0.004761\Omega$

The reactance component of pad transformer impedance would be

$X_{Ts} = \frac{5.87*0.69^2}{100*1.25} = \frac{2.673198}{125} = 0.021385584\Omega$

$Z_{Tm} = R_{Ts} + jX_{TS} = 0.004761 + j0.021385584\Omega$

Now the equivalent transformer impedance for each group can be found using equation (3.49).

4.3.2 Equivalence of Group Four (2.A) Pad-Mounted Transformers

Group four has five pad mounted transformer as shown in Figure 4.2. figure 4.2 (a) shows each transformers and figure 4.2 (b) shows the equivalent representation of group-four pad mounted transformers.

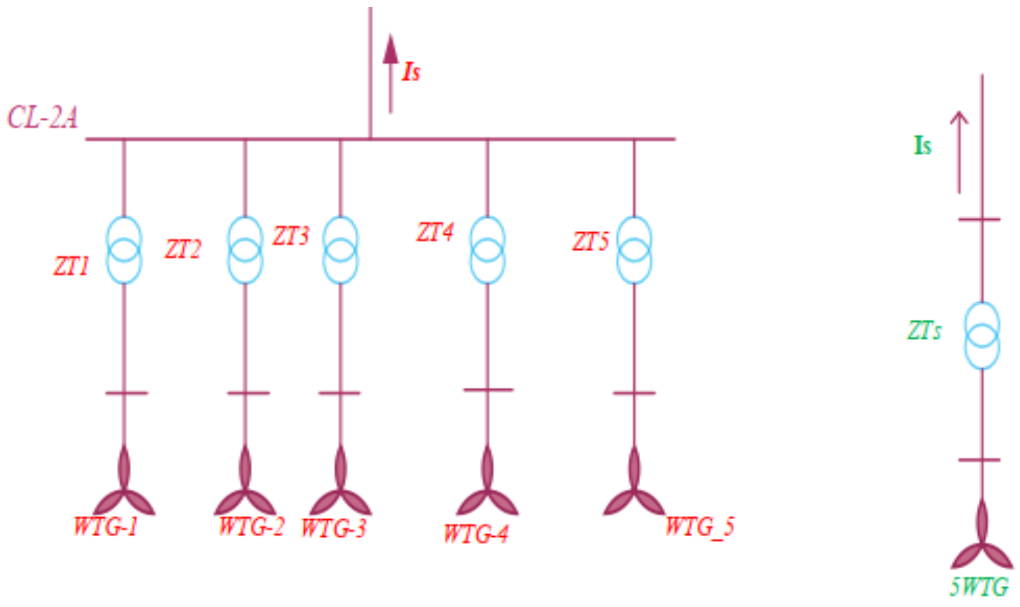

Figure 4.2: Full representation and (b) Equivalent representation of transformers

Substituting the value of ZTm and n=5 in equation (3.49),

$Z_{TS4} = \frac{0.004761+j0.021385584}{5} = 0.0009522 + j0.004277\Omega$

4.3.3 Equivalence of Group Five (2.B) Pad-Mounted Transformers

Similarly, for group five with seven pad mounted transformer, equivalent impedance would be;

$Z_{TS5} = \frac{0.004761+j0.021385584}{7} = 0.00068 + j0.003055\Omega$

The equivalent transformer impedance of cluster two can be calculated using equation (3.50) as:

$Z_{TS} = \frac{5^2*Z_{TS4}+7^2*Z_{TS5}}{(5+7)^2} = 0.0003967 + j0.00178\Omega$

4.3.4 Equivalency of Shunt Admittances

Equivalency of shunt admittances is calculated using equation (3.37).

I. Group four (2.A) shunt admittances

$B_{G4} = 45.37 + 12.57 + 10.24 + 10.24 + 10.24 = 88.66\mu s$

II. Group five (2.B) shunt admittances

$B_{G5} = 70.46 + 8.62 + 10.29 + 11.69 + 9.93 + 68.09 + 11.65 = 190.73\mu s$

4.3.5 Equivalency of Collector Circuit Impedance

The general expression to calculate the equivalence collector circuit impedance for any number of turbines in a group is given in equation (3.37). Since wind turbines are identical in each group to find the equivalence collector circuit impedance of group four and five, the equation (3.38) can be used.

I. Equivalency of Collector Impedance of Group Four (2.A)

In group four there are five wind turbines, the equation to calculate the equivalent collector impedance would be

$$Z_{CG4} = \frac{Z_1 + 2^2 Z_2 + 3^2 Z_3 + 4^2 Z_4 + 5^2 Z_5}{5^2} \tag{4.5}$$

Where Z1, Z2, Z3 and Z4 are the branch impedance between each wind turbines (WTG19-WTG20, WTG20-WTG21, WTG21-WTG22 and WTG22-WTG23 respectively) and Z5 are branch impedance between wind turbine 23 and end point CL2A as shown in appendix

A.2 in table A.2.

$Re\,[Z_{CG4}] = \frac{0.19+2^2*0.19+3^2*0.19+4^2*0.24+5^2*0.85}{5^2} = 1.11\Omega$

$\mathrm{Img}\,[Z_{CG4}] = \frac{0.03+2^2*0.03+3^2*0.03+4^2*0.04+5^2*0.15}{5^2} = 0.1924\Omega$

Hence, $Z_{CG4} = 1.11 + 0.1924\Omega$

II. Equivalency of collector impedance of group five (2.B)

In group five there are seven wind turbines, the equation to calculate the equivalent collector impedance would be

$$Z_{CG5} = \frac{\mathrm{Z}_1 + 2^2\mathrm{Z}_2 + 3^2\mathrm{Z}_3 + 4^2\mathrm{Z}_4 + 5^2 z_5 + 6^2 z_6 + 7^2 z_7}{7^2} \tag{4.6}$$

Where Z1, Z2, Z3, Z4, Z5 and Z6 are the branch impedance between each wind turbines (WTG30-WTG29, WTG29-WTG28, WTG28-WTG27, WTG27-WTG26, WTG26-WTG25 and WTG25-WTG24 respectively) and Z7 are branch impedance between wind turbine 24 and end point CL2B as shown in appendix A.2 in table A.2.

$\mathrm{Re}[Z_{CG5}] = \frac{0.22+1.27*2^2+0.19*3^2+0.22*4^2+0.19*5^2+0.16*6^2+0.54*7^2}{7^2} = 0.9696\Omega$

$\mathrm{Img}[Z_{CG5}] = \frac{0.04+0.23*2^2+0.03*3^2+0.04*4^2+0.04*5^2+0.03*6^2+0.17*7^2}{7^2} = 0.2506\Omega$

Hence, Z_{CG5} given as

$Z_{CG5} = 0.9696 + j0.2506\Omega$

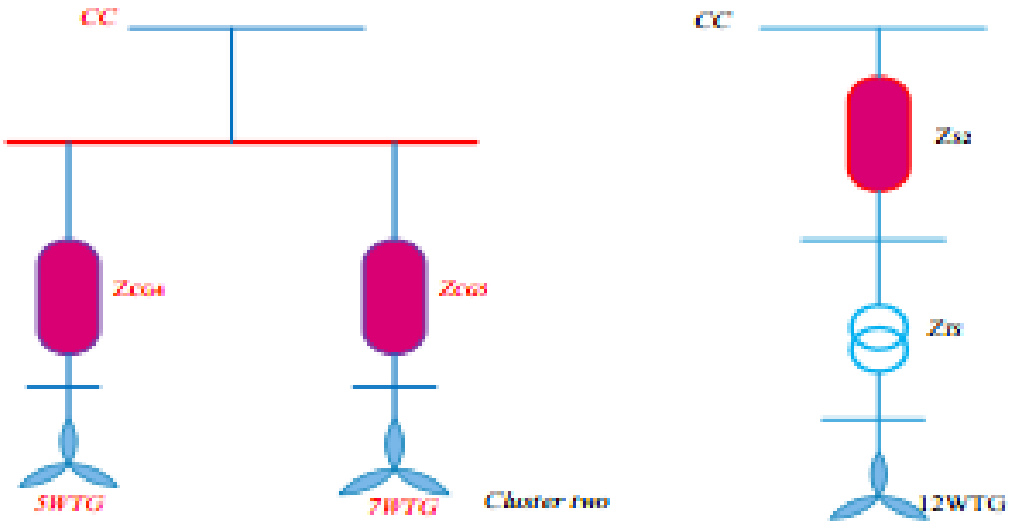

Figure 4.3: Reduced collector circuit impedance of cluster two collectors

By referring equation (3.39), collector circuit impedances of group four and five shown

in figure 4.3 can be reduced to single equivalence collector impedance. Hence,

$$Z_{s2} = \frac{\sum_{m=1}^{n} n_m^2 Z_m}{\left[\sum_{m=1}^{n} n_m\right]^2} \tag{4.7}$$

Where: Zm represents the equivalent impedance of the individual parallel groups. nm the number of turbine in each group.

Substituting the values in equation (4.6) Z_{S2} would be

$\mathrm{Re}[Z_{S2}] = \frac{1.11*5^2+0.9696*7^2}{(5+7)^2} = 0.5226\Omega$

$Img[Z_{S2}] = \frac{0.1924*5^2+0.2506*7^2}{(5+7)^2} = 0.1187\Omega$

$Z_{s2} = 0.5226 + j0.1187\Omega$

Hence, the final equivalence impedance of cluster two collector circuit is given by Z_{S2} and the pad mounted transformer equivalence impedance is given by Z_{ST}. Combining these two impedances and rescaling the output of a single generator (1 MW) by the number of wind turbine in cluster two (N=12), we can represent the cluster using single turbine representation shown in figure 4.4.

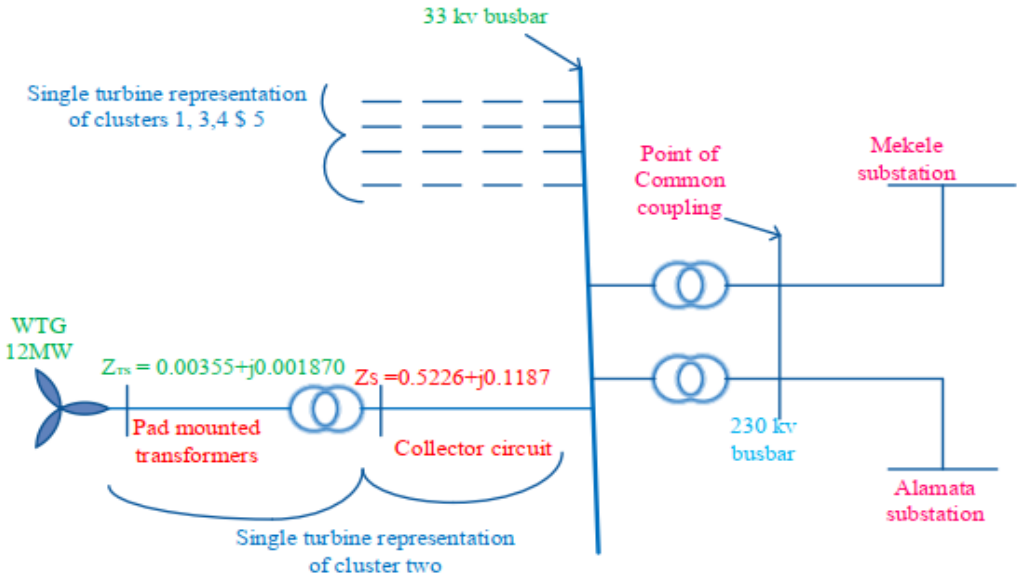

Figure 4.4: Single turbine representation of cluster two

In the wind farm considered as a case study there are two different variable-speed wind turbine generator types. For the first phase of the proposed (cluster one and two)

squirrel cage induction generators with full scale convertor are used and for the second phase (cluster three to five) double fed induction generators are used. In this case, it would be appropriate, in terms of the accuracy of analysis, to represent wind turbine generators by their respective single turbine equivalents for modeling of the wind farm for fault ride through capability studies.

The first phase of Ashegoda Wind Farm (AWF) (cluster one and two) would be represented by single equivalent FCG with its rating scaled up to 30MW and the second phase (cluster three to five) would be represented by single equivalent DFIG with its rating scaled up to 90MW. Figure 4.5 shows the single turbine representation of Phase I and II of AWF. The summary of single turbine representation of AWF phase I and phase II is provided in appendix in A.3 in table A.8 and table A.9. In this thesis the dynamic built-in models of FCG and DFIG in Visio software.

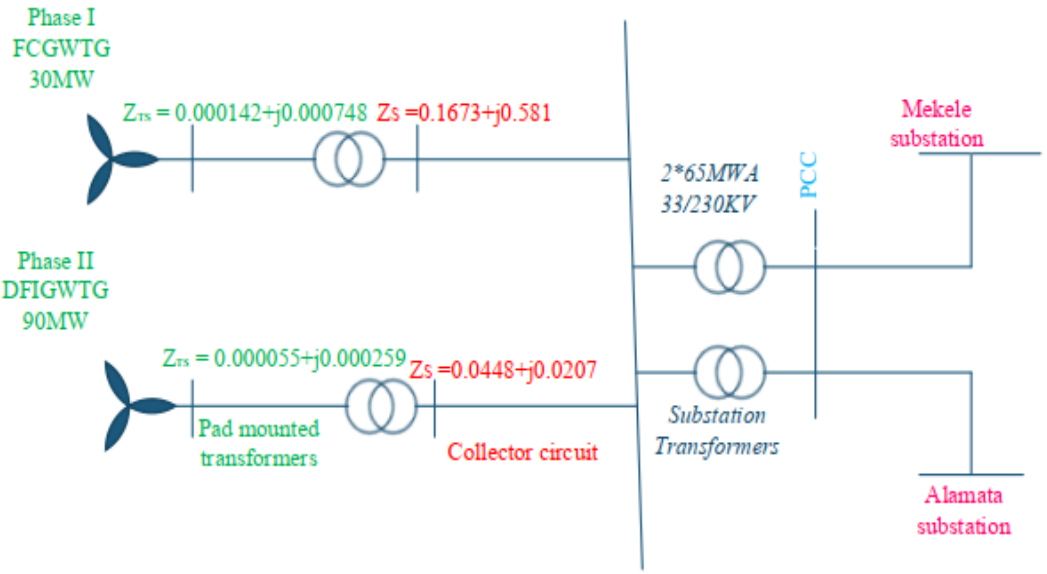

Figure 4.5: Single turbine representation of Phase I and II of AWF.

4.4 Control Techniques of Dynamic Voltage restorer

There are several techniques to implement and control methods of the Dynamic Voltage Restorer (DVR) device for power quality enhancements. The control of DVR is very important factor. Control methods for a Dynamic Voltage Restorer (DVR) device involve the detection of any disturbance in voltage by using the suitable algorithms. Proportional integral controller is used to minimize the error and to keep the voltage drop in to model

of dynamic voltage restorer and crowbar protection device in Mat Lab/Simulink software model in the system. All steps are discussed in the following section step by step and result Mat Lab/Simulink model software in appendix's A.5.

4.4.1 Proportional-Integral Controller technique

The main aim of the PI controller is to keep the constant voltage at load during any unwanted disturbances that occur in the system. The dynamic voltage restorer device and crowbar protection device in the simulation results of modeling in Mat Lab/Simulink software in the system. Comparing load voltage with reference voltage is considered as a controlling method here. First, all three-phase voltages are converted in p.u values then converted into dq with help of park transformation.

After that compare the d- voltage value with 1 and q- voltage value with 0 because as per IEEE stands rated voltage p.u d-component must be as well as q component must be 0. After comparing the original value with the reference value the difference is given to the PI controller for enhances.

The given signal by PI controller is converted into (abc) components by using clerk transformation because for generate switching signals to invert this signal is basic. Fig 4.6 shows the conventional PI controller to minimize unwanted disturbances of in the system. The major role of PI controller is to find voltage sags/swells, torque, active and reactive power in the system constant while voltage disturbances event modeling in the system appendix's A.5 models.

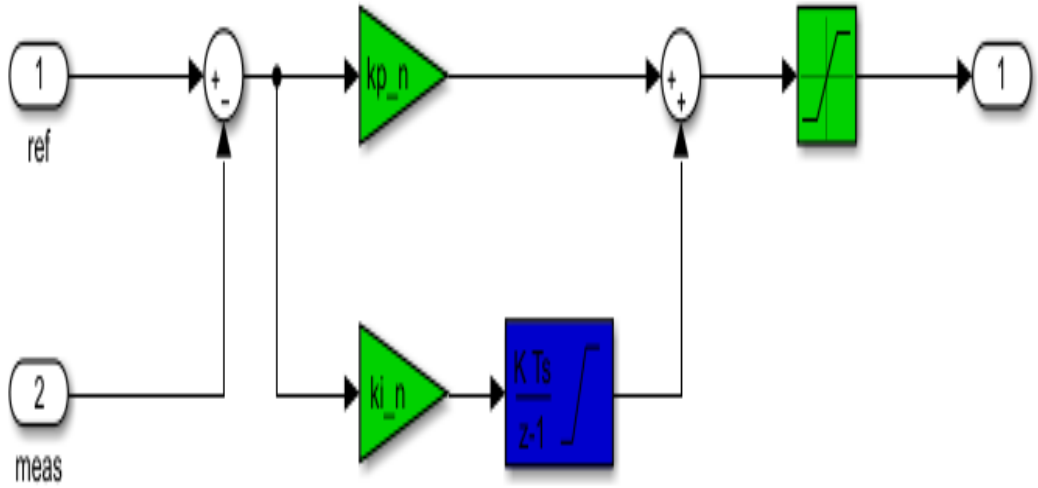

Figure 4.6: Proportional integral controllers

The currents and voltages are related by a first order transfer function. Since the slip value is weak, the will set up a control loop on each power with an independent regulator PI while compensating the disturbance terms in figure 4.6.

The Proportional Integral (PI) controller is still the most commonly used for controlling the Doubly Fed Induction Generators (DFIG), as well as in many industrial control systems. It is easy and quick to implement while providing acceptable performance. Regulators each axis role is to eliminate the gap between the active and reactive power references and the measured active and reactive power in [39].

Rotor Side Convertor in Power Control Mode

After the stator windings of the DFIG are connected to the grid, the DFIG starts to generate power to the grid. The DFIG is controlled through the RSC to generate active or reactive power according to the power command from the wind turbine central controller. The power command comes from the wind turbine central controller to realize Maximum Power Point Tracking (MPPT) or the requirements of the transmission system operators, etc. The grid synchronization for the RSC in power control is also needed. Under stator voltage orientation control, d-axis of dq reference frame is selected to be in the same direction as the grid voltage vector $\vec{V}$s, and the dq reference frame rotating angular speed is the same as the synchronous speed ωs in [40, 41].

The rotor voltages vrd and vrq are output voltages of the RSC. The stator voltages

V_{sd} and V_{sq} are regarded as the grid disturbance to the system. The stator three-phase voltage $\vec{V}$sabc, stator three-phase current $\vec{i}$sabc, and rotor three-phase current $\vec{i}$rabc are sampled and transformed into dq reference frame. The active power and reactive power is controlled by the outer power loops. For the active power, open-loop control is used, while closed-loop control with a PI regulator is used for the reactive power. The rotor d-axis current reference i_{rd}^{ref} is estimated from the active power command, while the rotor q-axis current reference i_{rq}^{ref} is generated by the outer reactive power control PI regulator.

There are two similar current loops, that is, d-axis rotor current-control loop and q-axis rotor current-control loop. The outputs of d-axis rotor current regulator and q-axis rotor current regulator are rotor voltage references V_{mrd} and V_{mrq}. The rotor voltage references are used to generate PWM signals for the converter. All steps are discussed in the following section step by step and result Mat lab/Simulink model software in appendix's A.5.

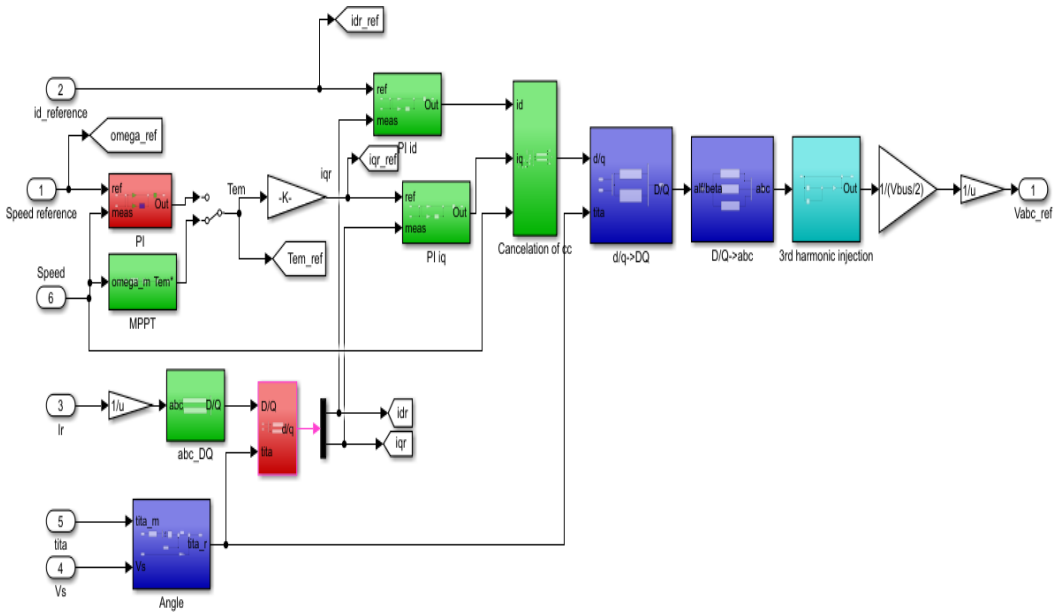

Figure 4.7: Diagram of control of rotor side the double fed induction generator inner part of system with DVR

Among the different available wind turbines of variable speed, Doubly Fed Induction Generator (DFIG) is the commonly used wind turbine in growing wind turbines. DFIG is usually used to fulfill standard grid requirements like power quality improvement, stability of the grid, grid synchronization, power control and fault ride through in grid tied wind energy system. The modeling of doubly fed induction generator in the inner part of with

and without devices in the systems. The all steps are DFIG parameters to models of the in the system discussed of Appedex's A.4 in table A.10.

4.4.2 PSO and GA Based Optimization Techniques

Two techniques have been proposed which are a particle swarm optimization and a genetic algorithm techniques are the best cost function optimization of the system.

4.4.2.1 Particle Swarm Optimization Algorithm Technique

particle swarm optimization is a computational opitimization technique developed by Kennedy and Eberhard in 1995. It uses a simple mechanism that mimics swarm behavior in birds flocking and fish schooling to guide the particles to search for global optimal solutions. The particles are initialized by a randomized position at the beginning of the search process, and then after every iteration, the position and velocity of each particle is changed in such a way that it moves towards the desired p_{best} and g_{best} location. The efficiency of local search and convergence to the global optimum solution are obtained by weighting the acceleration coefficients with random terms. Bothp_{best} and g_{best} locations generate separate random numbers for acceleration. PSO is proved to be a very efficient optimization algorithm by searching an entire high-dimensional problem spaces in [42, 43].

The PSO became a very popular evolutionary algorithm and successfully applied for a wide range of continuous optimization functions. The algorithm exploits the solution space by improving the trajectories as moving particles in multidimensional solution space. Population of PSO consists of personal positions called particles; denoted $\overrightarrow{X_1}$. Each particle has velocities $\overrightarrow{V_1}$ and a cost function evaluated by using the particle's position.

Positions and velocities are adjusted and cost function evaluated as the particle moves at each time step (Min f(x), xn = [x1, x2, x3.., xn]). Where n represents the number of decision variables.$Xn\varepsilon\,[L_{B,}U_B]$, n = 1, 2... n. L_B and U_B are the lower and upper bounds for the variable xn respectively. When the particle moves better position than any found formerly, personal best positions explored so far are stored in $\overrightarrow{P_1}$. The difference between personal best position and particle current position is added to velocity. Thus

velocities are used to move particles better coordinates.

$$V_{ij}(t+1) = wV_{ij}(t) + C_1 r_{1j}(t)(p_{ij}(t) - X_{ij}(t)) + C_2 r_{2j}(t)(g_j(t) - X_{ij}(t)) \tag{4.8}$$

Velocity consists of inertia term, cognitive component and social component as stated equation (4.8). Where w represents the inertia weight, r1j and r2j are uniformly distributed random numbers between the range of 0 and 1. C1 and c2 are constants, called cognitive and social scaling parameters; Vij the velocity of the particle, p_{ij} the personal best fitness value of the particle and g_j represents the best position and the global best in the whole population.

Using the PSO, the velocity can be represented under Eq. (4.10) in the PSO algorithm. Using Eq. (4.9), a certain velocity can be calculated as the position of individuals gradually moves closer to p_{best} and g_{best}. The current position can be modified by:

$$V_{(i,d)}^{(j+1)} = K * [V_{(i,d)}^{j} + C_1 * rand(0,1) * (Pbest_{(i,d)}^{j}) - X_{(i,d)}^{j} + C_2 * rand(0,1) * (Gbest^{i} - X_{(i,d)}^{j})] \tag{4.9}$$

$$X_{(i,d)}^{(j+1)} = X_{(i,d)}^{j} + V_{(i,d)}^{j} \tag{4.10}$$

$Where$

$K = \frac{2}{\left|2-c-\sqrt{c^2-4c}\right|}, c = c_1 + c_2 > 4$

C1, c2 is the acceleration constant, in this thesis, c1=c2= 4.05

Each particle represents a position and a potential solution of the search space.

Implementation of PSO: PSO is an evolutionary algorithm which requires the generation of random numbers. The performance of PSO algorithm is affected by the quantity and the quality of the numbers generated. The initial iteration is performed over the entire search space. The basic implementation of PSO is shown in the figure 4.8.

Table 4.3: The particle swarm optimization parameters used for this study

Indices	Value
Number of particles (d)	80
C1,c2	4.05
Var max,Varmin	10,-10
Number of iterations	100
nVar	5

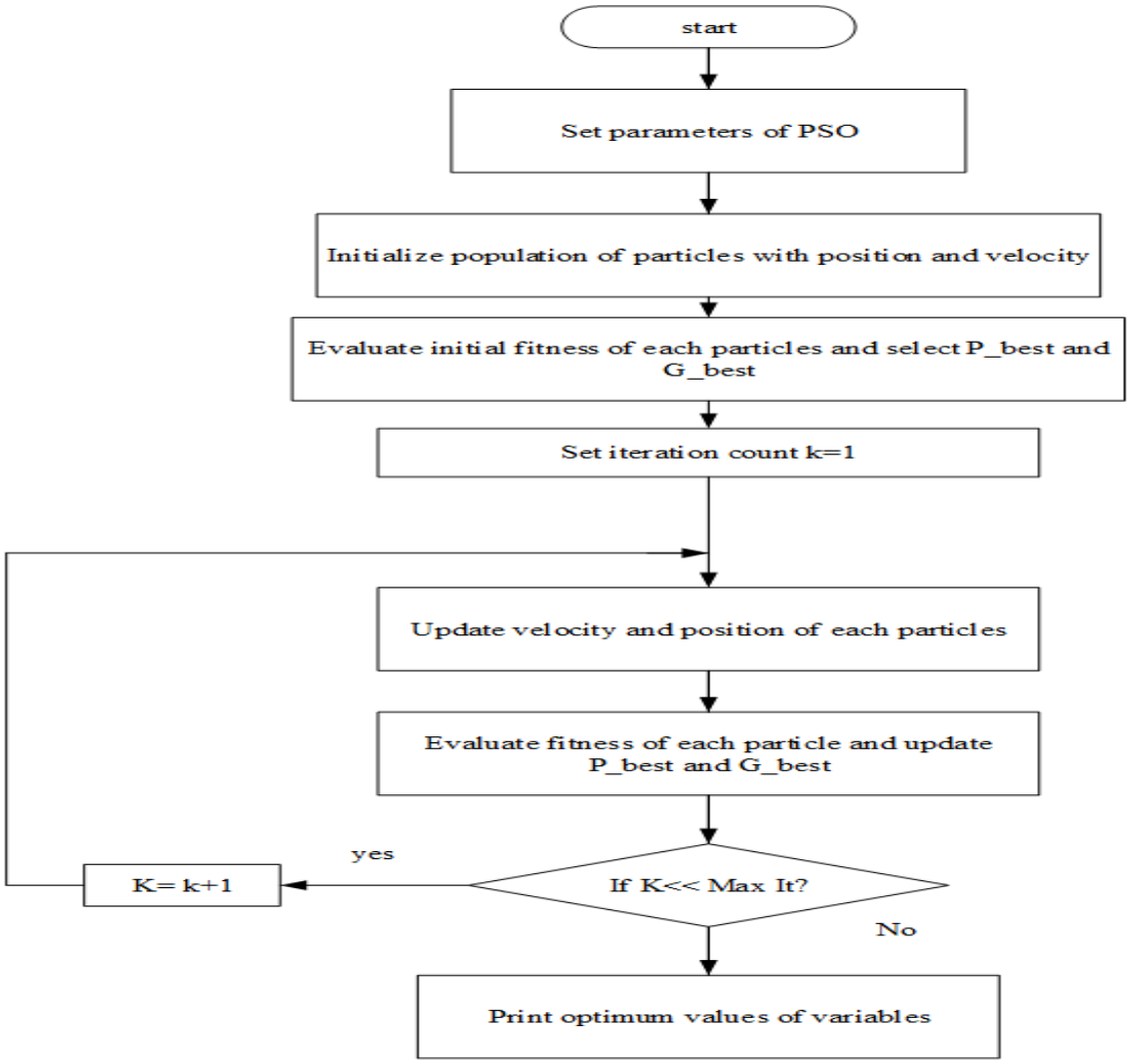

Figure 4.8: Flowchart basic implementation of particle swarm optimization algorithm

4.4.2.2 Genetic Algorithm Control Techniques

Genetic Algorithm (GA) is an important class of evolutionary algorithm. In 1975, the genetic algorithm was first of all used by Prof. John Holland (Holland, 1975) in[44]. GA usually provides approximate solutions to the various problems. GA uses various biological techniques such as inheritance, selection, crossover or recombination, mutation and reproduction. The various steps involved in this algorithm are:

1. Define an initial population randomly or heuristically.

2. Calculate the fitness value for every member inside the population.

3. Assign the selection probability for every member in such a way that it is proportional to its fitness value.

4. Formulate the next generation from the current generation by selecting the desired individuals to produce off springs.

5. Repeat the steps until suitable solution is found.

6. GA defines a collection of particles known as population and each individual particle is called as chromosome.

These chromosomes are then evaluated using the cost function also known as the fitness function. The cost function is usually the objective function of the given problem. Some of the processes associated with GA are:

a) Selection – this process is generally used to choose the chromosome which will go on to reproduce based on the fitness criterion.

b) Reproduction – this step is used for the formation of next generation from the current one.

c) Crossover – this process is used to exchange genetic material between the chromosomes. Single or multipoint crossover can be used.

d) Mutation – this process leads to the change in chromosomes for a single individual. Mutation prevents the algorithm from getting stuck at a particular point.

e) Stopping criteria – this is the final step in GA. The iteration stops when it reaches a desired solution or it achieves the maximum number of cycles.

Implementation Algorithm: GA results in the formation of fittest members after every iteration by using a predefined fitness function. Figure 4.9 ahead shows the basic flow chart of the Genetic Algorithm.

Table 4.4: The particle swarm optimization parameters used for this study

Induces	Value
Numbers of particles (d)	80
VarMax, VarMin	10,-10
Numbers of iteration	100
C1,c2	2
Crossover	0.8
Mutation	0.03
nVar	5

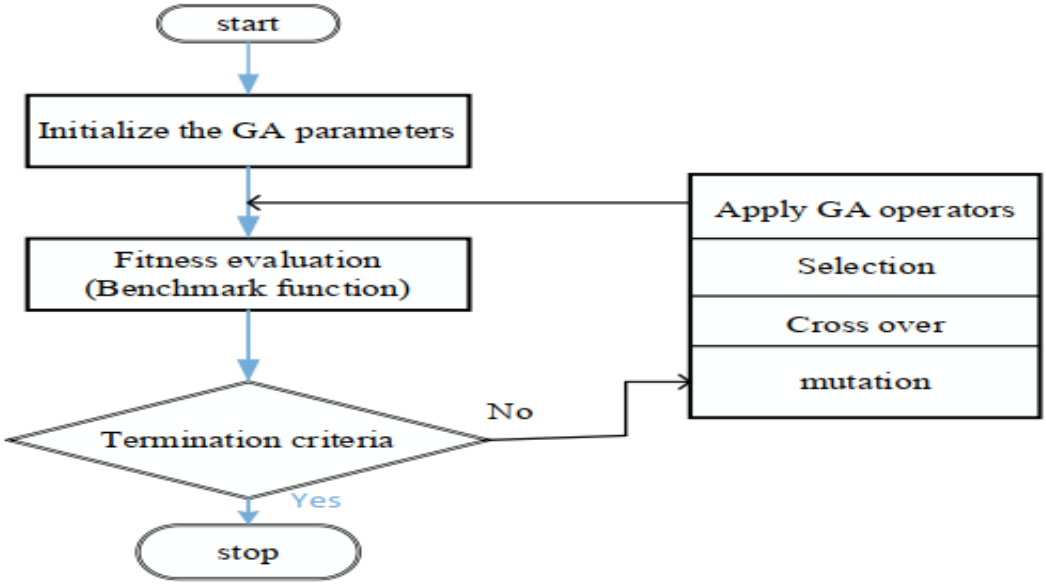

Figure 4.9: Flowchart basic implementation of GA algorithm

4.5 Economic Analysis of Ashegoda wind farm

Power supply authorities apply a tariff system which imposes penalties on the drawing of energy with a monthly average power factor lower than 0.9. The contracts applied are different from country to country and can vary also according to the typology of costumer. To protect a large sensitive load from voltage disturbances a dynamic voltage restorer (DVR) device with appropriate rating can be installed at load bus, however in an industrial state which various sensitive loads are available; it is not economically acceptable to install a Dynamic Voltage Restorer (DVR) device for each load. In this optimization problem the following objective functions to be considered in [45].

Maximizing the Cost Expenditure of DVR

According to the standard for sensitive loads the voltage limits should be within 80-90%. The total energy loss due to the fault was happened in 2017 G.C in Ashegoda wind farm only per years would be 15,544.75KW. To model of a Dynamic Voltage Restorer (DVR) device in Ashegoda wind farm used in rating generator 80MVA. In technical point of view this cost is proportional to the rating of DVR which is about 200-300$/KVA.

Table 4.5: Loss of load in 2017 G.C.

SL.No	Name of feeder/ unit	Date	Loss of load/generation (KW)
1	All 84 wind turbines	20/02/2017	741.876
2	All 84 wind turbines	30/03/2017	9,543
3	All 84 wind turbines	25/04/2017	5,259.87
Total loss			15,554.75

Yearly Cost of Energy Lost

Total energy loss due to the fault was happened in Ashegoda wind farm system only year would be 15,544.7478 KW =15,544.7478KW*8760hr =136,172,990.7KW.h. =136,172,990.738KW.h = 8,170,379.4$.

Also the model of the DVR in the system are rating of 80MVA = 80,000KVA*300$/KVA. = 24,000,000$

Saving = model of DVR – total energy loss = 24,000,000$- 8,170,379.4$ = 15,829,620.6$/year The Ashegoda wind farm would saving about 15,829,620.6$/year.

The total cost of dynamic voltage restorer device to model in Ashegoda wind farm rating 80MVA is about 24,000,000$ as in [43]. The payback period in year using equation would be:-

Payback period = $\frac{24{,}000{,}000}{8{,}170{,}379.4}$ = 2 years and 11mounths.

Chapter 5

Results and Discussions

5.1 System under Study

The northern region of Ethiopia national grid where Ashegoda Wind Farm (AWF) is connected has been considered as a system under study to evaluate the improvement facilitated by the introduction of Dynamic Voltage Restorer (DVR) device in to the system and to verify the application of DVR to improve the Fault Ride Through (FRT) capability of the DFIG based wind farm and helps to maintain the continuous connection of wind turbines to the grid during certain severe grid side voltage dips.

System modeling and simulation are performed in Mat Lab/Simulink software version 9.4. The system under study which represents the Northern region of the Ethiopian national grid which includes Tekeze hydro power plant (300MW installed capacity) and Ashegoda wind farm (120 MW installed capacity) and it is connected to the rest of Ethiopian interconnected system at Alamata substation through an External Grid of maximum short circuit capacity 1094 MVA. The test system has a total load of 139.21 MW and 73.64 Mvar connected at different load buses.

The 120 MW Ashegoda wind farm, at rated operation, has been represented by single machine equivalents of the two wind turbines types (DFIG and FCG), operating in voltage control mode, which are connected to a common bus called Point of Common Coupling (PCC) through which they are connected to the rest of the system via 230/33KV high voltage substation.

One of the objectives of this thesis is to evaluate the dynamic voltage restorer and

crowbar protection devices needs of the wind farm to meet the FRT requirements and to restorer the system to its initial state after the fault has been cleared. The DVR and Crowbar protection device capacity required restoring the system a three phase short circuit fault at PCC and to meet the FRT requirement of the wind farm is found to be ±80 MVA. The proposed DVR and crowbar protection, the dynamic voltage supporter, is connected at the PCC via a coupling transformer (15/33 kV).

Tekeze hydro power plant (Tekeze-PP) constitutes an aggregation of four generation units, with synchronous generators model type GENSAL (Salient Pole Generator Model), each equipped with EXST1(field excitation systems) and HYGOV governor system.

Data and dynamic parameters of the test system components used to model the test system are taken from the Ethiopian power system expansion master plan study final report in[46]. Scaled values and ratings of single machine equivalent of wind turbines and the synchronous generators are presented in appendix A.5. The detail of each type of wind turbine is available online at the manufactures' websites.

The test system is studied to evaluate the dynamic performance of the power system without and with the dynamic voltage support from DVR and Crowbar protection under different fault conditions such as three phase short circuit faults and sudden temporary step load change in the system. Such three phase short-circuit faults are balanced symmetrical events which are characterized by sudden and significant terminal voltage change. The balanced symmetrical events are often used as the worst-case scenarios in stability studies.

5.2 Simulation Results and Discussion

Particle swarm optimization is to make the existing system to most important Particle swarm optimization algorithm is used. Making PSO wind turbine generation more advantageous. The increases in the investment cost make the generation net economic benefits of each bus set decrease compared with that before the cost increases.

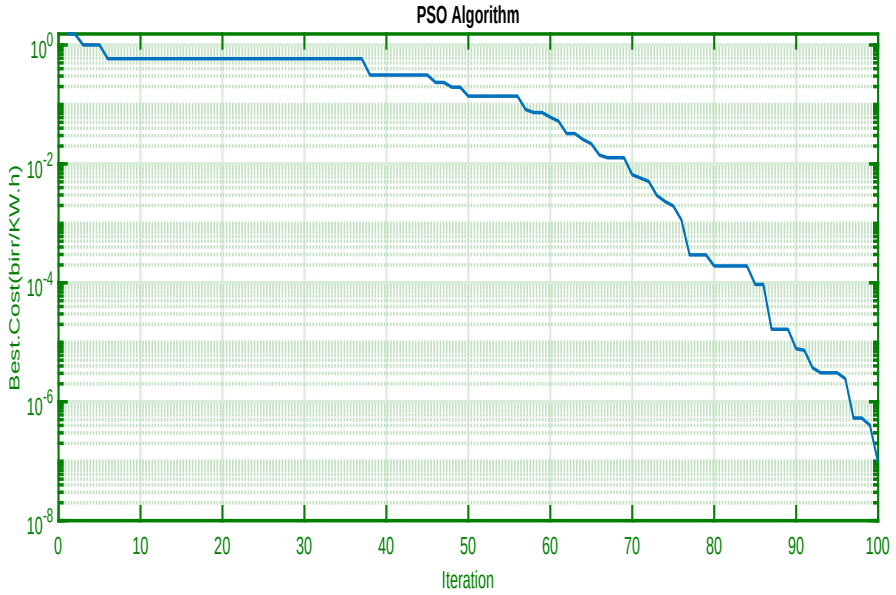

Figure 5.1: PSO represent best cost VS iteration curve

- In figure 5.1 iteration number between 6-37 is the best cost position of the Particle Swarm Optimization (PSO). The optimal place of best cost is 0.5883 birr/kWh. The maximum number of 100 and 80 using iteration and population size respectively in a particle swarm optimization. The curve shows particle swarm optimization is the optimal placement of the best cost of the system in appendix A.6.2.

Genetic algorithm is used in this work for comparison purpose to show the effectiveness of PSO based optimization; GA is selected from other swarm intelligence optimization algorithms for comparison purpose as expressed in the literature.

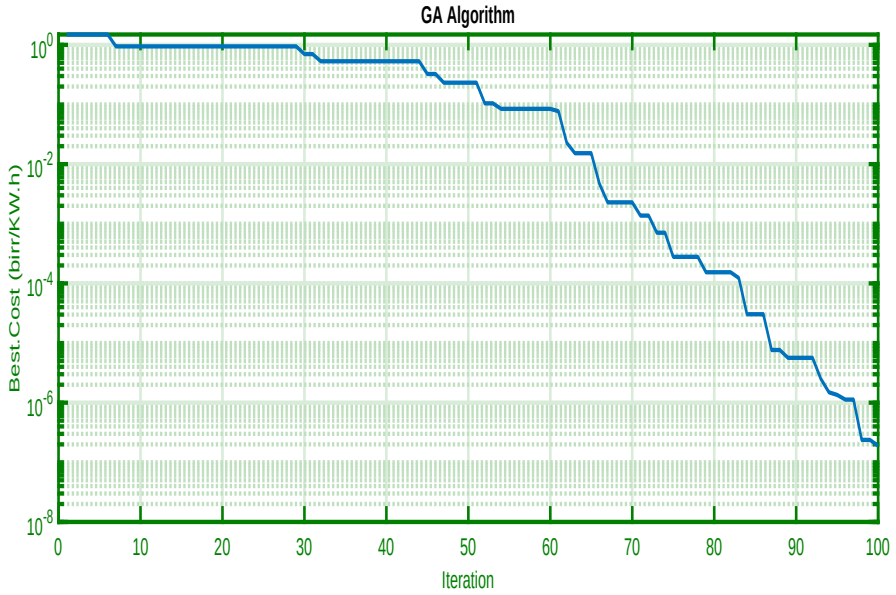

Figure 5.2: GA algorithm represent best cost VS iteration curve

- In figure 5.2 iteration number between 32-44 is the best cost position of the genetic algorithm. The optimal place of best cost is 0.5308 birr/kWh. The maximum number of 100 and 80 using iteration and population size respectively in a genetic algorithm. The curve shows Genetic algorithm is the optimal placement of the best cost of the system in appendix A.6.3.

Comparison of PSO and GA techniques

The comparison of PSO and GA are depending upon the curve shown in figure 5.1 and 5.2 the installation of dynamic voltage restorer the annual economic benefit of power system Ashegoda wind farm in table 5.1

Table 5.1: Comparison GA and PSO techniques

Method	Best cost (birr/kwh)	Optimize cost ($ /kwh)	Population size	Iteration
GA	0.5308	14,003,146.17	80	100
PSO	0.5883	15,453,930.89	80	100

- Table 5.1 the same number of iteration and population size a particle swarm optimization for the investment cost better than a genetic algorithm depend upon the modeling of a dynamic voltage restorer device.

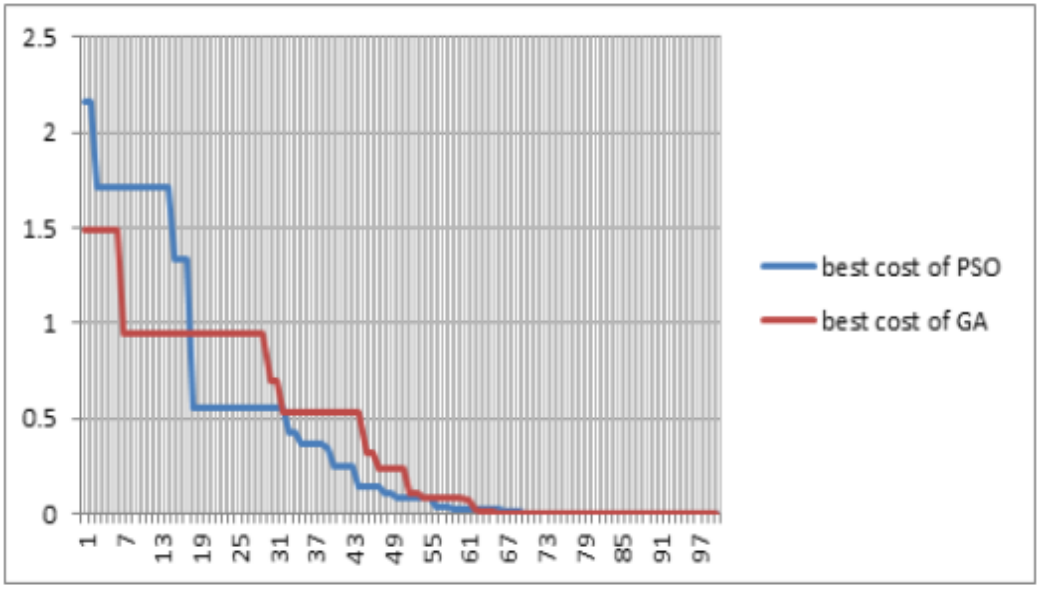

Figure 5.3: Comparison optimal best costs of GA and PSO

The optimal cost is calculated as 14,003,146.17 $/kWh and 15,453,930.89 $/kWh using GA and PSO respectively. The relative cost of GA wind turbine generation is lower before its investment cost increases, So, GA is more likely to be chosen. Furthermore, the generation net benefits of each bus set before the investment cost increases are superior. The relative cost of GA wind turbine generation increases after its investment cost increases, making PSO wind turbine generation more advantageous.

The increases the investment cost makes the generation net economic benefits of each bus set decreases compared with that before the cost increases. Therefore, improving the utilization efficiency and decreasing the investment cost of wind turbine generation. Can help improve the final generation net benefits resulting in the increase in the corresponding capital cost and M and O cost.

The devices are used to model of dynamic voltage restorer to minimize power loss, but Crowbar security to compare with dynamic voltage restorer in the system in using the mat lab simulation results.

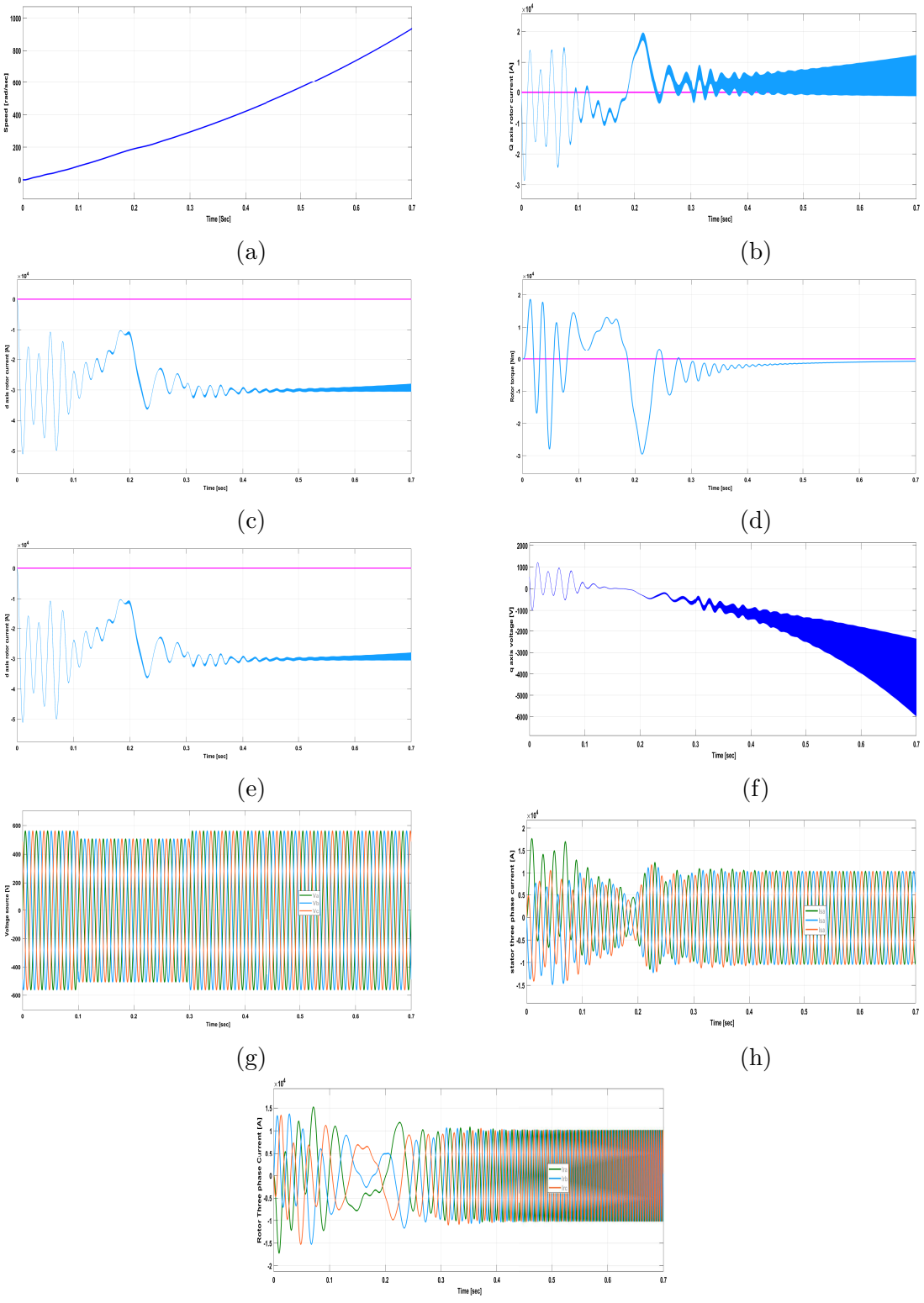

Figure 5.4: Rotor side control simulation result without any devices

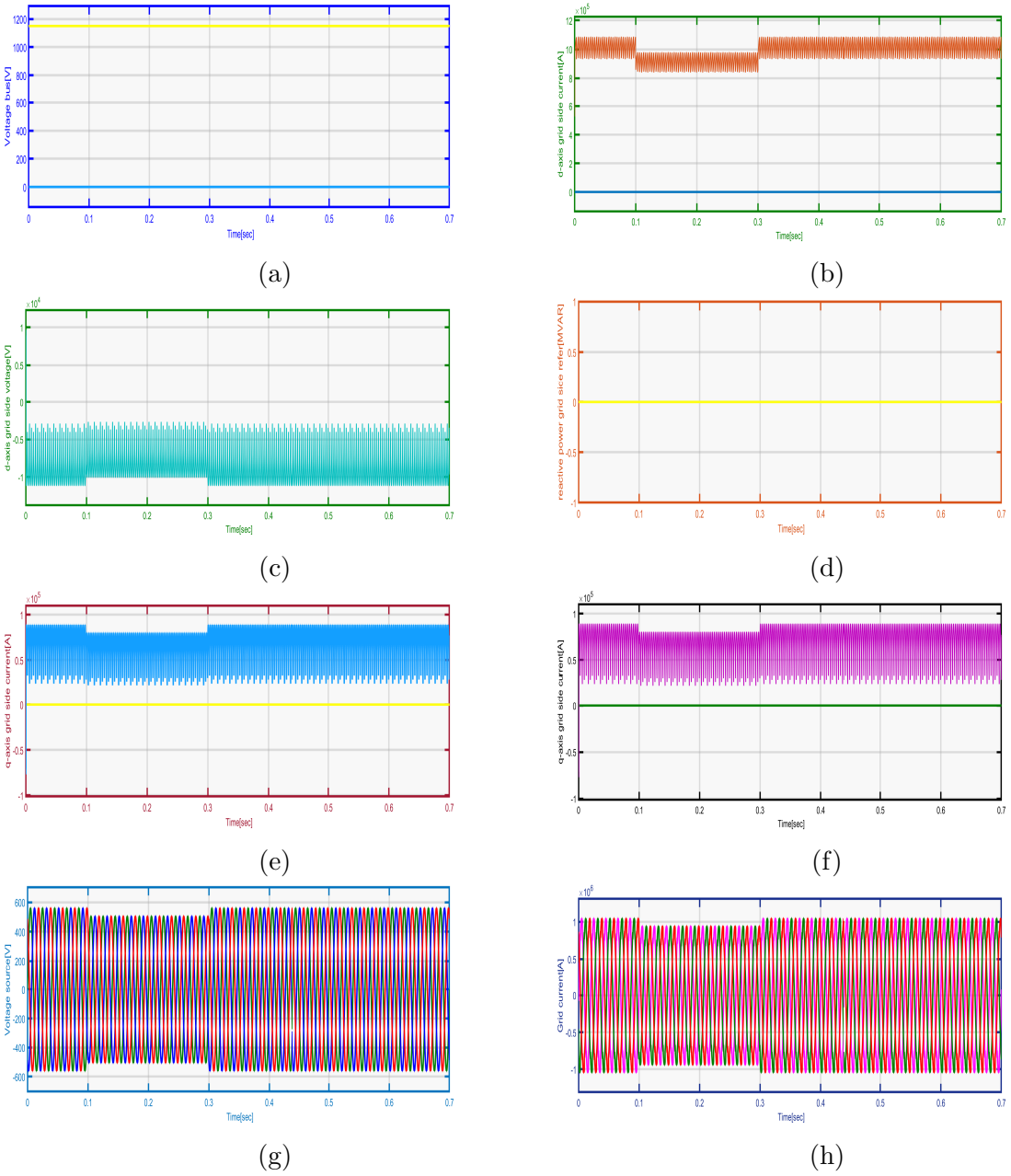

Figure 5.5: Grid side control simulation result without any devices

The rotor side current the range between 0.1-0.3second approach to direct current while the stator side current the range between 0.1-0.3 second the disturbance occur. The grid side and generator side voltage the range between 0.1-0.3 second the voltage dip occurs. Grid voltage unbalance causes numerous troubles in the doubly fed induction generator system. Since the stator of a DFIG is directly connected to the grid, negative sequence component is added to the stator flux under unbalanced grid voltage conditions. As a consequence, large negative-sequence current flow through the stator and the rotor of the DFIG, which causes a significant second-order harmonic fluctuation in the electromagnetic

torque and active and reactive powers are also fluctuating in the stator and the rotor.

The torque fluctuation causes fatigue in the mechanical parts such as the gearbox and the shaft. In addition, the active power fluctuations, which flow through the DC-link capacitors from both GSC and RSC, because a large second-order harmonic current in the DC capacitors as well as voltage ripples in the DC link. It results in higher power losses in the DC link capacitors and higher operation temperature, which will shorten the lifetime of the electrolytic capacitors.

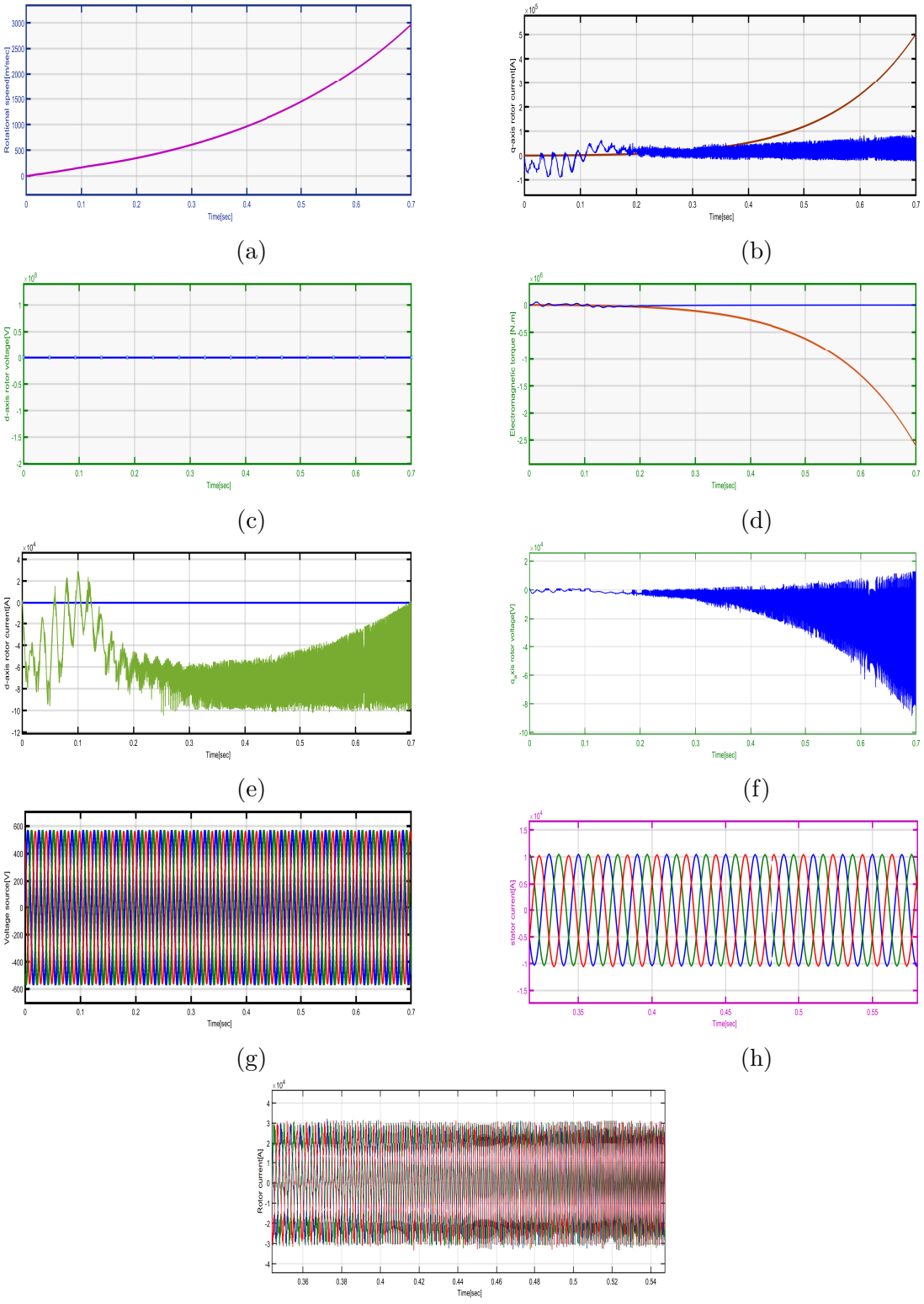

Figure 5.6: Rotor side control simulation result with dynamic voltage restorer

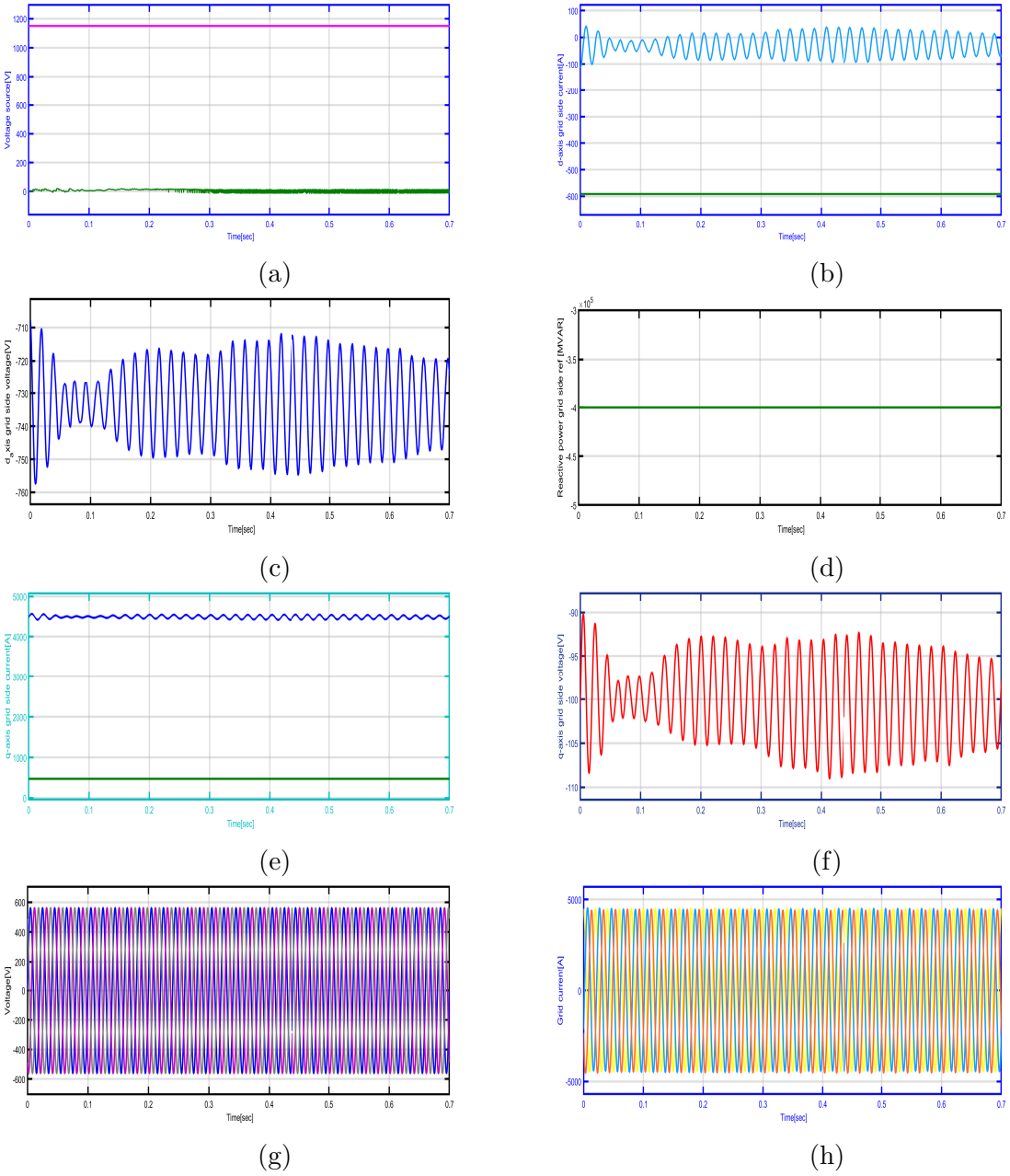

Figure 5.7: Grid side control simulation result with dynamic voltage restorer

The stator current balancing control provides a good solution for the negative effects caused by unbalanced grid voltage on the life time of the DFIG and enhancing the compatibility of the DFIG system in the unbalanced grid condition. Before the stator current balancing control is enabled, severe unbalance is present in the three-phase stator current, and the electro-magnetic torque experiences large fluctuations, and large harmonics can be observed in the rotor current.

After switching to the stator current balancing control, the system impedance for the negative-sequence voltage increases significantly and thus the negative-sequence cur-

rents are suppressed, leading to balanced stator currents, reduced electro-magnetic torque fluctuation, and reduced rotor current harmonics. Compared to the situation under the balanced grid, under unbalanced grid voltage, the capacitor current and core temperature are both increased.

Since the life time of the electrolytic capacitor decreases exponentially with the increase of core temperature, unbalanced grid conditions may accelerate the wear-out of the DC capacitors. Thus, from the perspective of enhancing the reliability of DC capacitors, reducing second-order harmonic current in the DC capacitor is required.By over-rating the DC link capacitors, the fluctuation in the DC voltage can be mitigated, however at the cost of higher material expense and higher weight. It would be desirable to develop an improved control scheme to suppress the DC voltage fluctuations without the necessity of increasing the DC bus capacitance.

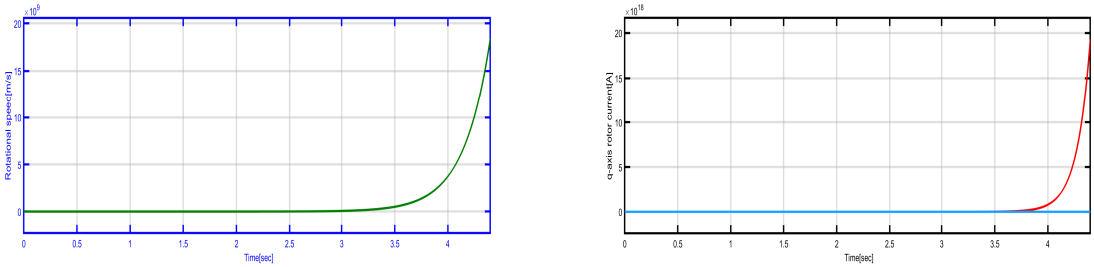

(a)

(b)

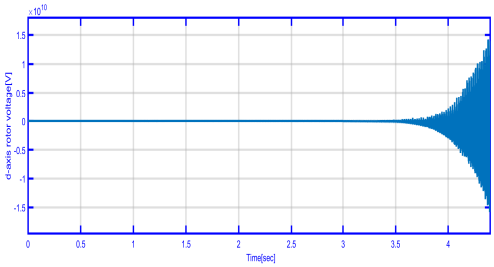

(c)

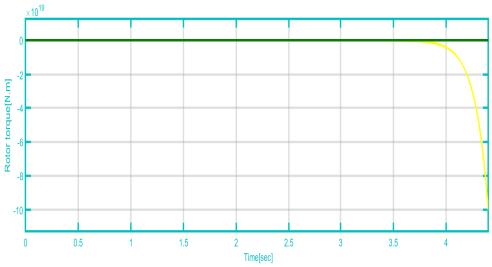

(d)

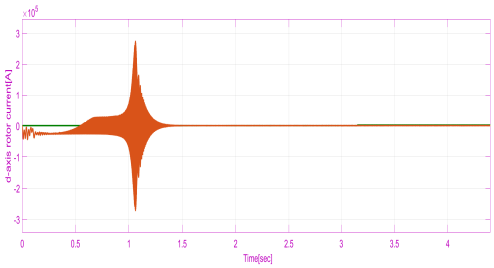

(e)

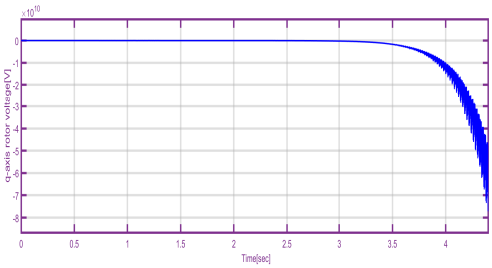

(f)

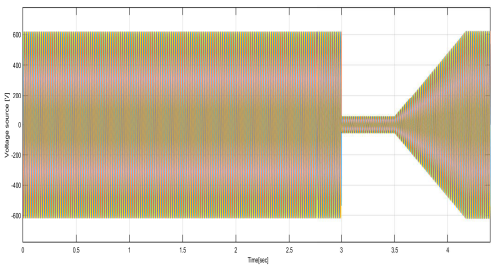

(g)

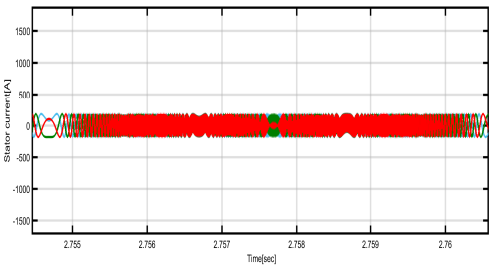

(h)

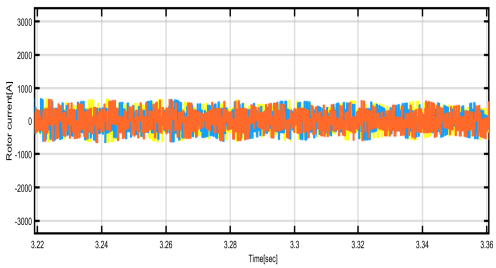

(i)

Figure 5.8: Rotor side control simulation result with crowbar protection

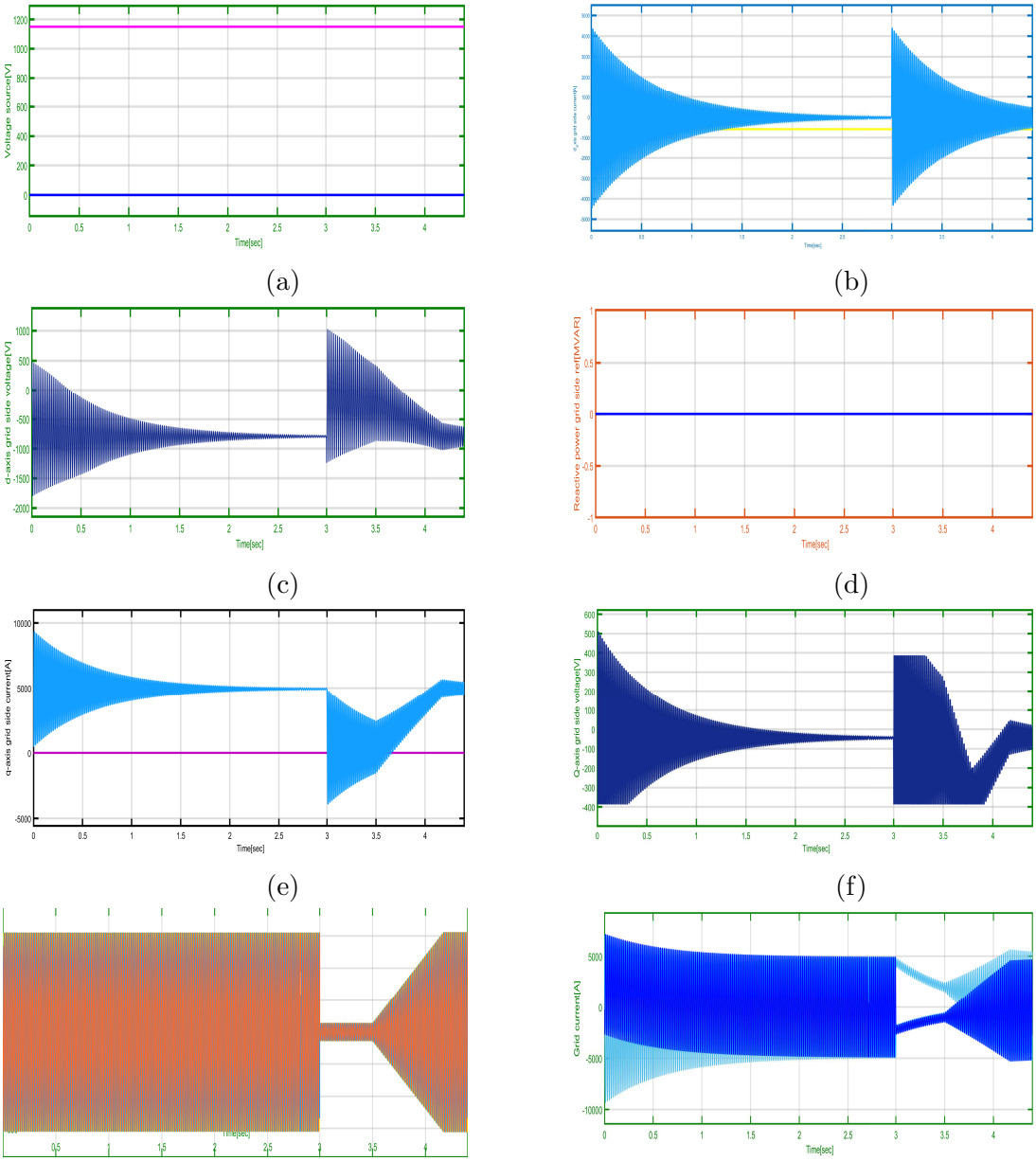

Figure 5.9: Grid side control simulation result with crowbar protection

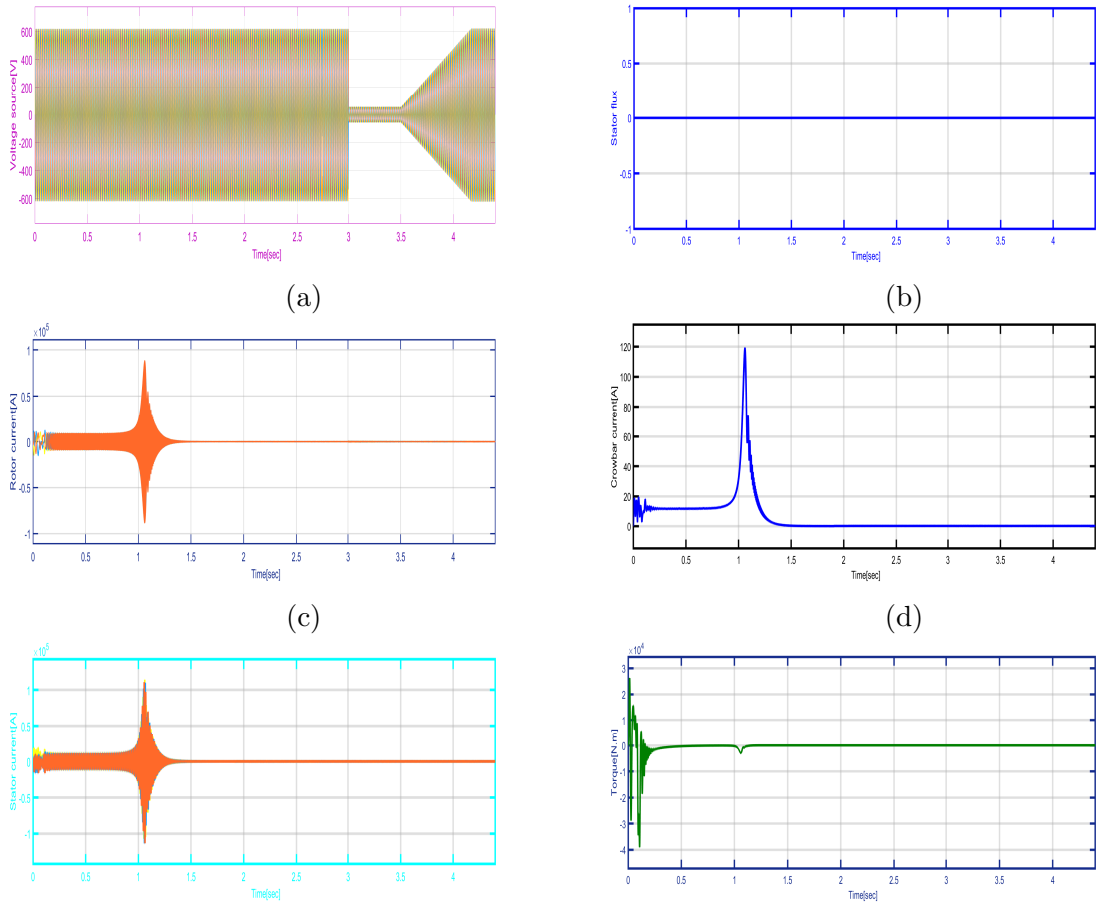

Figure 5.10: Fault analysis simulation result with crowbar protection

The crowbar firing is triggered by the rotor currents which rise due to the first rotor currents peak. The electronic switches of the convertor are usually stopped by the protection. However, the current and thus the energy continuous to flow in to the DC- link through the freewheeling diodes leading to a very fast voltage increases. The included parallel resistance in the rotor circuit and also connected resistance in the parallel with DC-link result in decreasing the stator currents and also the rotor current are decreased.

The DC-link voltage and torque fluctuations are significantly reduced. The rotor-side crowbar is widely used for the Low Voltage Ride-Through (LVRT) of a DFIG. It can be seen that the damping of stator natural flux is accelerated compared to the rotor and stator current is limited as well. Besides, the DC voltage will not rise and the electromagnet torque fluctuations are relatively small. The amplitude of the rotor current (refers to the stator side) and stator current, as well as the stator time constant with different crowbar resistance values under different voltage dip levels are simulated.

The rotor-side crowbar is one of the commonly used hardware solutions for the DFIG to ride through grid faults. The rotor-side crowbar short-circuits the rotor windings under grid faults, so that the transient rotor current can be limited and the RSC can be protected. The restart of the RSC is also an important issue. Normally, the crowbar needs to be disabled first, then after one or two switching periods, the RSC can be restarted. The integrator of the inner current control loop of the RSC should be reset to zero in order to prevent a transient overt current introduced by the restart of the RSC.

Chapter 6

Conclusion and Future Work

6.1 Conclusion

In simple terms, what have been accomplished in this thesis are firstly the analysis of the causes and the mechanisms of previous fault ride through of the Ashegoda wind farm and identification of the power system vulnerabilities and weaknesses of the system. Then, based on the identified fault causes and system weaknesses, some methods that can help mitigate system fault are proposed. This aim was achieved by modeling and simulating the Ashegoda wind farm by using Mat lab software.

From the vulnerabilities analysis, it is found that the most power loss between Mekele substation and Alamata substation in the point of common coupling (PCC). DVR is a feasible option to provide the necessary dynamic power compensation. Investigate the possibility of connecting of a DVR to the a wind power generation system for the purpose of transient stabilizing the grid voltage after grid- side disturbances such as a three phase short circuit fault and sudden load changes and hence enhance the stability of the power system which contains wind power generation system. Increasing amount of wind power generation requirement more appropriate solutions to address common voltage regulation requirements.

This thesis presents a single-objective function in economical optimal operation of wind turbines in wind farm in order to maximize net benefit cost of system. Therefore, it is possible to conclude that, the dynamic performance of the existing wind farm and hence the stability of the entire power system can be significantly improved through the

installation of DVR of a proper size, when severe network disturbances occur in the system.

Based on the studies and results found in this thesis, it is recommended to connect DVR with in the studied Ashegoda wind farm as it can enhance steady state and dynamic performances of the wind farm as well as the entire system when severe network disturbances abnormalities occur in the system.

6.2 Future Works

In this thesis, the Improved Fault Ride through Capability of DFIG -Wind Turbines Using Customized DVR is studied. That can be extended by considering other dynamic compensation technique such as UPFC and comparing the effectiveness in improving dynamic performance of the wind farm and hence system stability with DVR for the same studies case by considering technical and economic benefits.

Conventional PI controller based DVR has been studied in this thesis. For future work a Fuzzy Logic Controller (FLC) based DVR can also be considered as a mechanism to enhance stability of grid connected wind farms and to increase the LVRT capability of the wind turbines. Its performance could be compared with the conventional PI controlled DVR.

High wind power penetration presents many challenges to modern power systems. One of these challenges is power quality issue. An interesting future work could be analyzing the performance of DVR for power quality improvement in grid connected wind generating system.

Bibliography

[1] R. D. Richardson and G. M. McNerney, "Wind energy systems," *Proceedings of the IEEE*, vol. 81, no. 3, pp. 378–389, 1993.

[2] H. Jadhav and R. Roy, "A comprehensive review on the grid integration of doubly fed induction generator," *International Journal of Electrical Power and Energy Systems*, vol. 49, pp. 8–18, 07 2013.

[3] M. Tsili and S. Papathanassiou, "A review of grid code technical requirements for wind farms," *IET Renewable Power Generation*, vol. 3, no. 3, pp. 308–332, 2009.

[4] L. Yang, Z. Xu, J. Ostergaard, Z. Y. Dong, and K. P. Wong, "Advanced control strategy of dfig wind turbines for power system fault ride through," *IEEE Transactions on Power Systems*, vol. 27, no. 2, pp. 713–722, 2012.

[5] V. F. Mendes, C. V. de Sousa, S. Silva, B. C. Rabelo, and W. Hofmann, "Modeling and ride-through control of doubly fed induction generators during symmetrical voltage sags," *IEEE Transactions on Energy Conversion*, vol. 26, no. 4, pp. 1161–1171, 2011.

[6] G. Pannell, D. J. Atkinson, and B. Zahawi, "Minimum-threshold crowbar for a fault-ride-through grid-code-compliant dfig wind turbine," *IEEE Transactions on Energy Conversion*, vol. 25, no. 3, pp. 750–759, 2010.

[7] N. G. Hingorani, "Introducing custom power," *IEEE Spectrum*, vol. 32, no. 6, pp. 41–48, 1995.

[8] R. Sitharthan, M. Geethanjali, and T. Karpaga Senthil Pandy, "Adaptive protection scheme for smart microgrid with electronically coupled distributed generations," *Alexandria Engineering Journal*, vol. 55, no. 3, pp. 2539 – 2550, 2016.

[9] K. D. S. K. N. R. Sitharthana, C.K.Sundarabalanb and M. Karthikeyana, *A feed-forward transient current control method for Rotor Side Converter (RSC) of the DFIG has been proposed*, 3rd ed., ser. 10. Engineering and Technology Power Engineer Magazine, 2018, vol. 4.

[10] M. Rahimi and M. Parniani, "Grid-fault ride-through analysis and control of wind turbines with doubly fed induction generators," *Electric Power Systems Research*, vol. 80, no. 2, pp. 184 – 195, 2010.

[11] H. Berisso, "Fault ride through capability of double fed induction generator for wind energy system," Master's thesis, The school of the thesis A Master's Project Report presented to Ryerson University., The address of the publisher, 7 2010, an optional note.

[12] V. F. Mendes, C. V. de Sousa, S. Silva, B. C. Rabelo, and W. Hofmann, "Modeling and ride-through control of doubly fed induction generators during symmetrical voltage sags," *IEEE Transactions on Energy Conversion*, vol. 26, no. 4, pp. 1161–1171, 2011.

[13] G. Pannell, D. J. Atkinson, and B. Zahawi, "Minimum-threshold crowbar for a fault-ride-through grid-code-compliant dfig wind turbine," *IEEE Transactions on Energy Conversion*, vol. 25, no. 3, pp. 750–759, 2010.

[14] A. G. Abo-Khalil, D. Lee, and S. Lee, "Grid connection of doubly-fed induction generators in wind energy conversion system," in *2006 CES/IEEE 5th International Power Electronics and Motion Control Conference*, vol. 3, 2006, pp. 1–5.

[15] R. Pena, J. Clare, and G. Asher, "Doubly fed induction generator using back-to-back pwm converters and its application to variable-speed wind-energy generation," *IEE Proceedings-Electric power applications*, vol. 143, no. 3, pp. 231–241, 1996.

[16] S. Goel., "Comparison of the facts equipment operation in transmission and distribution systems," *17th International Conference on Electricity Distribution Barcelona, Session.*, no. 1, p. 49, 2014.

[17] M. Singh and V. Tiwari, "Modeling analysis and solution of power quality problems," *doi: http://eeeic. org/proc/papers/50. pdf*, 2009.

[18] Y. W. Li, D. M. Vilathgamuwa, P. C. Loh, and F. Blaabjerg, "A dual-functional medium voltage level dvr to limit downstream fault currents," *IEEE Transactions on Power Electronics*, vol. 22, no. 4, pp. 1330–1340, 2007.

[19] P. Roncero-Sánchez, E. Acha, J. E. Ortega-Calderon, V. Feliu, and A. García-Cerrada, "A versatile control scheme for a dynamic voltage restorer for power-quality improvement," *IEEE Transactions on power delivery*, vol. 24, no. 1, pp. 277–284, 2008.

[20] A. Falehi and M. Rafiee, "Enhancement of dfig-wind turbine's lvrt capability using novel dvr based odd-nary cascaded asymmetric multi-level inverter," *Engineering Science and Technology, an International Journal*, vol. 20, no. 3, pp. 805 – 824, 2017.

[21] C. Sundarabalan and K. Selvi, "Real coded ga optimized fuzzy logic controlled pemfc based dynamic voltage restorer for reparation of voltage disturbances in distribution system," *International Journal of Hydrogen Energy*, vol. 42, no. 1, pp. 603 – 613, 2017.

[22] R. Dastagir and M. Asif, "Power quality improvement using a dvr (dynamic voltage restorer)," 2014.

[23] N. Amutha and B. Kalyan Kumar.

[24] M. R. L. M. G. I. Gonzalo Abad, Jesús López, *Doubly Fed Induction Machine: Modeling and Control for Wind Energy Generation Applications (IEEE Press Series on Power Engineering)*. Wiley-IEEE Press, 2011.

[25] M. L, *Wind Power satisfies Network Demands*, 3rd ed., ser. 10. he Engineering and Technology Power Engineer Magazine, 2006, vol. 4.

[26] W. C. Dehong Xu, Frede Blaabjerg and N. Zhu, *Advanced Control of Doubly Fed Induction Generator for Wind Power Systems". IEEE Press series on power Engineering,*. Wiley-IEEE Press, 2018.

[27] T. Nadu, *Indian Wind Grid Code-Version 1.0,*, July,2009.

[28] X. D. C. W. Z. N. Blaabjerg, Frede, *Advanced Control of Doubly Fed Induction Generator for Wind Power Systems —— Introduction.* Elsevier, 2018, vol. 10-16.

[29] A. Etxegarai, P. Eguia, E. Torres, A. Iturregi, and V. Valverde, "Review of grid connection requirements for generation assets in weak power grids," *Renewable and Sustainable Energy Reviews*, vol. 41, pp. 1501–1514, 2015.

[30] T. Ackermann, *Wind Power in Power Systems (IEEE Press Series on Power Engineering).* Wiley-IEEE Press, 2005.

[31] V.Akhmatov, "Analysis of dynamic behavior of electric power systems with large amount of wind power," 04 2003.

[32] A. E.Muljadi, S.Pasupulati and D. Kosterovy, "Method of equivalencing for a large wind power plant with multiple turbine representation," vol. 49, no. 3, p. 20, 2008.

[33] A. J. J. H. R. Y. N. M. R. D. R. Z. J. S. E. Muljadi, C.P. Butterfield, "Equivalencing the collector system of a large wind power plant," vol. 49, no. 3, p. 18, 2006.

[34] D. Patil and D. Chavan, "Modelling of dynamic voltage restorer for mitigation of voltage sag and swell using phase locked loop."

[35] P. R. C. Beijing, "Renewable energy law of people's republic of china."

[36] G. Masters, *Renewable and efficient electric power systems.* Wiley-IEEE Press, 2004.

[37] A. P. Roses and B. Francois, "Practical determination of hvac–hvdc hybridization ratio for offshore transmission network architectures through technico-economic considerations," *IFAC-PapersOnLine*, vol. 49, no. 27, pp. 425–432, 2016.

[38] G. Bekele and A. Abdela, "Investigation of wind farm interaction with ethiopian electric power corporation's grid," *Energy Procedia*, vol. 14, pp. 1766–1773, 12 2012.

[39] C. Skoulidas, C. Vournas, and G. Papavassilopoulos, "An adaptive game for pay-as-bid and uniform pricing power pools comparison," 01 2002.

[40] M. R. L. M. G. I. Gonzalo Abad, Jesús López, *Doubly Fed Induction Machine: Modeling and Control for Wind Energy Generation Applications (IEEE Press Series on Power Engineering)*. Wiley-IEEE Press, 2011.

[41] H. Abu-Rub, M. Malinowski, and K. Al-Haddad, *Properties and Control of a Doubly Fed Induction Machine*, 2014, pp. 270–318.

[42] J. H. Holland, "Genetic algorithms and the optimal allocation of trials," *SIAM Journal on Computing*, vol. 2, no. 2, pp. 88–105, 1973.

[43] A. Ratnaweera, S. K. Halgamuge, and H. C. Watson, "Self-organizing hierarchical particle swarm optimizer with time-varying acceleration coefficients," *IEEE Transactions on evolutionary computation*, vol. 8, no. 3, pp. 240–255, 2004.

[44] D. Singh, "Modeling analysis and solution of power quality problems," 04 2020.

[45] C. Chang and S. Yang, "Tabu search application for optimal multiobjective planning of dynamic voltage restorer," vol. 4, 02 2000, pp. 2751 – 2756 vol.4.

[46] EEP, "Ethiopian power system expansion master plan study final report," *Renewable and Sustainable Energy Reviews*, vol. 4, pp. 326 – 333, 8 2014.

Appendix A

Appendix 1

A.1 values and ratings of the test system components

DFIG:

Power Rating: 90.18 MVA

Real power: 90 MW

Reactive power: +0.55 Mvar

Pad mounted transformer: 2000KVA (0.69/33kv)

FCG:

Power Rating: 31.17 MVA

Real power: 30 MW

Reactive power limits:± 0.8 Mvar

Pad mounted transformer: 1250KVA (0.69/33kv)

DVR

Power Rating:±80 MVA

Ac terminal voltage: 15kv

DC terminal voltage: 25kv

Coupling Transformer: 15 kV/33 kV

Transformer short circuit voltage: 10%

DC Capacitor: 3000μF

Tekeze-PP:

Power Rating: 350.4 MVA

Voltage: 13.8 kV

Power factor: 0.9

Reactive power limits:±38 Mvar

Total System Load:

Active power: 139.21 MW

Reactive power: 73.64 Mvar

EXTERNAL GRID:

The rest of the Ethiopian network is represented by EXTERNAL GRID at Alamata substation with the following short-circuit Characteristics.

Table A.1: Short-circuit characteristics of the EXTERNAL GRIG

Minimum three-phases short –circuit power	910.7 MVA
Maximum three-phases short –circuit power	1094 MVA

A.2 AWF Branch Impedance Parameters

Table A.2: Branch impedance of cluster one and two (Phase)

Group	Branches		Branch Flow (MV)	Cable Length (m)	Cable Cross Section (mm2)	Electrical Parameters		
	From	To				R (Ω)	XL (Ω)	B (µS)
1.A1	CL	2	2	204	50	0.17	0.03	8.97
	2	1	1	252	50	0.21	0.04	11.08
1.A2	CL	3	3	165	50	0.14	0.02	7.25
	3	4	2	243	50	0.20	0.04	10.68
	4	5	1	222	50	0.18	0.03	9.76
1.B	CL	6	13	825	240	0.13	0.09	69.94
	6	7	12	227	240	0.04	0.02	19.25
	7	8	11	220	150	0.06	0.03	14.51
	8	9	10	223	150	0.06	0.03	14.70
	9	10	9	218	150	0.06	0.03	14.37
	10	11	8	222	95	0.09	0.03	11.85
	11	12	7	218	95	0.09	0.03	11.64
	12	13	6	221	95	0.09	0.03	11.80
	13	14	5	651	95	0.27	0.08	34.75
	14	15	4	221	50	0.18	0.03	9.72
	15	16	3	322	50	0.26	0.05	14.16
	16	17	2	233	50	0.19	0.03	10.24
	17	18	1	233	50	0.19	0.03	10.24
2.A	CL	23	5	1032	50	0.85	0.15	45.37
	23	22	4	286	50	0.24	0.04	12.57
	22	21	3	233	50	0.19	0.03	10.24
	21	20	2	233	50	0.19	0.03	10.24
	20	19	1	233	50	0.19	0.03	10.24
2.B	CL	24	7	1320	95	0.54	0.17	70.46
	24	25	6	196	50	0.16	0.03	8.62
	25	26	5	234	50	0.19	0.04	10.29
	26	27	4	266	50	0.22	0.04	11.69
	27	28	3	226	50	0.19	0.03	9.93
	28	29	2	1549	50	1.27	0.23	68.09
	29	30	1	265	50	0.22	0.04	11.65

Table A.3: Branch impedance of clusters three, four and five (phase II)

Group	Branches		Branch	Cable	Cable Cross	Electrical Parameters		
	From	To	Flow(MW)	Length(m)	Section (mm2)	R (Ω)	XL (Ω)	B (µS)
3.A	CL	38	13.36	234	240	0.04	0.03	19.84
	38	37	11.69	416	240	0.07	0.05	35.27
	37	36	10.02	382	150	0.10	0.05	25.19
	36	35	8.35	269	95	0.11	0.04	14.36
	35	34	6.68	289	95	0.12	0.04	15.43
	34	33	5.01	523	50	0.43	0.08	22.99
	33	32	3.34	391	50	0.32	0.06	17.19
	32	31	1.67	324	50	0.27	0.05	14.24
3.B	CL	39	11.69	204	240	0.03	0.02	17.30
	39	40	10.02	437	150	0.12	0.05	28.82
	40	41	8.35	313	95	0.13	0.04	16.71
	41	42	6.68	486	95	0.20	0.06	25.94
	42	43	5.01	456	50	0.37	0.07	20.05
	43	44	3.34	284	50	0.23	0.04	12.48
	44	45	1.67	149	50	0.12	0.02	6.55
4.A	CL	55	16.70	50	2*150	0.01	0.01	4.55
	55	54	15.03	300	240	0.05	0.03	25.43
	54	53	13.36	274	240	0.04	0.03	23.23
	53	52	11.69	353	240	0.06	0.04	29.93
52		51	10.02	497	150	0.13	0.06	32.77
	51	50	8.35	368	95	0.15	0.05	19.64
	50	49	6.68	385	95	0.16	0.05	20.55
	49	48	5.01	752	50	0.62	0.11	33.06
	48	47	3.34	327	50	0.27	0.05	14.37
	47	46	1.67	380	50	0.31	0.06	16.70
4.B	CL	56	16.70	127	2*150	0.02	0.01	11.56
	56	57	15.03	446	240	0.07	0.05	37.81
	57	58	13.36	274	240	0.04	0.03	23.23
	58	59	11.69	278	240	0.04	0.03	23.57
	59	60	10.02	309	150	0.08	0.04	20.38
	60	61	8.35	300	95	0.12	0.04	16.01
	61	62	6.68	350	95	0.14	0.05	18.68
	62	63	5.01	292	50	0.24	0.04	12.84
	63	64	3.34	280	50	0.23	0.04	12.31
	64	65	1.67	305	50	0.25	0.05	13.41

A.3 Summary of Equivalent Impedance of AWF

Table A.4: Summary of equivalence of pad-mounted transformer impedance (phase I)

Cluster	No. of Transformers	Total power(MW)	Pad mounted transformer(ZTS)	
			Req (Ω)	Xeq (Ω)
1	18	18	0.000237	0.001246
2	12	12	0.000355	0.001870

Table A.5: Summary of equivalence of pad -mounted transformer impedance (phase II)

Cluster	No of Transformers	Total power(MW)	Pad mounted transformer(ZTS)	
			Req (Ω)	Xeq (Ω)
3	15	25	0.000197	0.000932
4	20	33	0.000148	0.000699
5	19	32	0.000155	0.000735

Table A.6: Summary of equivalence of collector circuit impedances AWF (phase I)

Cluster	No of turbine	Total power(MW)	Collector Impedance (ZS)		
			Req (Ω)	Xeq (Ω)	Beq (µS)
1	18	18	0.2324	0.1087	294.91
2	12	12	0.5226	0.1187	279.39

Table A.7: Summary of equivalence of collector circuit impedances AWF (phase II)

Cluster	No of turbine	Total power(MW)	Collector Impedance (ZS)		
			Req (Ω)	Xeq (Ω)	Beq (µS)
3	15	25	0.1613	0.0639	292.36
4	20	33	0.1304	0.0626	410.03
5	19	32	0.1171	0.0581	351.79

Table A.8: Summary of single turbine representation of AWF(phase I)

Cluster	No of Turbine	Total Power(MW)	Equivalent transformer Impedance (ZTS)		Equivalent Collector Impedance(ZS)		
			Req (Ω)	Xeq (Ω)	Req (Ω)	Xeq (Ω)	Beq (µS)
1 and 2	30	30	0.000142	0.000748	0.1673	0.0581	562.65
	Overhead line				0.51801	0.7065	1.41

Table A.9: Summary of single turbine representation of AWF (phase II)

Cluster	No of turbines	Total power (MV)	Eququivalent transformer Impedance (ZTS)		Equivalent Collector impendance(Zs)		
			Req (Ω)	Xeq (Ω)	Req (Ω)	Xeq (Ω)	Beq (µS)
3,4	54	90	0.000055	0.00026	0.0448	0.0207	1054.18
	Overhead lines				0.3189	0.435	7.44151
and 5	Cables and Overhead lines				0.3637	0.4557	1061.6215

A.4 parameters DFIG used for this study

Table A.10: The double fed induction generator parameters used for this study

Parameters	Value	Units
Nominal power	2	MW
Nominal torque	12732	N.m
Stator voltage	690	V
Nominal speed	1500	Rpm
Pole pairs	2	–
Magnetizing inductance (Lm)	2.5*10-3	H
Rotor leakage inductance	87*10-6	H
Stator leakage inductance	87*10-6	H
Rotor resistance	0.026	ohm
Stator resistance	0.029	ohm
Rated rotor voltage	2070	V
Rcrowbar	1/5	ohm

A.5 Modelling of the DFIG in System

A.5.1 DFIG without Any Devices

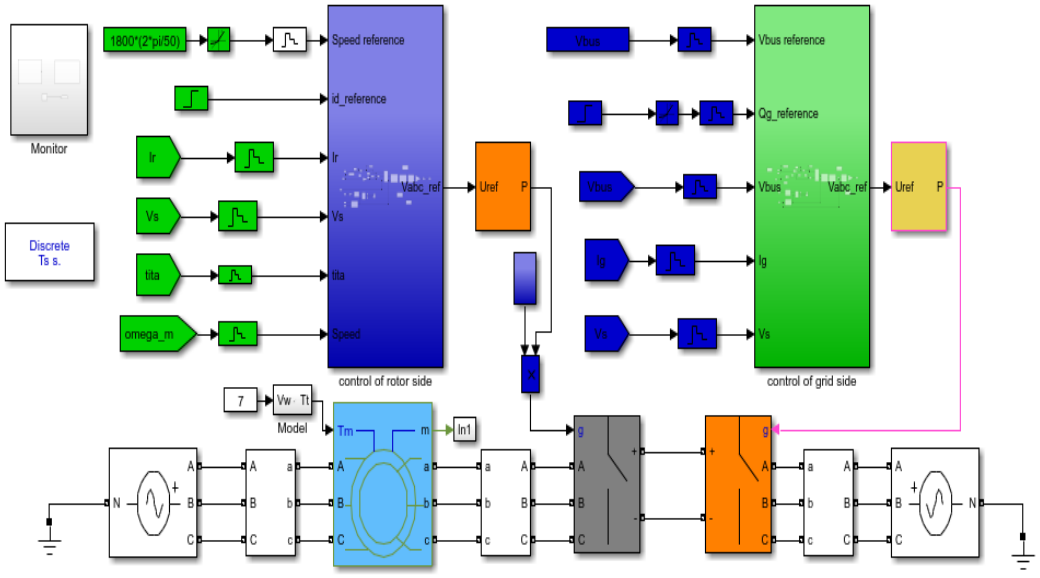

Figure A.1: Both rotor and stator side convertor without any devices block diagram of DFIG

A.5.2 DFIG with Dynamic Voltage Restorer

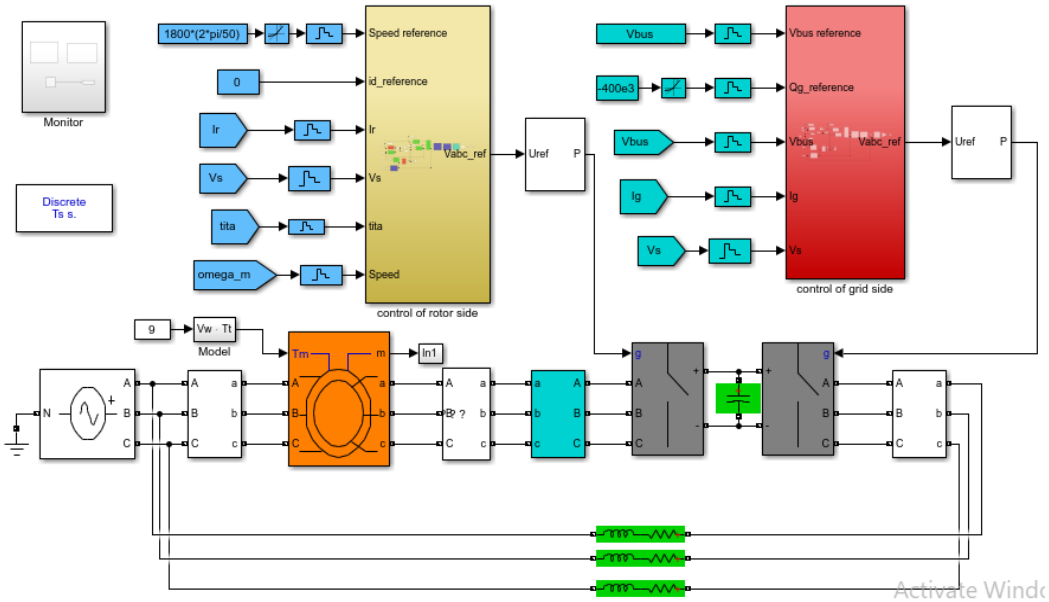

Figure A.2: Both rotor and stator side convertor with dynamic voltage restorer block diagram of DFIG Ashegoda wind farm

A.5.3 DFIG with Crowbar Protection

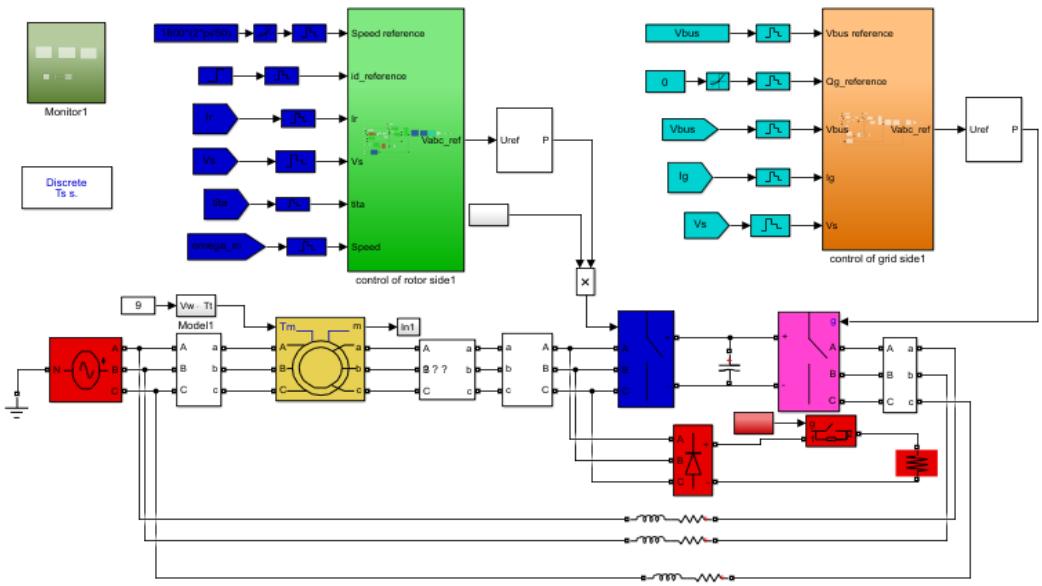

Figure A.3: Both rotor and stator side converter with crowbar protection block diagram of DFIG Ashegoda wind farm

A.6 codes of DFIG, PSO AND GAO

A.6.1 Double Fed Induction Generation System Code

```
 close all
 clear all
  clc
%% DFIG parameters -> rotor parameters referred to the stator
    side

f = 50;                          % stator frequency (Hz)
Ps = 2.5e6;                     % Rated stator power (W)
m = 1500;                        % Rated rotatetional speed (rev
   /min)
Vs = 690;                        % Rated stator voltage (v)
Is = 1760;                     % Rated stator current (A)
Tem = 12732;                      % Rated torque (N.m)

p = 2;                           % Pole pair
u = 1/3;                        % Stator/rotor turns ratio
vr = 2070;                      % Rated rotor voltage (non-
   reached)(v)
Smax = 1/3;                      % Maximum slip
vr_stator = (vr*Smax)*u;        % Rated rotor voltage referred
   to the stator (v)
Rs = 2.6e-3;                   % Stator resistance (ohm)
Lsi = 0.087e-3;               % leankage inductance (stator &
   rotor) (H)
Lm = 2.5e-3;                   % Magnitizing inductance (H)
Rr = 2.9e-3;                   % Rotor resistance referred to
   stator (ohm)
```

```
Ls = Lm + Lsi;                  % stator inductance (H)
Lr = Lm + Lsi;                  % Rotor inductance (H)
Vbus = 1150;                    % DC de bus voltage referred to
    stator (v)
sigma = 1- Lm^2/(Ls*Lr);
Fs = Vs*sqrt(2/3)/(2*pi*f);     % stator flux (aprox.)(kb)
J = 63.5;                       % inertia
D = 1e-3;                       % Damping
fsw = 4000;                      % switching frequency (Hz)
Ts = 1/fsw/50;                  % sample times  (sec)

          % PI regulators

tau_i = (sigma*Lr)/Rr;
tau_n = 0.05;
Wni = 100*(1/tau_i);
Wnn = 1/tau_i;
kp_id = (2*Wni*sigma*Lr)- Rr;
kp_iq = kp_id;
ki_id = (Wni^2)*Lr*sigma;
kp_id = ki_id;
kp_n = (2*Wnn*J)/p;
ki_n = ((Wnn^2)*J)/p;

         % three blade wind turbine model

N = 100;                        % gear box ratio
Radio = 42;                     % Radio
ro = 1.225;                     % Air density

          % Cp and Ct curves
```

```
beta = 0;                       % pitch angle
ind2 = 1;
for lambda =0.1:0.01:11.8
    lambdai(ind2)=(1./((1./(lambda-0.02*beta)+(0.003./(beta
       ^3+1)))));
    Cp(ind2)=0.73.*(151./lambdai(ind2)-0.58.*beta-0.002.*beta
       ^2.14-13.2).*(exp(-18.4./lambdai(ind2)));
    Ct(ind2) = Cp(ind2)/lambda;
    ind2 = ind2+1;
end
tab_lambda = [0.1:0.01:11.8];

       % Kopt for MPPT

Cp_max = 0.44;
lambda_opt = 7.2;
Kopt = ((0.5*ro*pi*(Radio^5)*Cp_max)/(lambda_opt^3));

       % Power curve in function of wind speed

 P =1.0e
    +06*[0,0,0,0,0,0,0,0.0472,0.1097,0.1815,0.2568,0.3418, ...
     0.4437,0.5642,0.7046,0.8667,1.0518,1.2616,1.4976,1.7613,2.0534,
         ...
     2.3513,2.4024,2.4024,2.4024,2.4024,2.4024,2.4024];
 V =
    [0.0000,0.5556,1.1111,1.6667,2.2222,2.7778,3.3333,3.8889,4.4444,
     ...
      5.0000,5.55556,6.1111,6.6667,7.2222,7.7778,8.3333,8.8889,9.4444,
         ...
```

```
      10.0000,10.5556,11.1111,11.6667,12.2222,12.7778,13.3333,13.8889,
         ...
      14.4444,15.0000];

  figure
  subplot(1,2,1)
  plot(tab_lambda,Ct,'linewidth',1.5)
  xlabel('lambda','fontsize',14)
  ylabel('Ct','fontsize',14)
  subplot(1,2,2)
  plot(V,P,'linewidth',1.5)
  grid
  xlabel('wind speed (m/s)','fontsize',14)
  ylabel('Power (W)','fontsize',14)

          % Grid side converter
 Cbus = 80e-3;      % DC bus capacitance
 Rg =20e-6;         % Grid side Filter's resistance
 Lg = 400e-6;       % Grid side Filter's inductance
 Kpg = 1/(1.5*Vs*sqrt(2/3));
 Kqg = -Kpg;
         % PI regulators
 tau_ig = Lg/Rg; Wnig  = 60*2*pi;
 Kp_idg = (2*Wnig*Lg)-Rg;
 Kp_iqg = Kp_idg;
 Ki_idg = (Wnig^2)*Lg;
 Ki_iqg = Ki_idg;

Kp_v = -1000;
Ki_v = -300000;
Rcrowbar = 1/5;           % Crowbar resistance
```

A.6.2 Particle Swarm Optimization Code

```
clc;
clear;
close all;



%% Problem Definition
CostFunction = @(x)Sphere(x);                    % Cost function
nVar = 5;                                        % Number of
   unknown (Decision) Variables
VarSize = [1 nVar];                              % Matrix size of
   Decision Variables
VarMin = -5;                                     % Lower Bound of
   Decision Variables
VarMax =  5;                                     % upper Bound of
   Decision Variables



%% parameters of PSO algorithm

MaxIt = 100;                                      % Maximum
   Numbers of Iteration
nPop  = 80;                                       % Population
   Size (Swarm Size)

w = 1;                                            % Inertia
   Coefficient
```

```
wdamp = 0.99;                                   % Damping Ratio
    of Inertia Weight
c1 = 2;                                         % Personal
   Accerelation Coefficient
c2 = 2;                                         % Social
   Accerelation Coefficient

%% Initialization

% The Particle Template

empty_particle.Position = [];
empty_particle.Velocity = [];
empty_particle.Cost = [];
empty_particle.Best.Position = [];
empty_particle.Best.Cost= [];

% Create Population Arrey

particle = repmat(empty_particle, nPop ,1);

% Initialize Global Best

GlobalBest.Cost = inf;

% Initialize Population Members

for i = 1: nPop

    % Generate Random Solution
```

```
    particle(i).Position = unifrnd(VarMin ,VarMax , VarSize);

  % Initialize Velocity

   particle(i).Velocity = zeros(VarSize) ;
    % Evaluation

    particle(i).Cost = CostFunction(particle(i).Position);

    % Update the Personal Best

    particle(i).Best.Position = particle(i).Position;
    particle(i).Best.Cost =  particle(i).Cost;

    % Update Global Best

    if particle(i).Best.Cost< GlobalBest.Cost
        GlobalBest = particle(i).Best;

    end
end
  % Arrey to Hold Best Cost Value on Each Iteration

  BestCosts = zeros(MaxIt , 1);

  %% Main Loop of GA algorithm
  for it = 1:MaxIt

      % Update Velocity
      for i = 1:nPop
          particle(i).Velocity = w*particle(i).Velocity ...
```

```
    + c1*rand(VarSize).*(particle(i).Best.Position -
       particle(i).Position) ...
    + c2*rand(VarSize).*(GlobalBest.Position -particle(i)
       .Position);

% Update Position
 particle(i).Position =  particle(i).Position +  particle
    (i).Velocity ;

 % Evaluation
  particle(i).Cost = CostFunction(particle(i).Position);

  % Update Personal Best
 if particle(i).Cost < particle(i).Best.Cost
     particle(i).Best.Position =  particle(i).Position;
     particle(i).Best.Cost =  particle(i).Cost;

      % Update Global Best
  if particle(i).Best.Cost< GlobalBest.Cost
    GlobalBest = particle(i).Best;
  end
 end
 end
 % Store the Best Cost Value
 BestCosts(it) = GlobalBest.Cost;

 % Display Iteration Information
 disp(['Iteration ' num2str(it) ' : Best Cost = ' num2str
    (BestCosts(it))]);

 % Damping Ratio of Inertia Weight
```

```
    w = w * wdamp;
  end

  %% Results

  figure;
  % plot(BestCosts,'LineWidth',2);
  semilogy(BestCosts,'LineWidth',2);
  xlabel('Iteration');
  ylabel('Best.Cost(birr/KW.h)');
  title('PSO Algorithm');
  grid on;
```

A.6.3 Genetic Algorthm Optimization Code

```
clc;
clear;
close all;



%% Problem Definition
CostFunction = @(x) Sphere(x);                 % Cost function
nVar = 5;                                      % Number of
   unknown (Decision) Variables
VarSize = [1 nVar];                             % Matrix size of
    Decision Variables
VarMin = -5;                                   % Lower Bound of
   Decision Variables
VarMax =  5;                                   % upper Bound of
   Decision Variables
```

```
%% parameters of GA algorithm

MaxIt = 100;                                    % Maximum
   Numbers of Iteration
nPop  = 80;                                     % Population
   Size (Swarm Size)

pc=0.8;                                         % Crossover
   probability
pm =0.03;                                        % Mutation
   probability
w = 1;                                          % Inertia
   Coefficient
wdamp = 0.99;                                    % Damping Ratio
    of Inertia Weight
c1 = 2;                                          % Mutation
   Acceleration Coefficient
c2 = 2;                                          % Social
   Acceleration Coefficient

%% Initialization

% The Particle Template

empty_particle.Position = [];
empty_particle.Velocity = [];
empty_particle.Cost = [];
empty_particle.Best.Position = [];
empty_particle.Best.Cost= [];
```

```
% Create Population Array

particle = repmat(empty_particle, nPop ,1);

% Initialize CrossoverBest

CrossoverBest.Cost = inf;

% Initialize Population Members

for i = 1: nPop

    % Generate Random Solution

    particle(i).Position = unifrnd(VarMin ,VarMax , VarSize);

  % Initialize Velocity

   particle(i).Velocity = zeros(VarSize) ;
    % Evaluation

    particle(i).Cost = CostFunction(particle(i).Position);

    % Update the MutationBest

    particle(i).Best.Position = particle(i).Position;
    particle(i).Best.Cost =  particle(i).Cost;

    % Update CrossoverBest

    if particle(i).Best.Cost< CrossoverBest.Cost
```

```
        CrossoverBest = particle(i).Best;

    end
end
  % Array to Hold Best Cost Value on Each Iteration

  BestCosts = zeros(MaxIt , 1);

  %% Main Loop of GA
  for it = 1:MaxIt

      % Update Velocity
      for i = 1:nPop
          particle(i).Velocity = w*particle(i).Velocity ...
        + c1*rand(VarSize).*(particle(i).Best.Position -
           particle(i).Position) ...
        + c2*rand(VarSize).*( CrossoverBest.Position -
           particle(i).Position);

    % Update Position
     particle(i).Position =  particle(i).Position +  particle
        (i).Velocity ;

     % Evaluation
      particle(i).Cost = CostFunction(particle(i).Position);

      % Update Mutation Best
     if particle(i).Cost < particle(i).Best.Cost
         particle(i).Best.Position =  particle(i).Position;
         particle(i).Best.Cost =  particle(i).Cost;
```

```
        % Update Crossover Best
     if particle(i).Best.Cost< CrossoverBest.Cost
       CrossoverBest = particle(i).Best;
     end
    end
     end
    % Store the Best Cost Value
    BestCosts(it) = CrossoverBest.Cost;

    % Display Iteration Information

   disp(['Iteration ' num2str(it) ' : Best Cost = ' num2str(
      BestCosts(it))]);



    % Damping Ratio of Inertia Weight
    w = w * wdamp;
end

%% Results

figure;
% plot(BestCosts,'LineWidth',2);
semilogy(BestCosts,'LineWidth',2);
xlabel('Iteration');
ylabel('Best.Cost (birr/KWh)');
title('GA Algorithm');
grid on;
```